

**Studies of the Thermal Protective Performance of Textile Fabrics used in Firefighters'
Clothing under Various Thermal Exposures**

by

Sumit Mandal

A thesis submitted in partial fulfillment of the requirements for the degree of

Doctor of Philosophy

Department of Human Ecology
University of Alberta

©Sumit Mandal, 2016

Abstract

This PhD study aims to thoroughly investigate the thermal protective performance of textile fabrics used in firefighters' clothing under various thermal exposures. This study has two key objectives – firstly, to characterize the thermal protective performances of different fabrics under a comprehensive range of thermal exposures; secondly, to empirically analyze the thermal protective performance of these fabrics under the thermal exposures. To accomplish both the objectives, physical properties (e.g., thickness, air permeability) of multi-layered fabrics that are commonly used in firefighters' clothing were measured; these multi-layered fabrics consisted different combinations of one type of shell fabric, three types of thermal liners, and one type of moisture barrier. Next, the thermal protective performances of these fabrics were evaluated in the Protective Clothing and Equipment Research Facility at the University of Alberta, Canada under the thermal exposures of flame, radiant heat, hot surface contact, steam, hot-water splash, and hot-water immersion with compression. The experimental data obtained were statistically analyzed to identify the effects of fabrics' physical properties on the performance under these thermal exposures. Also, the performances provided by the fabrics were compared, and the nature of heat and mass transfer through the fabrics under these exposures was explored. Using the significant fabric properties that affected the performance, numerical Multiple Linear Regression (MLR) and Artificial Neural Networks (ANN) modeling techniques were used to empirically predict the performance of the fabrics. The best prediction models were then employed for saliency testing to understand the relative importance of the significant fabric properties on the performance of the fabrics. The study demonstrates that the protective performance of textile fabrics varies with different types of thermal exposures. To provide effective protection in flame, radiant heat, and hot surface contact exposures, the most important

fabric properties to address are thickness and thermal resistance. Steam and hot-water (splash and immersion with compression) exposures allow mass transfer through fabrics. In the presence of steam jet pressure or water, fabric thickness, air or water vapor permeability, and evaporative resistance are primary properties to consider in protecting the human body. In this study, it has been identified that ANN models can be effectively used in comparison to MLR models for predicting the thermal protective performance of fabrics under different thermal exposures. By analyzing the best fit ANN models, it is identified that different fabric properties play a key role in predicting thermal protective performance of fabrics under various thermal exposures. Overall, this PhD study will enhance our understanding of fabric materials used in firefighters' clothing. This deeper understanding could be applied to engineer new test standards and fabric materials for clothing that can provide optimum occupational health and safety for firefighters.

Preface

This thesis contains 6 stand-alone but inter-connected journal articles that I have published from my PhD work. I prepared these articles under the valuable guidance of my previous PhD supervisor Dr. Guowen Song. He reviewed these articles before publication and provided technical as well as editorial feedback to improve the quality of these articles. These articles are listed below. In this list, my contribution to each article is clearly stated along with the contribution of co-authors.

1. Mandal, S., Song, G., Ackerman, M., Paskaluk, S., & Gholamreza, F. (2013). Characterization of textile fabrics under various thermal exposures. *Textile Research Journal*, 83(10), 1005-1019.

At the beginning of my PhD, I conceptualized this research article with the help of Dr. Song. In this article, I reviewed the literature, conducted the experiments, analyzed the data, and prepared the manuscript. For conducting the experiments, Mr. Ackerman and Mr. Paskaluk helped me to set up the testing instruments that I used to evaluate the thermal protective performance of fabrics under various thermal exposures: flame, radiant heat, hot surface contact, steam, and hot-water splash. Mr. Gholamreza also ran the tests to evaluate the thermal protective performance of some of my fabric samples under hot-water splash exposure. Before submitting this article to the *Textile Research Journal*, Mr. Ackerman and Mr. Paskaluk thoroughly reviewed the article and provided technical suggestions to improve the article.

2. Mandal, S., Lu, Y., Wang, F., & Song, G. (2014). Characterization of thermal protective clothing under hot water and pressurized steam exposure. *AATCC Journal of Research*, 1(5), 7-16.

In this article, I did the literature review, laboratory experiments to evaluate thermal protective performance of fabrics under steam and hot-water splash, data analysis, and

manuscript preparation. Dr. Lu evaluated thermal protective performance of clothing under hot-water spray using manikins (as this work is beyond the scope of my PhD, I did not incorporate this part in this thesis). Dr. Wang together with Dr. Song suggested a few changes during the galley proof of this article.

3. Mandal, S., Song, G., & Gholamreza, F. (2015). A novel protocol to characterize the thermal protective performance of fabrics in hot-water exposures. *Journal of Industrial Textiles*. doi 10.1177/1528083715580522

For this article, a thorough literature review and discussions with Dr. Song helped me to conceptualize the novel protocol to evaluate thermal protective performance of fabrics under hot-water exposures. In this article, I tested and evaluated the thermal protective performance of fabrics under hot-water immersion with compression exposure and further compared these experimental results with thermal protective performance values of fabrics against hot-water splash exposure. Here, Mr. Gholamreza ran the tests to evaluate the thermal protective performance of some of my fabric samples under hot-water splash exposure.

4. Mandal, S., & Song, G. (2016). Characterizing fabrics in firefighters' protective clothing: hot-water immersion and compression. *AATCC Journal of Research*, 3(2), 8-15.

I was responsible to review the literature, conduct the experiments, and analyze the data. Dr. Song provided me the technical guidance to understand the hot-water immersion with compression exposure, and its impact on thermal protective performance of fabrics. I prepared the manuscript and presented the paper at the conference.

5. Mandal, S., & Song, G. (2014). An empirical analysis of thermal protective performance of fabrics used in protective clothing. *The Annals of Occupational Hygiene*, 58(8), 1065-1077.

In this article, I have predicted thermal protective performance of fabrics using different empirical modelling techniques – Multiple Linear Regression (MLR) and Artificial Neural Networks (ANN). I used my experimental values of thermal protective performance of fabrics to create the empirical models. I further analysed these models and prepared the manuscript. Dr. Song provided valuable suggestions during the modelling of thermal protective performance of fabrics.

6. Mandal, S., & Song, G. (2015). Thermal sensors for performance evaluation of protective clothing against heat and fire: a review. *Textile Research Journal*, 85(1), 101-112.

In this article, I thoroughly reviewed the literature and composed the manuscript. For preparing the manuscript, Dr. Song provided me the technical knowledge and many relevant classic literatures on thermal sensors.

Dedication

My parents always encouraged me to be a good academician. Although I lost my father in the third year of my PhD, I strongly believe that his blessings were with me throughout my PhD. After my father's death, my younger brother wholeheartedly took care of my mother in India; it gave me an opportunity to peacefully complete my PhD in Canada. Also, my loving wife left her Assistant Professorship in India and accompanied me in Canada to support and encourage at every step of my PhD. Hence, I like to dedicate this thesis to my grandparents (Late Kiriti Mandal and Late Nalini Mandal), parents (Late Ranajit Kumar Mandal and Mrs. Sulekha Mandal), parents-in-laws (Late Prem Lal and Late Wanti Bai), younger brother (Mr. Sunit Mandal), and wife (Ms. Indu Mandal) for their inspiration, never-ending love, emotional support, and understanding.

Also, I would like to dedicate this thesis to my philosophical mentor, Dr. Daisaku Ikeda (President, Soka Gakkai International Association), for his guidance about the world peace, culture, and education based on the wonderful life philosophy of Nichiren Buddhism.

'As the heat of a fire reduces wood to ashes, the fire of knowledge burns to ashes all karma'

– Bhagavad Gita (Song of the Lord)

Acknowledgements

At first, I wish to thank to the gracious God for giving me the opportunity and potential to pursue this PhD study and the wisdom and strength to complete this successfully. The process of this study has made me realize that I am a very fortunate person: my excellent supervisors, loving family, and friends have always supported and helped me, without any hesitation.

I started my PhD under the supervision of Dr. Guowen Song. During the fourth year of my PhD, Dr. Song resigned from the University of Alberta (U of A), Canada. Thereafter, I have continued my PhD under the supervision of Dr. Jane Batcheller at the U of A. Dr. Song and Dr. Batcheller are incredible supervisors. Without their unflinching support, guidance, patience, and encouragement, I could never have finished my PhD with the title of ‘Killam Laureate’. They were not just my supervisors, but excellent mentors: they set a good example of excellent academicians. I would like to take this opportunity to express my most sincere gratitude to them.

I express my sincere gratitude to my PhD supervisory committee members – Dr. Rene Rossi (Head, Protection and Physiology Laboratory, EMPA, Switzerland) and Dr. Hongbo Zeng (Associate Professor, Chemical and Materials Engineering, U of A) – for their guidance and support. I am thankful to Dr. Rossi for giving me a short term research opportunity under his guidance at the EMPA (Swiss Federal Laboratories for Materials Science and Technology), Switzerland. I am indebted to the incredible support and encouragement I received from my arm’s length PhD examiners – Dr. David Torvi (Professor and Chair, Department of Mechanical Engineering, University of Saskatchewan, Canada) and Dr. Rachel McQueen (Associate Professor, Textile and Apparel Science, U of A). I am thankful to Dr. Rhonda Breitzkreuz (Associate Professor, Human Ecology, U of A) for helping me to learn and understand about the theory and practice of human ecology.

I greatly appreciate the technical support from Mr. Mark Ackerman (Adjunct Professor, Mechanical Engineering, U of A), Mr. Stephen Paskaluk (Research Engineer, Human Ecology, U of A), and Ms. Mary Glasper (Graduate Student, Human Ecology, U of A) for my PhD. I also appreciate the technical support provided by Dr. Martin Camenzind, Ms. Leonie Elissawi, Mr. Max Aeberhard, and Mr. Ivo Rechsteiner during my research at the EMPA, Switzerland.

I am indebted to U of A Human Ecology Graduate Coordinators – Dr. Berna Skrypnek, Dr. Deanna Williamson, Dr. Janet Fast, and Dr. Arlene Oak – for showing confidence in my abilities by nominating me for various institutional, provincial, and international scholarships or awards. For my PhD study, I received FS Chia Scholarship, Provost Doctoral Entrance Award, Alberta Innovates Scholarship, Izaak Walton Killam Scholarship, Andrew Stewart Prize, Betty Crown Scholarship, Joanne A. Vincenten Scholarship, Pansy and George Scholarship, Edmonton Consular Ball Scholarship, Martha Piper Award, International Graduate Student Award, Human Ecology Research Grant, Travelling Grant for Advancement of Scholarship, Professional Development Grant, Alberta Citizenship Award, and AATCC (American Association of Textile Chemists and Colorists) Herman and Myrtle Goldstein Student Paper Competition Award.

During my PhD study, members of Soka Gakkai International Association of Canada were my extended family. In particular, I would like to thank Mr. Richard Bornhuse, Ms. Debra Bornhuse, Mr. Paul Reich, Ms. Paula Reich, Mr. Albert Lim, Dr. Mukul Jain, Ms. Sarika Jain, Dr. Nidhi Sharma, and Dr. Prasanna Bhomkar for their unwavering emotional support and care.

I also acknowledge the friendships of my neighbors – Mr. Jai Singh, Dr. Vandana Singh, Dr. Avinash Parashar, Ms. Akansha Parashar, Mr. Gautam Bardoloi, Dr. Prajjita Bardoloi, Mr. Shiva Sivaskandan, Ms. Uma Sivaskandan, Mr. Vikram Chauhan, Ms. Priyali Chauhan, Mr. Rahul Pandey, Dr. Madhur Pandey, Mr. Deva, and Ms. Karen – at the Michener Park residence.

Table of Contents

	Page No.
Chapter 1: Introduction	1
1.1 Background.....	1
1.2 Objectives and impacts.....	2
1.3 Definitions.....	4
1.4 Outline of the thesis.....	9
Chapter 2: Literature Review	11
2.1 Previous research on thermal protective performance of fabrics.....	11
2.2 Remaining gaps in the previous research.....	16
Chapter 3: Research Methodology	19
3.1 Fabric selection and properties evaluation.....	19
3.2 Test conditions and approaches.....	23
3.2.1 Flame exposure test.....	26
3.2.2 Radiant heat exposure test.....	27
3.2.3 Hot surface contact exposure test.....	28
3.2.4 Steam exposure test.....	30
3.2.5 Hot-water splash exposure test.....	31
3.2.6 Hot-water immersion with compression exposure test.....	34
3.3 Procedure to analyze the experimental results.....	36
3.3.1 MLR modeling.....	38
3.3.2 ANN modeling.....	38

Chapter 4: Results and Discussion	42
4.1 Characterization of thermal protective performance of fabrics under various thermal exposures.....	42
4.1.1 Thermal protective performance in flame, radiant heat, and hot surface contact exposures.....	44
4.1.2 Thermal protective performance in steam, hot-water splash, and hot-water immersion with compression exposures.....	52
4.2 Empirical analysis of thermal protective performance of fabrics under various thermal exposures.....	67
4.2.1 MLR models.....	68
4.2.2 ANN models.....	69
4.2.3 Comparison between MLR and ANN models.....	71
4.2.4 Relative importance of each significant fabric property on thermal protective performance.....	72
Chapter 5: Summary and Conclusion	75
References	79
Appendices	92

List of Tables

	Page No.
Table 1: Constructional features of fabrics used in this work.....	21
Table 2: Structural configurations and physical properties of the fabric systems.....	22
Table 3: Thermal protective performance (second-degree burn time in seconds) under flame, radiant heat, and hot surface contact exposures.....	44
Table 4: Results of t-tests between fabric system properties and second-degree burn time in flame, radiant heat, and hot surface contact exposures.....	45
Table 5: Thermal protective performance (second-degree burn time in seconds) in steam, hot-water splash, and hot-water immersion with compression exposures.....	52
Table 6: Results of t-tests between fabric system properties and second-degree burn times in steam, hot-water splash, and hot-water immersion with compression exposures.....	54
Table 7: Significant fabric properties that affected thermal protective performance under various thermal exposures.....	68
Table 8: The R^2 , RMSE, and P-values of the MLR and ANN models.....	71
Table 9: The results of saliency tests.....	73

List of Figures

Figure 1: Skin simulant sensor.....	24
Figure 2: Human skin model.....	25
Figure 3: Schematic diagram of the flame exposure test.....	27
Figure 4: Schematic diagram of the radiant heat exposure test.....	28
Figure 5: Schematic diagram of the hot surface contact exposure test.....	30
Figure 6: Schematic diagram of the steam exposure test.....	31
Figure 7: Schematic diagram of the hot-water splash exposure test.....	33
Figure 8: Schematic diagram of the hot-water immersion with compression exposure test.....	35
Figure 9: Schematic diagram of three-layered feed-forward back propagation ANN model with five hidden neurons.....	41
Figure 10: Relationship between fabric thickness and second-degree burn time in flame, radiant heat, and hot surface contact exposures.....	47
Figure 11: Behavior of thermal energy imposed on a fabric system in a hot surface contact exposure.....	50
Figure 12: Thermal energy transfer through the interface between hot surface contact and fabric system.....	50
Figure 13: Association between air permeability and second-degree burn time in steam.....	57
Figure 14: Association between air permeability and second-degree burn time in hot-water splash.....	57
Figure 15: Association between air permeability and second-degree burn time in hot-water immersion with compression at a pressure of 56 kPa and temperature of 75°C.....	58
Figure 16: Proposed behavior of high pressurized steam inside a fabric system.....	61

Figure 17: Heat and mass transfer mechanisms through fabric systems in steam and hot-water exposures.....63

Figure 18: Relationship between fabric evaporative resistance and second-degree burn time in hot-water immersion with compression exposure of different temperatures and pressures.....64

Chapter 1

Introduction

1.1 Background

The National Fire Protection Association (NFPA) reported that 1,375,000 fire incidents occurred across the U.S. in 2012 (Karter, 2013a). These fire incidents resulted in a total of 16,500 civilian injuries, 2,855 civilian deaths, and \$12.4 billion loss of capital. Human cost in terms of firefighter injuries and deaths were also very high. The NFPA fire statistics confirmed injuries to 69,400 firefighters and a death toll of 97 firefighters in various fire incidents across the U.S. in 2012. From these totals, 31,490 burn injuries occurred when firefighters were working in fire hazards (Fahy, LeBlanc, & Molis, 2014; Karter & Molis, 2013). Although Canada does not have a national fire commissioners' office to compile detailed statistics on casualties of Canadian firefighters, the Canadian Fallen Firefighters Foundation reported that every year approximately 20 on-duty firefighter fatalities occur in Canada (*The Fallen*, n.d.). As protective clothing is the only barrier between firefighters and their occupational fire hazards, the majority of burn injuries result from the inadequate performance of their clothing (Kahn, Patel, Lentz, & Bell, 2012). The performance of thermal protective clothing is strongly associated with the nature of the thermal environments faced by on-duty firefighters (Lawson, 1996). In order to understand the performance of thermal protective clothing, many researchers have investigated the thermal environments faced by on-duty firefighters (Abbott & Schulman, 1976; Foster & Roberts, 1995; Lawson, 1996; Lawson, 1997; Rossi, 2003). Through these investigations, it has been established that firefighters are exposed to flames, radiant heat, hot surface contact, steam, and hot liquids of varying intensities and durations. In these thermal exposures, the performance of thermal protective clothing varies depending upon the characteristics of the textile fabrics

used in the clothing. Thus, to improve firefighters' protection, there is a need to study and understand the performance of the textile fabrics used in firefighters' clothing under different thermal exposures.

Considering the need, extant research has focused on the thermal protective performance of fabrics used in firefighters' clothing under specific thermal exposures, primarily, flame, radiant heat, hot surface contact, steam, and hot-water splash (Benisek & Phillips, 1981; Lu, Song, Zeng, Zhang, & Li, 2014; Rossi, Indelicato, & Bolli, 2004; Rossi & Zimmerli, 1994; Shalev & Barker, 1984). Most of the research has focused on a single thermal exposure and characterized the performance of different fabrics under the exposure. At present, there has been no comprehensive study of the performance of fabrics considering the full range of thermal exposures likely to be encountered by firefighters. Firefighters also experience burn injuries from the exposure to hot-water when they kneel and crawl on the fire-ground (Barker, 2005; Lawson, 1996; Lawson, Twilley, & Malley, 2000); however, no research has investigated the performance of fabrics under this important exposure. Thus, our knowledge of the fabric properties that can improve the thermal protection of firefighters' clothing is still limited and fragmented. Furthermore, the performance evaluation methods used in the previous research are fabric-destructive in nature, expensive, and cumbersome to employ on a routine basis (Benisek & Phillips, 1979; Stull, 1997). To date, no empirical analysis has been carried out to predict the performances using numerical models (Hui & Ng, 2009).

1.2 Objectives and impacts

The objectives of this study are to characterize the thermal protective performance of selected multi-layered textile fabrics used in firefighters' clothing under various thermal exposures and empirically analyze the thermal protective performance of these fabrics (Mandal,

Lu, Wang, & Song, 2014; Mandal & Song, 2014a; Mandal & Song, 2014b; Mandal & Song, 2015; Mandal, Song, Ackerman, Paskaluk, & Gholamreza, 2013a; Mandal, Song, & Gholamreza, 2015; Mandal & Song, 2016). To accomplish these objectives, the physical properties of the fabrics are experimentally measured, and the thermal protective performances of these fabrics are evaluated under various laboratory-simulated thermal exposures. A novel test protocol is used to evaluate the thermal protective performance under hot-water immersion with compression. For the characterization, based on the data obtained from the laboratory experiments, this study statistically analyzes the effect of fabric physical properties on the thermal protective performances of the selected fabrics under various thermal exposures. Also, the performance of the fabrics is compared, and the nature of the heat and mass transfer through the fabrics under these exposures is comprehensively discussed. Using the significant fabric properties that affect thermal protective performance, empirical Multiple Linear Regression (MLR) and Artificial Neural Networks (ANN) models are further used to predict thermal protective performance. The best prediction models are then employed to understand the relative importance of the significant fabric properties on performance.

This study contributes to develop a thorough understanding of thermal protective performance of fabrics under various thermal exposures by acknowledging various significant fabric properties that affect the performance. This study also advances the theory of heat and mass transfer through these fabrics under selected thermal exposures. Furthermore, empirical models for predicting thermal protective performance of fabrics are established, and the relative importance of different significant fabric properties on this prediction is thoroughly demonstrated. In future, this understanding will help to develop new fabric materials and test standards that can be used to provide better protection and comfort to firefighters in Canada and

worldwide.

1.3 Definitions

Air permeability of a fabric: is the volume of air passed per second through a known area of the fabric at a particular pressure differential between the two surfaces of the fabric ([ASTM International, 2013a](#)).

Artificial Neural Networks (ANN) model: are families of statistical learning models (in machine learning and cognitive science discipline) inspired by biological neural networks and are used to estimate or approximate a variable that is dependent on a large number of input variables ([Hassoun, 1995](#); [Yegnanarayana, 2006](#)).

Conduction or conductive heat transfer: is the transfer of heat between substances that are in direct contact with each other ([Arpaci, 1966](#)). When a substance is heated, its molecules gain more thermal energy and vibrate more. These molecules then bump into nearby molecules and transfer some of their thermal energy to them. This process then continues and passes the thermal energy from the hot end down to the colder end of the substance.

Condensation: is the change of water from its gaseous form (water vapor) into liquid water ([Bergman, Lavine, Incropera, & Dewitt, 2011](#)).

Coefficient of Variation (CV): is a statistical measure of the dispersion of data points in a data series around the mean. It represents the ratio of the standard deviation to the mean, and it is a useful statistic for comparing degree of variation from one data series to another, even if the means are drastically different from each other ([Agresti & Franklin, 2009](#)).

Coefficient of determination (denoted by R^2): is interpreted as the proportion of the variance in the dependent variable that is predictable from the independent variable ([Agresti & Franklin, 2009](#)).

Confidence interval: is a range of values so defined that there is a specified probability that the value of a parameter lies within it (Agresti & Franklin, 2009).

Constrictivity: is a dimensionless parameter that describes the mass transport processes in a porous media and it depends on the ratio of the diameter of the diffusing particle to the pore (Bergman, et al., 2011).

Convection or convective heat transfer: is the transfer of heat from one place to another by the movement of fluids. This heat transfer involves the combined processes of conduction (heat diffusion) and advection heat transfer by bulk fluid flow (Arpaci & Larsen, 1984).

Density: or more precisely, the volumetric mass density, of a material is its mass per unit volume (Bergman, et al., 2011).

Diffusion: is the net movement of molecules or atoms from a region of high concentration to a region of low concentration (Bergman, et al., 2011).

Emissivity: is defined as the ratio of the thermal energy radiated from a material's surface to that radiated from a blackbody (a perfect emitter) at the same temperature and wavelength under the same viewing conditions (Hsu, 1963).

Evaporative resistance of a fabric: is the resistance of the fabric to the flow of moisture vapor from a surface with a higher vapor pressure to an environment with a lower vapor pressure (ISO, 2014).

Extinction coefficient: determines how strongly a material absorbs thermal energy in a thermal exposure (Lienhard & Lienhard, 2011).

Heat capacity: is the number of heat units needed to raise the temperature of a material by one degree (Bergman, et al., 2011).

Heat flux: is the thermal intensity indicated by the amount of energy transmitted per unit area per unit time (Lienhard & Lienhard, 2011).

Heat transfer: is the movement of thermal energy from one object to another object of different temperature (Lienhard & Lienhard, 2011).

Hypothesis test: is an inferential procedure that uses sample data to evaluate the credibility of a hypothesis about a population (i.e., a set of fabric system) (Agresti & Franklin, 2009).

Linear regression t-test: determines whether there is a significant linear relationship between an independent variable (fabric properties) and dependent variable (thermal protective performance) (Agresti & Franklin, 2009; Yan & Su, 2009).

Mass of a fabric: is one of the ways to classify fabric, and it is measured by weighing a standardized width of a yard or meter of fabric on a scale (ASTM International, 2013a).

Mass transfer: is the net movement of mass from one location (usually meaning a stream, phase, fraction, or component) to another location. Mass transfer occurs in many processes, such as absorption, evaporation, adsorption, drying, precipitation, and membrane filtration (Bergman, et al., 2011).

Multiple Linear Regression (MLR) model: attempts to model the relationship between two or more independent variables and a dependent variable by fitting a linear equation to observed data. Here, every value of the independent variable is associated with a value of the dependent variable (Orme & Orme, 2009; Yan & Su, 2009).

Nonwoven fabric: is a textile sheet or web structure bonded together by entangling fibers or filaments through mechanical, thermal, or chemical process (Batra & Pourdeyhimi, 2012; Massenaux, 2003).

Porosity of a fabric: is a measure of the void (i.e., empty) spaces in a fabric, and is a fraction of the volume of voids over the total volume ([ASTM International, 2013a](#)). The porosity values lie between 0 and 1 or it can be expressed as a percentage between 0 and 100%.

P-value: is a function of the observed sample results (a statistic) that is used for testing a statistical hypothesis ([Agresti & Franklin, 2009](#)).

Radiation or radiative heat transfer: is the transfer of heat from one place to another through infrared radiation (a type of electromagnetic radiation). This heat transfer can also occur through empty spaces ([Siegel & Howell, 2002](#)).

Root Mean Square Error (RMSE): is frequently used to measure the differences between values predicted by a model (e.g., MLR, ANN) or an estimator and the values actually observed ([Agresti & Franklin, 2009](#)).

Specific heat: is the heat required to raise the temperature of the unit mass of a given substance by a given amount (usually one degree) ([Bergman, et al., 2011](#)).

Standard deviation: is a measure that is used to quantify the amount of variation or dispersion of a set of data values ([Agresti & Franklin, 2009](#)).

Thermal absorptivity: is the property of a material that determines the fraction of incident thermal radiation absorbed by the material ([Bergman, et al., 2011](#); [Hsu, 1963](#)).

Thermal conductivity: is the rate at which heat passes through a specified material, expressed as the amount of heat that flows per unit time through a unit area with a temperature gradient of one degree per unit distance ([Bergman, et al., 2011](#); [Hsu, 1963](#)).

Thermal insulation of a fabric: is the reduction of heat transfer (the transfer of thermal energy between objects of differing temperature) between objects in thermal contact or in range of radiative influence ([Abdel-Rehim, Saad, Ei-shakankery, & Hanafy, 2006](#); [Song, 2009](#)).

Thermal inertia: is the degree of slowness with which the temperature of a material approaches that of its surrounding and which is dependent upon its absorptivity, thermal conductivity, specific heat, and dimensions (Bergman, et al., 2011; Hsu, 1963).

Thermal protective performance of a fabric: According to American Society for Testing and Materials (ASTM) D 4108 and Canadian General Standards Board (CGSB) 78.1 standards, thermal protective performance of a fabric is defined as the minimum exposure energy required to cause the accumulated energy received by the copper sensor to equal the energy that can cause a second-degree burn in human tissue (ASTM International, 1987; CGSB, 2001). For this study, thermal protective performance is the time to a predicted second-degree burn injury as defined using a skin simulant sensor and skin burn model when the fabric is tested under various thermal exposures (Mandal, et al., 2013a; Song, et al., 2011a). Here, thermal protective performance of the fabric is defined as the time to second-degree burn injury because this could help to realistically understand wearers' protection under a thermal exposure while wearing the thermal protective clothing.

Thermal resistance of a fabric: is the resistance of the fabric to the heat transfer through conduction, convection, and/or radiation (ASTM International, 2014a).

Thickness of a fabric: is a precise measurement of the distance between two plane parallel plates separated by the fabric when a known pressure is applied and maintained on the plates (ASTM International, 2013a).

Tortuosity of a fabric: is a ratio that characterizes the convoluted pathways of fluid diffusion through the porous media such as fabric. In the fluid mechanics of porous media, tortuosity is the ratio of the length of a streamline – a flow line or path – between two points to the straight-line distance between these points (Bear, 1972).

Transmissivity of a fabric: is the degree to which a fabric allows thermal energy, in particular electromagnetic radiation, to pass through it (Haghi, 2011).

Woven fabric: is a structure produced when at least two sets of yarns are interlaced, usually at right angles to each other, according to a predetermined pattern of interlacing, and such that at least one set is parallel to the axis along the lengthwise direction of the fabric (ASTM International, 2013a).

1.4 Outline of the thesis

This doctoral thesis is divided into 5 chapters. **Chapter 1** introduces the research and provides background for this study. The research problem is stated and the objectives and contributions of the study are explained. **Chapter 2** thoroughly reviews the literature on thermal protective performance of fabrics under various thermal exposures. Through this review, various fabric properties that affect the thermal protective performance of fabrics are presented. The important knowledge gaps in the existing research are identified to provide the rationale for the objectives of this study. **Chapter 3** describes the research methodologies used to fulfil the objectives of this study. This chapter describes the fabrics selected for this study and their properties. Also, the experimental approaches to evaluate the thermal protective performance of these fabrics under various thermal exposures are demonstrated, and the procedures for analyzing the experimental results are stated. **Chapter 4** presents the results and discussion of this study. Here, thermal protective performances of fabrics are characterized under various thermal exposures and are explained based on the theory of heat and/or mass transfer. This characterization process helps to identify the fabric properties that significantly affected the thermal protective performance. Furthermore, using the significant fabric properties as input variables, thermal protective performance of fabric as an output variable is empirically predicted. These predictions are actualized using MLR and ANN modeling techniques. These MLR and

ANN models are also statistically compared and best fit models for predicting thermal protective performance of fabrics are identified. By utilizing the best fit models for predicting thermal protective performance of fabrics, the relative importance of the significant fabric properties on protective performance is thoroughly examined. **Chapter 5** reports the summary and conclusion of this study. Here, the limitations of the study are clearly mentioned in order to provide the future research direction in the field of thermal protective clothing or textiles and materials science.

Chapter 2

Literature Review

2.1 Previous research on thermal protective performance of fabrics

Many researchers have studied the thermal protective performance of fabrics used in firefighters' clothing under single or specific thermal exposures ([Benisek & Phillips, 1981](#); [Lu, et al., 2014](#); [Rossi, et al., 2004](#); [Rossi & Zimmerli, 1994](#); [Shalev & Barker, 1984](#)). In these studies, the thermal protective performance of the fabrics was evaluated using the test methods developed by many national and international organizations such as ASTM, International Organization for Standardization (ISO), and NFPA ([ASTM International, 2008a](#); [ASTM International, 2008b](#); [ASTM International, 2008c](#); [ASTM International, 2013b](#); [ISO, 1995](#); [NFPA, 2013](#)). These studies have also characterized the fabrics in order to recognize and explain fabric properties affecting the thermal protective performance.

In the late 1970s and early 1980s, [Benisek and Phillips \(1979, 1981\)](#) analyzed single- and double-layered fabrics in the high intensity flame exposures. They found that the thickness and weight of fabrics affected the thermal protective performance, and that the protection of double-layered fabrics was much higher than that of single-layered fabrics. [Barker and Lee \(1987\)](#), and [Shalev and Barker \(1983\)](#) demonstrated that the thermal protective performance of single-layered fabrics was affected by changes in the intensity of the flame exposure and also by the thickness and weight of the fabrics. [Barker and Lee \(1987\)](#) further explained that the fabric's density (mass per unit volume) does have a significant impact on thermal protective performance. Here, if the density of a fabric gradually increases, the thermal protective performance proportionately decreases. However, over the density of $\sim 60 \text{ kg/m}^3$, the thermal protective performance drops very rapidly. This is because, beyond this density, the dead air

trapped inside the fabric structure starts conducting the thermal energy toward the wearer's skin. This situation rapidly lowers the thermal protective performance of the fabric. Furthermore, [Morris \(1953\)](#) explained that when two fabrics are of equal thickness, the one with lower density shows greater thermal protective performance. In this context, it is necessary to remember that the structural properties of two fabrics with the same density can be quite different. One fabric might be loosely woven from tightly twisted, hard yarns and the other might be closely woven from loosely twisted, soft yarns. This variation in structural properties may affect the thermal protective performance of the fabrics. Contextually, [Torvi and Dale \(1998\)](#), and [Torvi, Dale, and Faulkner \(1999\)](#) found that a fabric with high thermal conductivity and low specific heat could quickly transfer thermal energy through it and lower the thermal protective performance. They also noted that such a fabric could decompose in a flame exposure. Here, the thermal decomposition reactions of the fabric are generally endothermic because little oxygen is available for exothermic oxidation reactions to happen ([Torvi, 1997](#)). This endothermic decomposition reaction could generate considerable thermal energy depending upon the intensity and duration of the flame exposure. This thermal energy generated by decomposition could also lower the thermal protective performance of the fabric.

In a bench-top configuration that simulated a combined exposure of flame and radiant heat, [Shalev and Barker \(1984\)](#) observed that the thermal energy transfer rate was lower for thick fabrics than for thin fabrics, and that the air permeability of the fabrics did not significantly affect the transfer of thermal energy. They concluded that air permeability has little or no impact on thermal protective performance of fabrics. [Perkins \(1979\)](#) concluded that fabric weight and thickness are the main properties to consider when analyzing fabric performance in low intensity ($\sim < 20 \text{ kW/m}^2$), radiant heat exposures. Through statistical analysis, he confirmed that fabric

weight and thickness are positively associated with thermal protective performance of fabrics. Fabrics with high thickness entrap more dead air than thinner fabrics, and this air helps to insulate wearers (Sun, Yoo, Zhang, & Pan, 2000; Torvi & Dale, 1999; Zhu, Zhang, & Chen, 2007). However, Song, et al. (2011a) observed that thick fabrics store more thermal energy than thin fabrics in the low intensity radiant heat exposures, and this stored energy may be released due to compression during and after the exposure. The release of the stored energy causes burn injury on a wearer's skin and consequently lowers the performance of the clothing (Eni, 2005). Barker, Guerth-Schacher, Grimes, and Hamouda (2006) stated that fabrics may absorb moisture due to perspiration from a sweating firefighter; thus increasing the thermal conductivity of fibers, and lowering the thermal protective performance of the fabric (Lee & Barker, 1986; Lu, Li, Li, & Song, 2013a). In contrast, it was also found that if a fabric absorbs a significantly high amount of water (over 15% of its weight), this situation provides a cooling effect to firefighters by reducing the thermal energy transfer (Song, Cao, & Gholamreza, 2011b).

Rossi and Zimmerli (1994) also investigated the impact of moisture on thermal protective performance of multi-layered fabric systems during hot surface contact. They found that the presence of water in the outer layer of the fabric system (exposed to the hot surface contact) enhanced the thermal conductivity of the fabric system. As a result, the thermal protective performance of the fabric system dropped by 50-60%. In this context, a multi-layered fabric system with a separate moisture barrier in the inner layer exhibited better thermal protective performance than a multi-layered fabric system with a laminated moisture barrier on the outer shell fabric. However, both of these fabric systems exhibited a similar drop in performance when their inner layers were wet. If the inner layer of the fabric system was wet, the thermal protective performance was found to drop by 10-25% for all of the selected fabric systems of this study.

Here, the decrease in thermal protective performance was greater at lower temperatures because the water accumulated in the fabric layers without any significant evaporation, enhancing thermal conductivity and lowering the thermal protective performance of the fabric systems.

If moisture that has accumulated inside the fabric structure turns into steam during a thermal exposure, the steam may diffuse toward the skin depending upon the fabric's characteristics, leading to skin burns (Keiser, Becker, & Rossi, 2008; Keiser & Rossi, 2008; Keiser, Wyss, & Rossi, 2010; Rossi, et al., 2004). Similarly, water used by firefighters to extinguish fire may generate steam in the environment and thus be transferred through their clothing to produce skin burns. Rossi, et al. (2004) concluded that water vapor permeability is the most important fabric property to consider for effective protection in steam exposures. They suggested that a water vapor impermeable membrane inside the fabric layers might significantly prevent steam transfer and reduce burn injuries. It was also confirmed that a thick fabric with a water vapor impermeable membrane provides better protection from steam than a thick fabric with a semi-permeable membrane (Keiser, et al., 2010; Keiser & Rossi, 2008; Sati, Crown, Ackerman, Gonzalez, & Dale, 2008).

Lu, Song, Ackerman, Paskaluk, and Li (2013b), and Lu, Song, Li, and Paskaluk (2013c) studied the performance of single-layered fabric systems against hot liquid splash at 85°C. They used water, drilling mud (manufactured by SAGDRIL), and canola oil to simulate various workplace hazards. They observed that the properties of water, e.g., density, thermal conductivity, surface tension, and heat capacity, at 85°C were the highest among all liquids evaluated; whereas, the dynamic viscosity of water was the lowest of all the liquids at this temperature. They found that the thermal protective performance of the fabric systems evaluated depended on the properties of the fabrics (e.g., weight, thickness, air permeability, fiber content,

weave structure) and liquids. They found that the air permeability of a fabric system was negatively associated with thermal protective performance under all types of hot liquid splashes. This is an important finding since previous studies did not find any relationship between air permeability and thermal protective performance under flame and radiant heat exposures (Perkins, 1979; Shalev & Barker, 1984). Lu, et al. (2013b, 2013c) also found that fabric performance was lower when exposed to water or drilling mud than when exposed to canola oil. This was thought to be because the heat capacity of hot-water or drilling mud is higher than the heat capacity of canola oil. Basically, the amount of heat energy per unit mass of hot-water or drilling mud was higher due to their high heat capacity; this high heat content lowered the thermal protective performance of selected fabrics in Lu, et al.'s study. Gholamreza and Song (2013) found that a multi-layered fabric system with an air-impermeable outer layer provided better protection against hot liquid splash than a multi-layered fabric system with an air-permeable outer layer. Recently, Lu, et al. (2014) investigated the thermal protective performance of different single-layered fabrics under hot liquid splash. They found that the flow pattern of liquids on the fabrics varied depending on the surface energy between the liquid molecule and fabric. Generally, a very hot liquid or highly rough fabric surface could influence the surface tension of the liquid; in turn, increasing the wettability of the fabric. In the case of a fabric with high wettability, the liquid could penetrate through the fabric due to wicking and cause burns on wearers' skins. Lu, et al. (2014) further mentioned that the liquid applied can be stored in fabric or transmitted through the fabric depending upon fabric properties (thickness, density, air permeability). If a fabric can store more and transmit less liquid, it will show high initial thermal protective performance. They also found that the addition of a thermal liner with a

single-layered shell fabric can help to store more and transmit less liquid and this enhances the performance of the shell fabric.

2.2 Remaining gaps in the previous research

Based on the above discussion, it is evident that much research has focused on the thermal protective performance of multi-layered fabrics used in firefighters' clothing under specific thermal exposures, namely flames, radiant heat, hot surface contact, steam, and/or hot-water splash. From these studies, important fabric properties influencing thermal protective performance under specific thermal exposures and test conditions have been identified (Benisek & Phillips, 1981; Lu, et al., 2014; Rossi, et al., 2004; Rossi & Zimmerli, 1994; Shalev & Barker, 1984). However, no study has evaluated the thermal protective performance of fabrics under all of these thermal exposures. As a consequence, knowledge of the fabric properties that influence thermal protective performance is still limited. Contextually, Barker (2005), and Lawson (1997) suggested that the studies on thermal protective performance of firefighters' clothing over a wide range of thermal exposures are needed in order to holistically understand the effects of various thermal exposures on the performance. Furthermore, previous researchers focused on the thermal protective performance of fabrics (for industrial use) under hot-water splash conditions (Gholamreza & Song, 2013; Lu, et al., 2013b; Lu, et al., 2013c; Lu, et al., 2014). However, on-duty firefighters are not so likely to be exposed to hot-water splash only. They do kneel and crawl on the floor while working to extinguish fires and rescue fire-victims. While performing these activities, their clothing is compressed specifically in the knees, elbows, and lower-legs. The clothing may also be immersed in hot-water. This hot-water immersion with compression can cause skin burns to firefighters' arms, hands, legs, and feet (Barker, 2005; Lawson, 1996; Lawson, et al., 2000). Burn injury statistics indicated that nearly 38% of burn injuries occurred

on firefighters' arms/hands and legs/feet during the period 2007-2011 in the U.S. (Karter, 2013b). However, the thermal protective performance of fabrics under the hot-water immersion with compression has not been widely studied.

As mentioned in the previous section, many national and international organizations (e.g., ASTM, ISO, NFPA) have developed standard test methods (e.g., ASTM F 2703, ASTM F 1939, ASTM F 2702, ASTM F 2701, ISO 9151, NFPA 1971) to evaluate the performance of fabrics in particular thermal exposures. By evaluating the thermal protective performances of fabrics using these experimental methods, many researchers have also explained the relationship between fabric properties and thermal protective performance (Benisek & Phillips, 1981; Lu, et al., 2014; Rossi, et al., 2004; Rossi & Zimmerli, 1994; Shalev & Barker, 1984). However, these experimental methods are fabric-destructive in nature, expensive, and difficult to carry out on a routine basis (Benisek & Phillips, 1979; Stull, 1997). Therefore, an empirical analysis for predicting the thermal protective performance of fabrics could save time and reduce costs. MLR and ANN techniques have been successfully employed to empirically model the complex relationships between input and output variables in the textile fabrics and clothing fields. For example, they have been used to predict the fabric spirality, seam quality (Hui & Ng, 2009; Majumdar & Majumdar, 2004; Murrells, Tao, Xu, & Cheng, 2009; Pynckels, Kiekens, Sette, Van-Langenhove, & Impe, 1995). Although MLR models provide simple predictions of the output variables, the prediction accuracy of ANN models is greater in most fields where they have been applied. To date, no empirical MLR and ANN models have been used for predicting the thermal protective performance (output variable) of textile fabrics from fabric properties (input variables). Also, as previous researchers have not explained the significant fabric properties affecting thermal protective performance (Benisek & Phillips, 1981; Lu, et al., 2014;

Rossi, et al., 2004; Rossi & Zimmerli, 1994; Shalev & Barker, 1984), the implementation of these empirical MLR or ANN models for predicting the performance could be instrumental in determining the relative importance of the significant fabric properties influencing thermal protective performance.

Chapter 3

Research Methodology

3.1 Fabric selection and properties evaluation

In the manufactured thermal protective clothing for firefighters, layered fabric systems are generally used. These fabric systems consist of different types of high-performance fabrics (an outer shell, a moisture barrier, and/or a thermal liner) in an assembly (Makinen, 2008). The high-performance fabrics used in this study were selected based on the fiber content, weave structure, mass, thickness, and air permeability (Table 1). These fabrics are commercially available and commonly used in the manufacturing of thermal protective clothing. By assembling these fabrics in different combinations, layered fabric systems (single-, double-, and triple-layered) were prepared to fulfil the objectives of this study (Table 2). Notably, the number of prepared fabric systems or the sample size for this study was relatively small; however, the small sample size is common to most textile experimental research and this does not adversely affect the data analysis (Andersson, 1999; Wen, 2014). In these fabric systems, the outer layer (OL) is facing the thermal exposure, the inner layer (IL) is closest to the skin simulant sensor or the wearers' skin, and the middle layer (ML) is sandwiched between OL and IL. The physical properties (mass, thickness, air permeability, thermal resistance, and evaporative resistance) of each of these fabrics or fabric systems were measured according to ASTM standards and their mean value is calculated by maintaining a Coefficient of Variation (CV) between 1-2.5% (see Appendices 1-3). These mean values are presented in Table 1 and Table 2. It should be noted that the mean values of three specimens are presented in my published papers (Mandal, et al., 2013a; Mandal, et al., 2014), but I calculated the mean values of ten specimens for the thesis. As a consequence, the mean values reported in the thesis are slightly different from the values

reported in my published papers. Furthermore, the measured physical properties (mass, thickness, air permeability, thermal resistance, and evaporative resistance) were considered as independent variables with respect to the dependent variable (thermal protective performance) for the statistical data analysis. Here, the number of physical properties considered was limited to four because the sample size of this study is relatively small. Generally, fewer independent variables are recommended for statistical analysis, especially where the sample size is small (Wen, 2014).

Table 1. Constructional features of fabrics used in this work

Fabric types	Fiber content	Weave structure	Mass ^a (g/m ²)	Thickness ^b (mm)	Air permeability ^c (cm ³ /cm ² /s)
A (Outer Shell)	60% Kevlar [®] aramid and 40% Polybenzimidazole	Plain weave, rip-stop woven	248	0.69	15.7
B (Thermal liner)	100% Nomex [®] aramid	Plain weave Nomex [®] layer quilted to two thin Nomex [®] oriented webs	209	1.63	43.2
C (Thermal liner)	100% Nomex [®] aramid	Plain weave Nomex [®] layer quilted to Nomex [®] needle-felted batt	289	2.13	40.6
D (Thermal liner)	100% Nomex [®] aramid	Plain weave Nomex [®] layer quilted to Nomex [®] scrim, needle-felted batt, and scrim	351	3.18	38.4
E (Moisture Barrier)	85% Nomex-III [®] A and 15% polyurethane	Plain weave Nomex [®] back-coated with polyurethane film	211	0.85	0

^aMeasured according to ASTM D 3776 (ASTM International, 2009).

^bMeasured according to ASTM D 1777 under 1kPa pressure (ASTM International, 1996).

^cMeasured according to ASTM D 737 under air pressure differential 125Pa (ASTM International, 2004).

Table 2. Structural configurations and physical properties of the fabric systems

Fabric construction	Fabric systems	Structural configurations	Thick-ness (mm)	Air permeability (cm³/cm²/s)	Thermal resistance^f (°K·m²/W)	Evaporative resistance^g (m²·Pa/W)
Single-layered	A	Fabric A	0.69	15.71	0.073	4.40
Double-layered	AB	Fabric A (OL) + Fabric B ^a (IL)	2.18	13.59	0.117	9.87
	AD	Fabric A (OL) + Fabric D ^b (IL)	3.53	13.30	0.169	12.70
	AE	Fabric A (OL) + Fabric E ^d (IL)	1.42	0	0.095	20.70
	EA	Fabric E ^c (OL) + Fabric A (IL)	1.42	0	0.095	21.17
Triple-layered	AEB	Fabric A (OL) + Fabric E ^d (ML) + Fabric B ^a (IL)	2.88	0	0.129	25.90
	AEC	Fabric A (OL) + Fabric E ^d (ML) + Fabric C ^c (IL)	3.49	0	0.151	25.40
	AED	Fabric A (OL) + Fabric E ^d (ML) + Fabric D ^b (IL)	4.23	0	0.184	28.03
	EAC	Fabric E ^c (OL) + Fabric A (ML) + Fabric C ^c (IL)	3.49	0	0.151	25.37

^aThe web side of Fabric B is in contact with wearers' skin.

^bThe scrim side of Fabric D is in contact to wearers' skin.

^cThe batt side of Fabric C is in contact with wearers' skin.

^dThe polyurethane coated side of Fabric E faces Fabric A.

^eThe polyurethane coated side of Fabric E faces a thermal exposure.

^fMeasured according to ASTM D 1518 (ASTM International, 2014a).

^gMeasured according to ISO 11092 (ISO, 2014).

3.2 Test conditions and approaches

The protective performances of three specimens of each selected single-, double-, and triple-layered fabric system were evaluated for each thermal exposure using bench-scale tests. Before testing, the specimens were conditioned at $20\pm 2^{\circ}\text{C}$ temperature and $65\pm 5\%$ relative humidity for at least 24 hours in accordance with ASTM D 1776 (ASTM International, 2015). Then, these specimens were subjected to the laboratory-simulated thermal exposure until the time required to generate a second-degree burn on human skin was reached (see details in sections 3.2.1-3.2.6). The standard deviation (SD) of the mean burn time for three specimens of each fabric system in the thermal exposure was maintained within the limits of 2.5%. If the standard deviation of mean burn time obtained from three specimens was not within this limit, more specimens were tested to maintain the limit (see Appendices 4-9). The mean result of second-degree burn time of a fabric system is defined as its ‘thermal protective performance’ under the specific test.

In order to predict the time required for a second-degree burn injury, the calculation procedure of ASTM F 1930 standard test method was followed (ASTM International, 2013c). Skin simulant sensors specified in the method were used (Mandal, et al., 2013a; Mandal & Song, 2015). The sensor consisted of a slab, 32 mm length and 19 mm diameter, of colorceron, an inorganic material consisting of a mixture of various compounds such as calcium, aluminum, silicate, asbestos fiber, and a binder (Figure 1). This inorganic material does not have the same values of density (ρ), thermal conductivity (k), or specific heat (C_p) when compared with human skin; however, thermal inertia [a product of ρ (kg/m^3), k ($\text{W}/\text{m}^{\circ}\text{C}$), and C_p ($\text{J}/\text{kg}^{\circ}\text{C}$)] or thermal absorptivity (a square root of thermal inertia) of the material is similar to that of human skin (Barker, Hamouda, Shalev, & Johnson, 1999; Dale, Crown, Ackerman, Leung, & Rigakis, 1992;

Torvi, 1997). Here, a type-T thermocouple (copper-constantan) is held on the surface of the colorceron slab (by an epoxy-phenolic adhesive that can tolerate temperatures up to 370°C) to measure the temperature increase of the slab during the thermal exposure. During the thermal exposures, the energy transmitted through the fabric systems is processed at every 0.1s by the skin simulant sensor. In this process, the skin simulant sensor works according to the skin model (Figure 2). Based on this model, the thermal energy transmitted within the sensor is represented as a transient, one dimensional heat diffusion problem in which the temperature within the human skin (epidermis layer) and under the human skin (dermis, subcutaneous layers) varies with skin depth and exposure time (ASTM International, 2013c). In this study, using the surface (epidermis skin) temperatures of the slab measured by thermocouple, the time for a second-degree skin burn injury was calculated using Henriques Burn Integral (HBI) equation (Equations 1 and 2) (Henriques, 1947; Henriques & Moritz, 1947).

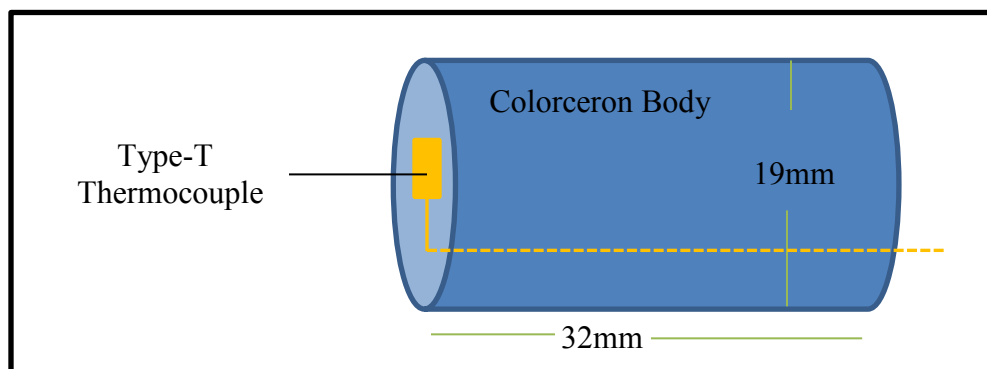


Figure 1. Skin simulant sensor

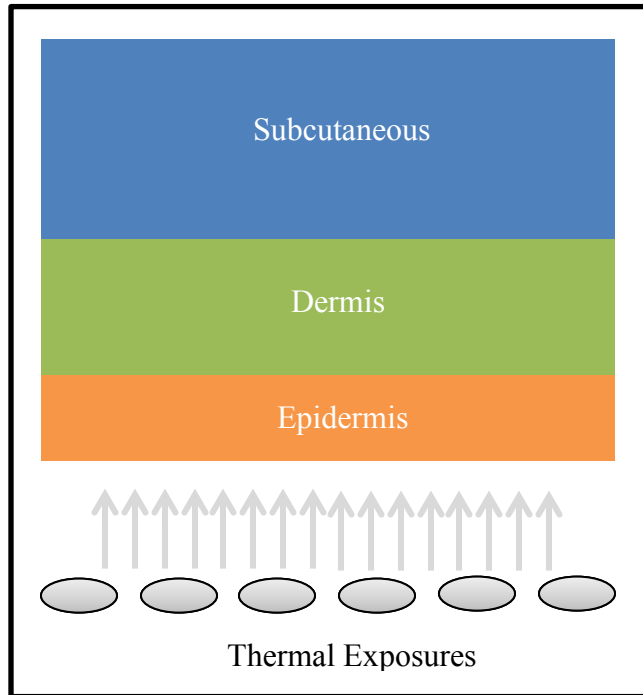


Figure 2. Human skin model

$$\frac{d\Omega}{dt} = P \exp\left(\frac{-\Delta E}{RT}\right) \dots \dots \dots \text{Equation 1}$$

Mathematical integration of Equation 1 yields,

$$\Omega = \int_0^t P \exp^{-\left(\frac{\Delta E}{RT}\right)} dt \dots \dots \dots \text{Equation 2}$$

where,

Ω = burn injury parameter (dimensionless),

P = frequency factor (2.185×10^{124} seconds⁻¹ at $T < 50^\circ\text{C}$ and 1.823×10^{51} seconds⁻¹ at $T > 50^\circ\text{C}$),

ΔE = activation energy (J/kmol),

R = universal gas constant (8.315 J/kmolK) (i.e., $\Delta E/R = 93534.9$ K at $T < 50^\circ\text{C}$ and $\Delta E/R = 39109.8$ K at $T > 50^\circ\text{C}$),

T = temperature (K) at epidermis skin depth of 75×10^{-6} m, and

t = time (seconds) for which T is above 317.15 K (44°C).

The time at which Ω reaches a value of 1 in Equation 2 is called the ‘second-degree burn time’ (Heath, 2000).

3.2.1 Flame exposure test

Protective performance in flame exposure was measured using a modified ISO 9151 testing approach as shown in Figure 3. The modification was primarily associated with the type of sensor and data calculation technique to predict the thermal protective performance in terms of time required for a second-degree burn injury. In the original ISO 9151 standard, a horizontally oriented specimen of the fabric system (14×14 cm) is subjected to an incident heat flux of 80 kW/m² from the flame of a gas burner placed beneath it (ISO, 1995). The heat passing through the specimen is measured by means of a small copper calorimeter placed on top of and in contact with the specimen. The time, in seconds, required to raise the temperature at 24±0.2°C in the calorimeter is recorded; the mean result for three test specimens is calculated as the ‘heat transfer index (flame)’. In the modified ISO 9151 standard, the flame was delivered from a Meker propane gas burner with a diameter of 38 mm (Figure 3, a) (Mandal, et al., 2013a). The burner was adjusted to deliver a heat flux of 84 kW/m². The fabric specimen of size 10×10 cm (Figure 3, b) was mounted above the burner using the specimen support frame (Figure 3, c) with the outer layer of the fabric system facing the burner. The fabric specimen was protected from the heat source before and after the test run. At the time of the test, the burner was placed beneath the fabric specimen and the flame was delivered for a time that depended on the structure (i.e., the composition and number of layers) of fabric system. The thermal energy transferred through the fabric specimen was processed using a skin simulant sensor (Figure 3, d) mounted on an insulating board and located behind the fabric specimen. The surface (epidermis skin) temperature of the sensor was recorded and the second-degree burn time was calculated using the customized software (Figure 3, e) that was programmed according to HBI equation.

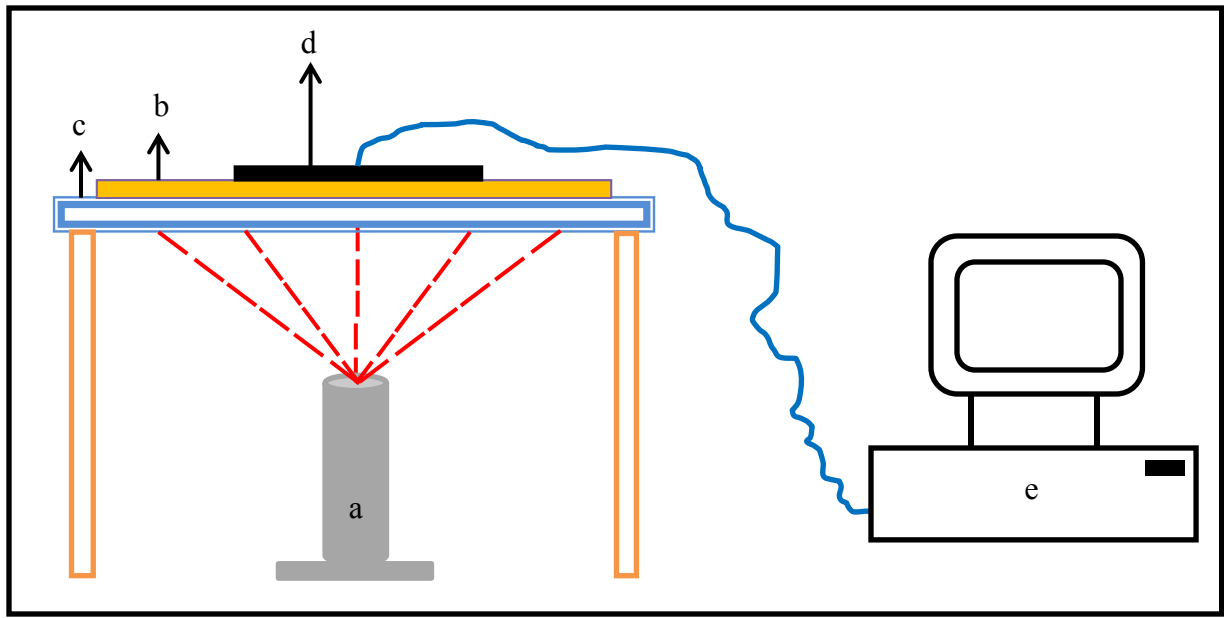


Figure 3. Schematic diagram of the flame exposure test (a = gas burner, b = fabric specimen, c = specimen support frame, d = skin simulant sensor, and e = HBI software)

3.2.2 Radiant heat exposure test

To measure thermal protective performance of fabrics in radiant heat exposure, the cone calorimeter (Figure 4) test was conducted following a modified ASTM E 1354 testing approach. The modification involved the use of a data acquisition technique for predicting the time required for a second-degree burn injury as the means of evaluating the thermal protective performance of fabrics. In the original ASTM E 1354 standard, a horizontally oriented specimen of the fabric system (10×10 cm) is subjected to an incident radiant heat flux of 0-100 kW/m² generated from an electric spark placed on top of it; the ignitability, heat release rates, mass loss rates, effective heat of combustion, and visible smoke development of the specimen in the certain duration exposure are measured using an oxygen consumption calorimeter (ASTM International, 2014b). In the modified ASTM E 1354 test, heat was generated by a truncated cone-shaped electrically heated (5000W, 240V) coil (Figure 4, a) adjusted to deliver a heat flux of 84 kW/m² (Mandal, et al., 2013a). The specimen of the fabric system (15×15 cm) (Figure 4, b) was horizontally mounted beneath the heated coil. The heat flux was kept uniform within the central 50 by 50 mm

area of the specimen. A transverse shutter was used to protect the fabric specimen from the heat source before and after the test. The radiant heat exposure time for different fabric specimens was varied according to the structure of the fabric system. A skin simulant sensor attached on a frame (Figure 4, c) was placed behind the test specimen to process the thermal energy transferred through the fabric system during the exposure. The surface (epidermis skin) temperature of the sensor was recorded and the second-degree skin burn time was calculated using the customized and programmed HBI software (Figure 4, d).

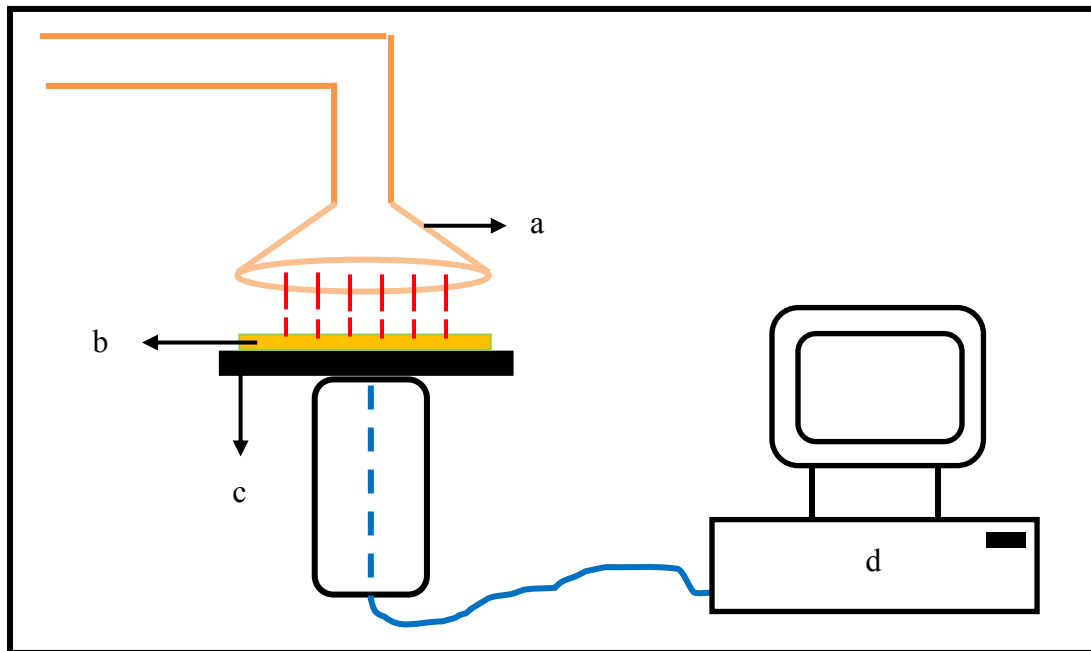


Figure 4. Schematic diagram of the radiant heat exposure test (a = cone-shaped electrically heated coil, b = fabric specimen, c = skin simulant sensor on a frame, and d = HBI software)

3.2.3 Hot surface contact exposure test

Thermal protective performance of fabrics in hot surface contact exposure was measured according to a modified ASTM F 1060 (Figure 5) method. The modification was primarily associated with the hot surface temperature, type of sensor, and data calculation procedure to predict the thermal protective performance. In the original ASTM F 1060 standard, a specimen of the fabric system (10×15 cm) is horizontally placed in contact (contact-pressure is 3 kPa) with

a standard hot surface (temperature is up to 316°C) (ASTM International, 2008d). The amount of heat transmitted through the specimen is measured by a copper calorimeter placed on top of the specimen; this calorimeter is mounted in an insulating block with added weight. Finally, the heat measured is compared with the human tissue tolerance (pain sensation or a second-degree burn) and the obvious effects of heat on the specimen (physical damage and degradation) are noted. In the modified ASTM F 1060 test used, the specimen of the fabric system (10×15 cm) was placed horizontally (Figure 5, a) on a hot surface plate of electrolytic copper (Figure 5, b) under a load of 1 kg (Figure 5, c) (Mandal, et al., 2013a) . The temperature of the hot surface (Figure 5, d) was controlled at 400°C using variable power supply with a thermocouple (Figure 5, e). Heat transmitted through the test specimen was processed by a skin simulant sensor (Figure 5, f) mounted above the fabric specimen on an insulated board. The exposure time varied depending on the composition and number of layers of the fabric system, since the test ran until the transferred energy was sufficient to generate a second-degree skin burn injury. The skin simulant sensor (Figure 5, f) and customized HBI software (Figure 5, g) were used to calculate the time required for a second-degree skin burn injury.

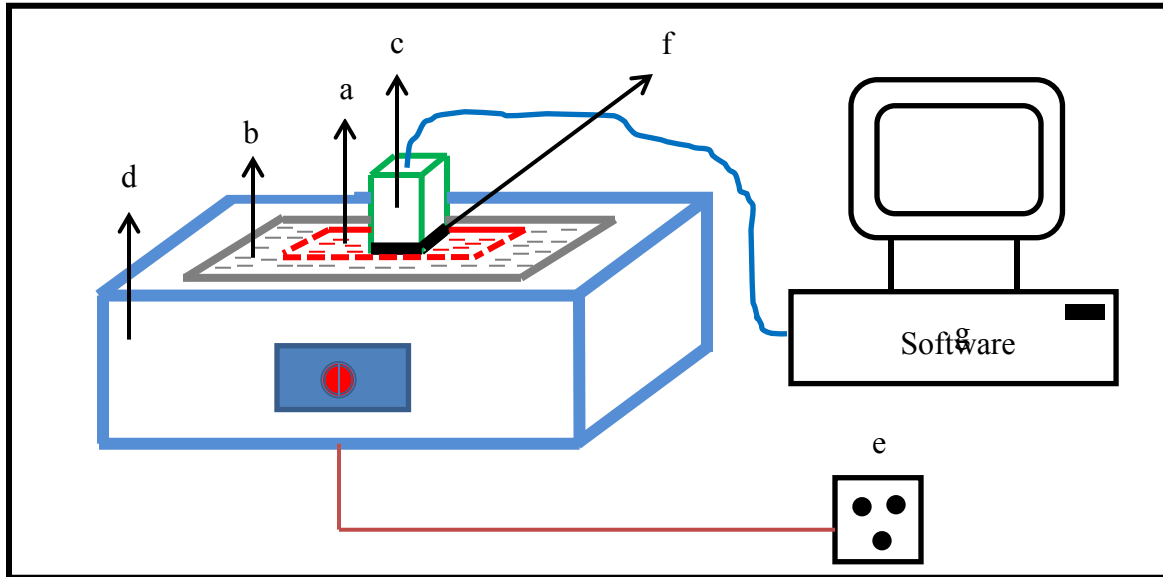


Figure 5. Schematic diagram of the hot surface contact exposure test (a = fabric specimen, b = hot surface plate of electrolytic copper, c = a load of 1 kg, d = hot surface, e = variable power supply with a thermocouple, f = skin simulant sensor, and g = HBI software)

3.2.4 Steam exposure test

A schematic diagram of the steam tester developed by the research team of Protective Clothing and Equipment Research Facility (PCERF) at the University of Alberta (U of A), Canada is illustrated in Figure 6 (Ackerman, et al., 2012; Murtaza, 2012). Steam (Figure 6, a) was generated through a 3 kW boiler at a temperature of 150°C. The fabric specimen (20×20 cm) was placed on Teflon plated specimen holder (Figure 6, b) attached with an embedded skin simulant sensor (Figure 6, c). The steam was impinged at a pressure of 200 kPa from 50 mm above the fabric specimen through a nozzle having a diameter of 4.6 mm (Figure 6, d). The duration of the steam exposure was controlled according to the structure of the fabric specimen or system to generate a second-degree burn injury. Notably, although the normal steam exposure time for this tester is 10s, the steam exposure time was 30s for the thickest fabric specimen used in this study. During and after the steam exposure, the heat flux through the fabric specimen was processed by the skin simulant sensor and the time required to generate a second-degree skin burn was calculated by the customized and programmed HBI software (Figure 6, e).

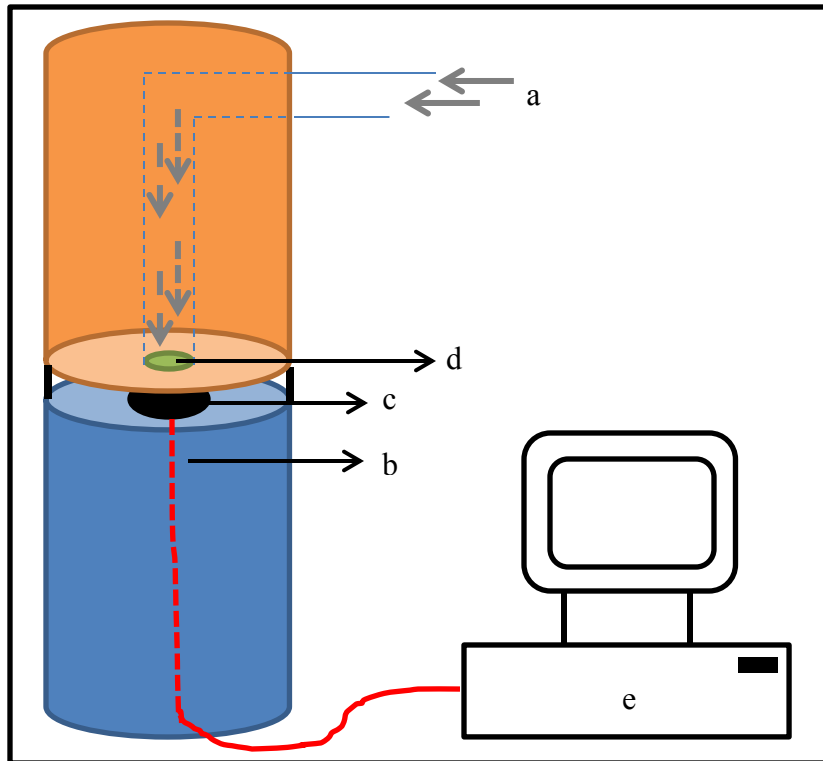


Figure 6. Schematic diagram of the steam exposure test (a = steam from boiler, b = fabric specimen holder, c = skin simulant sensor, d = steam impingement nozzle, and e = HBI software)

3.2.5 Hot-water splash exposure test

The hot-water splash test was conducted using a modified ASTM F 2701 (Figure 7) method (Jalbani, Ackerman, Crown, Keulen, & Song, 2012; Lu, et al., 2013b). In the original ASTM F 2701 standard, hot-water is hand-poured on the fabric specimen through a funnel to create a 10s hot-water splash exposure for evaluating the thermal protective performance of the specimen using copper calorimeters (ASTM International, 2008c). However, Jalbani, et al. (2012) found that this pouring procedure is unrealistic and can affect the hot-water flow rate and repeatability, resulting in an increase in measurement errors. They replaced the funnel with a small pipe, directly fed by a circulating hot-water bath via a small pump through a hose and valve system; this modification provides a consistent application of a given quantity of water at a consistent temperature and flow rate. The equipment was further modified as described by Mandal, et al. (2013a) to replace the copper calorimeters with skin simulant sensors. Each fabric

specimen (30×30 cm) was mounted on an inclined (45°) sensor board (Figure 7, a) made of a nonconductive, liquid and heat resistant material. The sensor board had two skin simulant sensors – an upper sensor (Figure 7, b₁) representing a direct exposure point of the fabric system to the hot-water, and a lower sensor (Figure 7, b₂) representing an off-direct exposure point of the fabric system to the hot-water. Notably, only the data obtained from the upper sensor was used for this study. Here, hot-water was prepared in a circulating bath (Figure 7, c) and its temperature was maintained at 85°C using a temperature control device (Figure 7, d). The hot-water was initially circulated by a pump (Figure 7, e) through a circulation valve attached with a flow control valve (Figure 7, f) in order to regulate the water temperature within the pipe at 85°C. Using a water tap (Figure 7, g), the hot-water was then passed through the water outlet (Figure 7, h). By employing a thermocouple at the front of the outlet, the water temperature was constantly monitored. Next, the fabric specimen was continuously exposed to the hot-water until a second-degree burn was predicted. The duration of the water flow depended upon the structure of the fabric specimen or system being tested. The thermal energy (in the form of heat and mass transmitted through the specimen) at the direct exposure point was processed using the skin simulant sensor (Figure 7, b₁). The surface (epidermis skin) temperature of the sensor was recorded and used to calculate the time required for a second-degree skin burn injury using the customized and programmed HBI software (Figure 7, i).

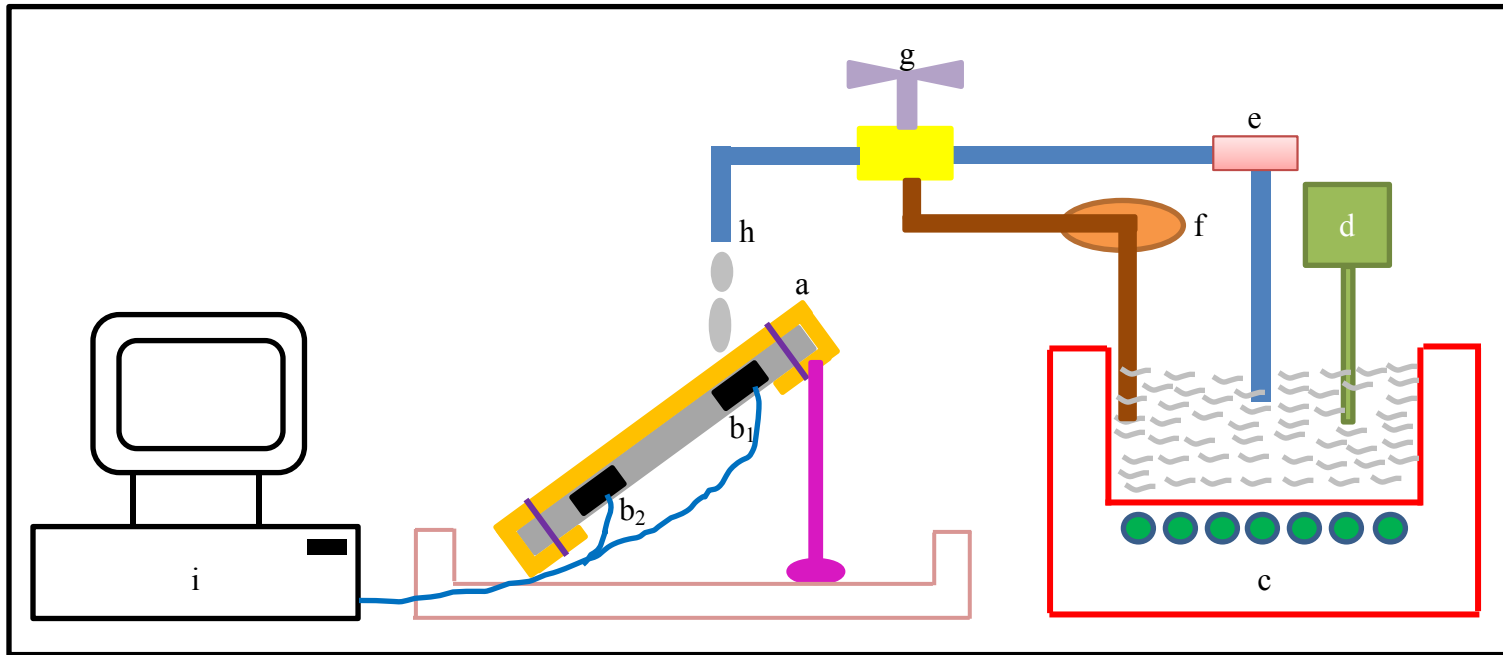


Figure 7. Schematic diagram of the hot-water splash exposure test (a = inclined sensor board, b₁ = upper skin simulant sensor, b₂ = lower skin simulant sensor, c = hot-water bath, d = temperature control device, e = pump, f = circulation valve attached with flow control valve, g = water tap, h = water outlet, and i = HBI software)

3.2.6 Hot-water immersion with compression exposure test

The hot-water immersion with compression test was carried out using a new test apparatus available at the U of A, Canada (Mandal & Song, 2014b; Mandal & Song, 2014c). In this study, a metal platform with perforated top surface (Figure 8, a) was positioned at the bottom-center of a hot-water bath (Figure 8, b). Then, water (Figure 8, c) was poured into the bath up to a level 6 cm above the perforated top surface. The water temperature was maintained at 75°C, 85°C, or 95°C using a temperature control device (Figure 8, d). Next, a 30.5×30.5 cm fabric specimen (Figure 8, e) was attached with a rubber band (Figure 8, f) to the skin simulant sensor (Figure 8, g) mounted on a cylindrical weight (Figure 8, h). This specimen-covered sensor was immersed into the hot-water bath using a pneumatic device (Figure 8, i) until the whole assembly (specimen + sensor) rested flatly on the center of the perforated surface. Pressure was applied to compress the specimen between the sensor and perforated surface and was pneumatically controlled at 14 kPa (~2.0 psi), 28 kPa (~4.0 psi), or 56 kPa (~8.0 psi). Thermal energy transmitted through the compressed specimen was processed by the sensor for a period of 120s. From the thermal energy, time required to generate a second-degree skin burn was calculated by the customized HBI software (Figure 8, j).

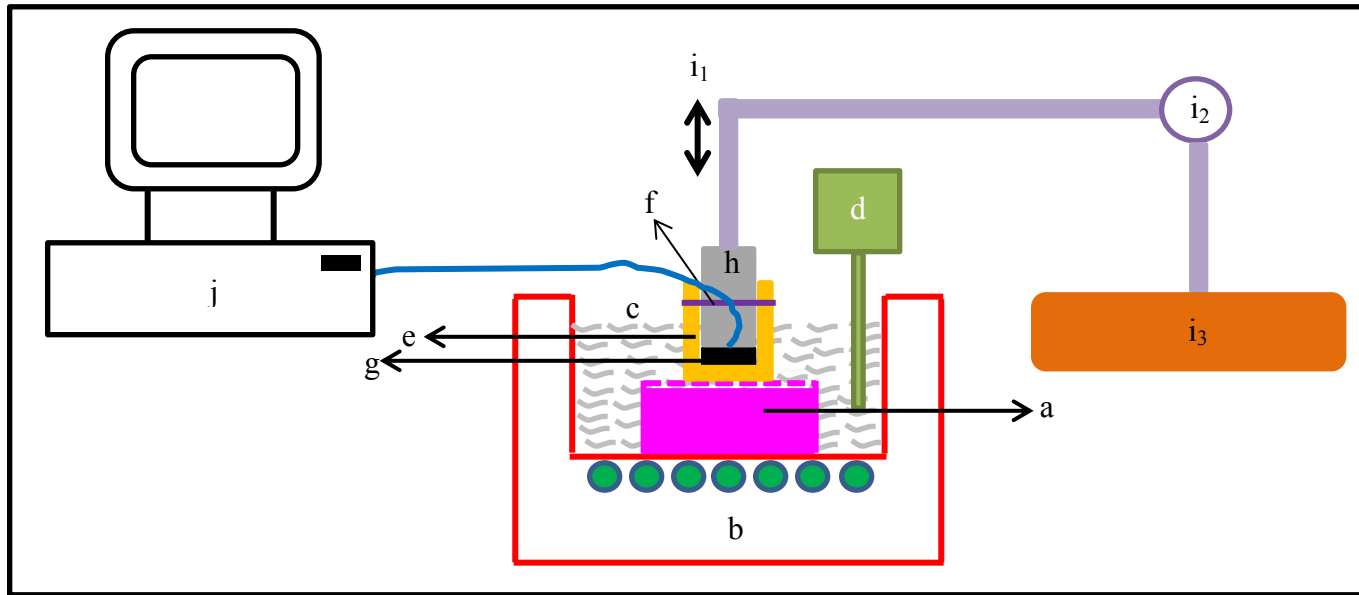


Figure 8. Schematic diagram of the hot-water immersion with compression exposure test [a = metal platform with perforated top surface, b = hot-water bath, c = hot-water, d = temperature control device, e = fabric specimen, f = rubber band, g = skin simulant sensor, h = cylindrical weight, i = pneumatic device (i_1 = pneumatically controlled up and down device, i_2 = pressure gauge, i_3 = air compressor), and j = HBI software]

3.3 Procedure to analyze the experimental results

The second-degree skin burn times of the selected fabric systems obtained from the tests described above were tabulated. The thermal protective performances of the fabric systems were ranked or rated according to the time required to generate a second-degree burn injury in each thermal exposure. The physical properties (e.g., thickness, air permeability, thermal resistance, and evaporative resistance) and thermal protective performances (second-degree burn times) of the fabric systems were normalized between -1 and $+1$, with the average value set to zero. The normalized variable $X_{i,norm}$ was calculated by Equation 3, where,

$R_{i,max} = \text{Maximum}[(X_{i,max} - X_{i,avg}), (X_{i,avg} - X_{i,min})]$. This normalization process reduced the redundancy rates in the data by pulling out abnormal factors, and it helped to distribute the data with normal probability plot.

$$X_{i,norm} = \frac{X_i - X_{i,avg}}{R_{i,max}} \dots\dots\dots \text{Equation 3}$$

In Equation 3,

X_i is the value of a selected variable (thickness, air permeability, thermal resistance, evaporative resistance, or second-degree burn time),

$X_{i,avg}$ is the average value of that particular variable,

$X_{i,min}$ is the minimum value of that variable,

$X_{i,max}$ is the maximum value of that variable, and

$R_{i,max}$ is the maximum range between the average value and either the minimum or the maximum of that variable.

In order to understand the association between the physical properties of fabric systems and thermal protective performance in a thermal exposure, a linear regression t-test of the normalized data set was conducted using the StatCrunch™ 5.0 software ([StatCrunch, n.d.](#)). The

association was inferred based on the + or – sign of the T-stat value obtained from the t-test; this association was further justified through the theories of heat and mass transfer. P-values obtained from the t-test for individual fabric properties were analyzed to identify the fabric properties that significantly affected the thermal protective performance. Significance tests were carried out at the significance level 0.05. Thus, if the obtained P-value for any considered property was less than 0.05, that property was inferred to be statistically significant. Relationships between the significant fabric properties and the thermal protective performance were plotted, and the coefficients of determination (R^2) of these plots were calculated. An R^2 value with proximity to 1 was inferred as a strong association between the significant fabric property and thermal protective performance. Inference tests [hypothesis test (P-value) and confidence interval (upper and lower limits)] were carried out to understand the differences in thermal protective performances of different fabric systems in various thermal exposures. The significant properties were further used in the MLR and ANN models for predicting the thermal protective performance in a thermal exposure; for the modeling, a linear relationship was assumed between the significant fabric properties and thermal protective performance. These MLR and ANN models were then statistically compared based on their predicting performance parameters [R^2 , Root Mean Square Error (RMSE), P-values]. This comparison process was applied to identify the best-fit high-performance models to predict the thermal protective performance. During the comparison, a model with high R^2 , low RMSE, and P-values of <0.05 was inferred as the best-fit high-performance model. The best-fit high-performance model was further used in a saliency test to understand the relative importance of the significant fabric properties on thermal protective performance. Here, the saliency test was conducted by eliminating only one designated significant fabric property from the best-fit model at a time. The increase in RMSE value in the

saliency test compared to the best-fit model was considered as the indicator of importance of the eliminated significant fabric property; the eliminated property that generated the highest RMSE was inferred to be the most important property for thermal protective performance. In the following section, the modeling methodologies of MLR and ANN are thoroughly discussed.

3.3.1 MLR modeling

In this study, the standard MLR models were used to predict the thermal protective performance using the significant properties (under various thermal exposures) obtained from the t-test analysis. This modeling was carried out using the StatCrunch™ 5.0 statistical software ([StatCrunch, n.d.](#)). A generic form of these MLR models used is shown in Equation 4.

$$(Performance) = C + \beta_1 \times (SFP)_1 + \beta_2 \times (SFP)_2 + \dots + \beta_n \times (SFP)_n \dots\dots\dots \text{Equation 4}$$

where,

C = identically distributed constant normal error,

$(SFP)_1 \dots (SFP)_n$ = significant fabric properties, and

$\beta_1 \dots \beta_n$ = regression coefficients that determine relative strength of the respective significant fabric properties.

Here, a notable inherent limitation of the MLR model is that it should not be used to predict the output variable (thermal protective performance) beyond the range of the values of the input variables (significant fabric properties) employed in the model ([Hui & Ng, 2009](#); [Majumdar & Majumdar, 2004](#); [Murrells, et al., 2009](#); [Pynckels, et al., 1995](#)).

3.3.2 ANN modeling

The ANN used is a powerful data modeling tool that could capture and represent any kind of relationship between the input (significant fabric properties obtained from the t-tests) and output (thermal protective performance) variables ([Arupjoyti & Iragavarapu, 1998](#); [Hui & Ng, 2009](#); [Majumdar & Majumdar, 2004](#); [Murrells, et al., 2009](#); [Pynckels, et al., 1995](#); [Zaefizadeh,](#)

Khayatnezhad, & Gholamin, 2011). By using the ANN modeling technique, different ANN models were developed in this study for predicting the thermal protective performance of fabrics under various thermal exposures. In these ANN models, three layers were used – input layer, hidden layer, and output layer. These models were constructed using the MATLAB[®] 6.1 software (MATLAB, n.d.). For constructing a suitable model, an important point to consider was to decide upon the architecture of the ANN as it can have different architectures. Keeping all this in mind, various ANN architectures were deployed and investigated considering one hidden layer. Through this investigation, it was found that a three-layered feed-forward back propagation ANN model (with one hidden layer) can be a universal technique to model a complex linear function (Figure 9). In this three-layered feed-forward model, each layer of the neural network contained connections to the next layer (e.g., from the input to the hidden layer), but there were no connections back. Here, all the neurons in a particular layer received a signal from the neurons of the previous layer. The signal received was then multiplied by a weight factor known as a synaptic weight. Next, the weighted inputs were summed up and passed through a transfer function to generate the output in a fixed range of values. This output was then transferred to the neurons of the next layer. As the models used back propagation supervised training form (the gradient descent with momentum constant), the final outputs predicted were always compared with the actual output. Through this comparison, the back propagation training algorithm calculated the prediction error and adjusted the synaptic weight of various layers backward from the output to the input layer. This weight adjustment process worked based on a delta rule and decreased the error signal iteratively. Eventually, the model got closer and closer to produce the desired final output. The delta rule used is shown in Equation 5, where, $W(n)$ = the weight connecting between two neurons at the n^{th} iteration, $\Delta W(n)$ = the weight correction

applied to the $W(n)$ at the n^{th} iteration, E = predicted error signal at the n^{th} iteration, and η = learning rate parameter constant. The hyperbolic tangent sigmoid transfer function (Equation 6) was assigned as an activation function in the hidden layer, and the linear function (Equation 7) was used in the output layer. These specific functions were used because they can easily be applied with all types of data and can provide the best performance for an ANN model (Hui & Ng, 2009). In the Equations 6 and 7, x is the weighted sum of inputs to a neuron and $f(x)$ is the transformed output from that neuron. In this regard, a challenge in using the feed-forward back propagation ANN model was to decide the number of neurons in the hidden layer. If the neurons are too few in the hidden layer, the model is unable to differentiate between complex patterns, and it might lead to a linear estimate of the actual relationship between the inputs and output variables; whereas, if the neurons are too many, the model follows a noise in the data set, and it might lead to an inaccurate output (Murrells, et al., 2009). In order to choose the optimum number of neurons in the hidden layer, the feed-forward ANN models were trained with two to ten neurons, and the best predictive ANN models was found with five hidden neurons (Figure 9) (Mandal & Song, 2012a; Mandal & Song, 2014a). In the present study, by default, MATLAB software randomly used 70% of the data (significant properties and thermal protective performance) for the training, 15% of the data for the validation, and the remaining 15% of the data to test the predicting performance of the ANN models. Contextually, it is notable that these ANN models were trained with a small dataset. As a consequence, these models could be unstable and may not be generalized for use in predicting thermal protective performance of all types of fabrics.

$$\Delta W(n) = -\eta[\partial E / \partial W(n)] \dots\dots\dots \text{Equation 5}$$

$$f(x) = \frac{\sinh x}{\cosh x} = \frac{e^x - e^{-x}}{e^x + e^{-x}} = \frac{e^{2x} - 1}{e^{2x} + 1} \dots\dots\dots \text{Equation 6}$$

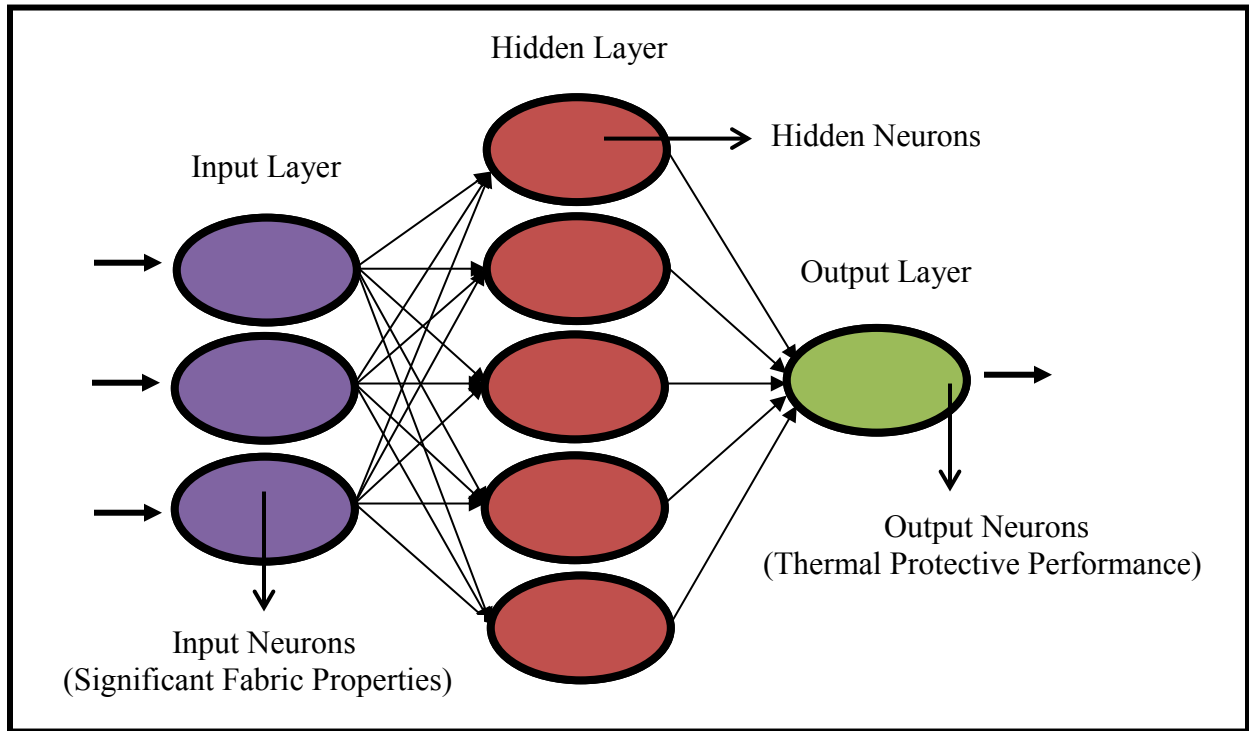


Figure 9. Schematic diagram of three-layered feed-forward back propagation ANN model with five hidden neurons

Chapter 4

Results and Discussion

This results and discussion chapter is broadly divided into two sections (sections 4.1 and 4.2). In section 4.1, the results of the characterization of the thermal protective performance of the fabrics under various thermal exposures (flame, radiant heat, hot surface contact, steam, hot-water splash, and hot-water immersion with compression) are reported. Here, based on the statistical significance tests [e.g., t-test, coefficient of determination (R^2)], different fabric properties significantly affecting the thermal protective performance are identified and discussed through the theory of heat and mass transfer. Additionally, the differences in thermal protective performance of two sets of fabric systems (e.g., air-permeable, air-impermeable) are demonstrated through statistical inference tests (hypothesis test, confidence interval test). In section 4.2, the thermal protective performance of the fabric systems are empirically analyzed by employing the MLR and ANN modeling techniques. Here, the significant fabric properties (identified in section 4.1) are used in the empirical MLR and ANN models to predict the thermal protective performance of the fabric systems under each thermal exposure. Then, these empirical MLR and ANN models are compared to identify the best fit model for predicting the thermal protective performance of the fabric systems. The best fit model for each thermal exposure is further used for saliency testing to find the relative importance of each significant fabric property for the thermal protective performance of the fabric systems.

4.1 Characterization of thermal protective performance of fabrics under various thermal exposures

During the flame exposure, a flame is produced through controlled combustion of flammable propane gas. The flame generates a jet of hot gaseous molecules that move toward the

fabric surface. As the moving air mass imposes thermal energy on the fabric system, convection is the primary mode of heat transfer in flame exposure (Arpaci & Larsen, 1984; Burnmeister, 1993). As some thermal energy also radiates from the flame surface toward the fabric, radiation is the secondary mode of heat transfer in flame exposure. In radiant heat exposure, electromagnetic waves radiate from a conical electrical heat source toward the fabric system imposing electromagnetic energy on the fabric system; therefore, radiation is the primary mode of heat transfer (Hsu, 1963; Siegel & Howell, 2002). Physical contact between the fabric system and hot surfaces results in conduction being the primary mode of heat transfer in hot surface contact exposure (Arpaci, 1966). Convection and/or diffusion are the primary modes of mass (water molecules) and heat transfer through the fabric system, especially in steam, hot-water splash, and hot-water immersion with compression exposures (Bergman, et al., 2011).

The thermal protective performance of the fabric systems varies under each type of thermal exposure, depending upon heat and/or mass transfer through the fabric system. Flame, radiant heat, and hot surface contact exposures transfer mainly heat through the fabric systems (Arpaci, 1966; Arpaci & Larsen, 1984; Hsu, 1963); whereas, mainly mass transfer (through water containing a large amount of thermal energy) occurs in steam, hot-water splash, and hot-water immersion with compression exposures (Bergman, et al., 2011). During mass transfer, liquid and vaporized water molecules diffuse along their concentration gradients i.e., from the high concentration regions towards the low concentration regions. As the steam exposure occurs under high pressure, it is expected that the vaporized water molecules have a greater momentum than the liquid water molecules present in the hot-water exposures (splash, and immersion with compression). In turn, the mass transfer rate is greater during steam exposures than during hot-water exposures.

4.1.1 Thermal protective performance in flame, radiant heat, and hot surface contact exposures

The thermal protective performance (second-degree burn times) of the selected fabric systems (A–EAC) obtained through laboratory-simulated flame, radiant heat, and hot surface contact exposures are presented in Table 3. In agreement with previous literature (Benisek & Phillips, 1981; Shalev & Barker, 1984), second-degree burn times of triple-layered fabric systems are mostly higher than second-degree burn times of single- and double-layered fabric systems, inferring that triple-layered fabric systems will provide more protection to a wearer than single- and double-layered fabric systems in flame, radiant heat, or hot surface contact exposures. Actually, the greater number of air layers and extra trapped air inside the triple-layered fabric systems contribute to their high second-degree burn times (Song, et al., 2011a; Song, et al., 2011b).

Table 3. Thermal protective performance (second-degree burn time in seconds) under flame, radiant heat, and hot surface contact exposures

Fabric construction	Fabric systems	Second-degree burn time in seconds		
		Flame	Radiant heat	Hot surface contact
Single-layered	A	2.75	4.64	1.51
Double-layered	AB	12.81	11.90	4.77
	AD	16.59	24.18	6.87
	AE	9.58	9.22	5.16
	EA	5.72	7.91	3.54
Triple-layered	AEB	11.79	17.60	9.45
	AEC	15.74	23.19	16.27
	AED	20.84	27.93	17.30
	EAC	15.47	20.59	7.22

To understand the impact of the fabric systems’ properties on the second-degree burn times, the experimental dataset comprising fabric thickness, air permeability, thermal resistance, evaporative resistance, and second-degree burn time of each thermal exposure was normalized following the procedure indicated in section 3.3 titled “Procedure to analyze the experimental

results” and t-tests were carried out. Results obtained from the t-tests (T-stat and P-value) are shown in Table 4.

Table 4. Results of t-tests between fabric system properties and second-degree burn time in flame, radiant heat, and hot surface contact exposures

Fabric system properties	Second-degree burn time in seconds					
	Flame		Radiant heat		Hot surface contact	
	T-Stat	P-value	T-Stat	P-value	T-Stat	P-value
Thickness	8.96	0.0001	17.68	0.0001	3.78	0.007
Air permeability	-0.76	0.47	-0.82	0.43	-1.59	0.15
Thermal resistance	9.72	0.003	17.78	0.002	3.33	0.01
Evaporative resistance	1.71	0.13	1.87	0.11	2.67	0.16

As shown in Table 4, the T-stat values for fabric air permeability and evaporative resistance are negative and positive, respectively, in the exposures of flame, radiant heat, and hot surface contact. The negative and positive T-stat values indicate a negative and positive association between fabric air permeability and second-degree burn time (as air permeability increases or evaporative resistance decreases, second-degree burn time decreases). Basically, a fabric system with high air permeability generally reduces the evaporative resistance of the fabric system and that helps to move the thermal energy through the fabric system. However, the impact of air permeability and evaporative resistance is not significant as indicated by the P-values which are all much greater than 0.05. In the flame, radiant heat, and hot surface contact exposures, fabric air permeability and evaporative resistance did not significantly impact the second-degree burn times.

The T-stat values for fabric thickness and thermal resistance are also positive in the exposures of flame, radiant heat, and hot surface contact. Hence, the association between these two fabric properties (fabric thickness and thermal resistance) and second-degree burn time is positive in these exposures. Furthermore, P-values of fabric thickness and thermal resistance under these exposures are all less than 0.05. These P-values as expected indicate that thickness

and thermal resistance are highly significant fabric properties for effective protection under flame, radiant heat, and hot surface contact exposures. However, P-values of fabric thickness are significantly less than the P-values of fabric thermal resistance. From this, it can be inferred that fabric thickness is a more significant property than fabric thermal resistance. In the same context, it is notable that the thickness could affect the thermal resistance of the fabric. The values in Table 4 also suggest that P-value of fabric thickness in hot surface contact exposure is significantly higher than flame and radiant heat exposures. This indicates that fabric thickness is less significant property for second-degree burn time in hot surface contact exposure. Basically, heat or thermal energy transfer in hot surface contact exposure proceeds through a pressure or load on the fabric system that is not present in flame and radiant heat exposures. Consequently, heat or thermal energy transfer mechanism through the fabric systems in hot surface contact exposure differs from both the flame and radiant heat exposures. Relationships between fabric thickness and second-degree burn time in flame, radiant heat, and hot surface contact exposures are shown in Figure 10 to individually explain and compare the exposures in detail. In this context, it has been hypothesized that thermal energy transfer mechanisms through multiphase (solid fiber and gaseous air), non-homogeneous fabric systems entail a combination of absorption, re-radiation/reflection, conduction, and possibly forced convection (Chitphiomsri & Kuznetsov, 2005; Shalev & Barker, 1984; Song, Chitphiomsri, & Ding, 2008).

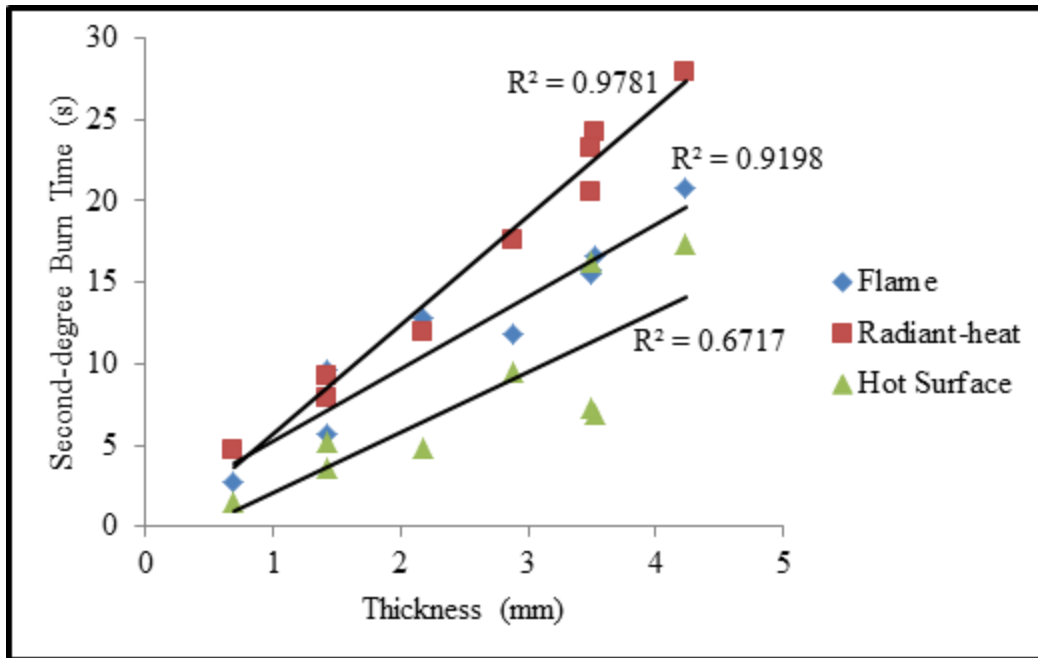


Figure 10. Relationship between fabric thickness and second-degree burn time in flame, radiant heat, and hot surface contact exposures

Figure 10 confirms the T-stat values that showed a positive association between fabric thickness and second-degree burn time. In comparison between flame and radiant heat exposures, it is clear that the R^2 values between fabric thickness and second-degree burn time are different. This infers that a different level of association between fabric thickness and second-degree burn time exists in flame and radiant heat exposures. In flame and radiant heat exposures, thermal energy is imposed on the multiphase (solid fiber and gaseous air) fabric systems and this incident thermal energy may partially be reflected, and/or absorbed, and/or transmitted depending on the fabric system's emissivity or absorptivity (Shalev & Barker, 1984; Song, 2004). The emissivity (ϵ) of a fabric system is strongly dependent upon the nature of its surface optical properties. The surface optical properties are basically influenced by the fiber content, method of fabrication, finishing, temperature/thermal cycling, and/or chemical reactions during thermal exposures. A fabric system with maximum emissivity ($\epsilon \sim 1$) reflects less thermal energy than a fabric system with minimum emissivity ($\epsilon \sim 0$); therefore, thermal energy imposed on

fabrics with high emissivity is mostly absorbed inside the fabric system and/or transmitted toward the skin. In this study, the fabrics consist mainly of Kevlar[®]/PBI and Nomex[®] fibers. According to [Song \(2004\)](#), the emissivity of fabrics made from these fibers is nearly 0.9; in turn, these fabrics have a significant contribution to absorb and/or transmit thermal energy toward human skin. The thermal energy transmitted through a fabric system comes in direct contact with the skin and may generate a burn injury. Also, thermal energy absorbed inside the fabric system can move toward the wearer's skin and generate a burn injury. Normally, thick fabric systems provide higher protection against thermal exposure because they contain more trapped air than thin fabric systems. The trapped air volumes act as an insulator, lowering the transmissivity of the fabric system; hence, reducing the penetration rate of thermal energy from the fabric system toward the skin. Adding a moisture barrier and a thermal liner to a shell fabric will substantially increase wearers' protection by increasing the number of air layers and the trapped air volume. Although a triple-layered fabric system might contain more air between its layers than a single-layered fabric contains in its pores, the insulating effect of the additional air space might be compromised by the increase in thermal energy that can be stored inside the fabric layers. This stored energy might also be transmitted toward the wearer's skin over time. This energy would transmit regardless of whether the fabric is compressed or not. As fabrics usually get compressed at various locations (elbows, knees) when the wearer moves, this compression may reduce the second-degree burn time or thermal protective performance of the fabric system ([Song, et al., 2011a](#); [Song, et al., 2011b](#)). Interestingly, as the R^2 values between fabric thickness and second-degree burn time in flame and radiant heat exposures are 0.92 and 0.98, respectively (Figure 10), this infers that fabric thickness may be more strongly related to thermal protective performance (second-degree burn time) in radiant heat exposure compared to flame exposure. This is because

in radiant heat exposure thermal energy is mostly transmitted through the fabric system (Torvi & Threlfall, 2006) while in flame exposure, thermal energy imposed on the surface of the fabric system mainly spreads horizontally and/or bounces back to the environment depending upon the configuration of the exposure (e.g., angle of flame impingement, intensity of flame). Therefore, fabric thickness plays a more significant role in heat or thermal energy transmission to the wearer in radiant heat exposure than in flame exposure.

Furthermore, it can be identified from Figure 10 that the R^2 in the hot surface contact ($R^2=0.67$) exposure is much lower than the flame ($R^2=0.92$) and radiant heat ($R^2=0.98$) exposures. At any given thickness, the second-degree burn time in hot surface contact exposure is also much lower than the flame and radiant heat exposures. To explain these phenomena, it is necessary to understand the behavior of thermal energy imposed on a fabric system in a hot surface contact exposure (Figure 11). Figure 11 shows that a physical contact establishes between the hot surface and the fabric system in a hot surface contact exposure. The contact resistance between the fabric system and the hot surface may vary depending on the surface roughness of the fabric system (Figure 12). A fabric system with a rough surface (i.e., with high contact resistance or a high static frictional coefficient) will have a tiny air gap at the interface between the fabric system and the hot surface, which reduces the thermal energy transfer inside the fabric system. A smooth fabric system surface (i.e., with a low contact resistance or low static frictional coefficient) allows good thermal contact between the hot surface and the fabric system, increasing the thermal energy transfer inside the fabric system. In the hot surface contact exposure, compression of the fabric system also decreases the air volume in the fabric. Absence of an air phase inside a compressed fabric system (between the wearer's skin and a hot surface contact) lowers the thermal insulation of the fabric system; hence, the second-degree burn time

or thermal protective performance is decreased. When the solid fiber phase inside the fabric system predominates, the thermal conductivity of the fabric system is enhanced and its extinction coefficient (i.e. how strongly the fabric system absorbs thermal energy) becomes high. Thermo-physical properties (e.g., density, volumetric heat capacity) of the fabric system may also change depending on the compression in the fabric system (Shalev & Barker, 1983). The rapid transmission of thermal energy through a compressed fabric system generates a quick burn on the wearer's skin. Contact resistance between the fabric system and the wearer's skin is also reduced with fabric compression, and this situation aggravates the thermal energy transmission toward the skin.

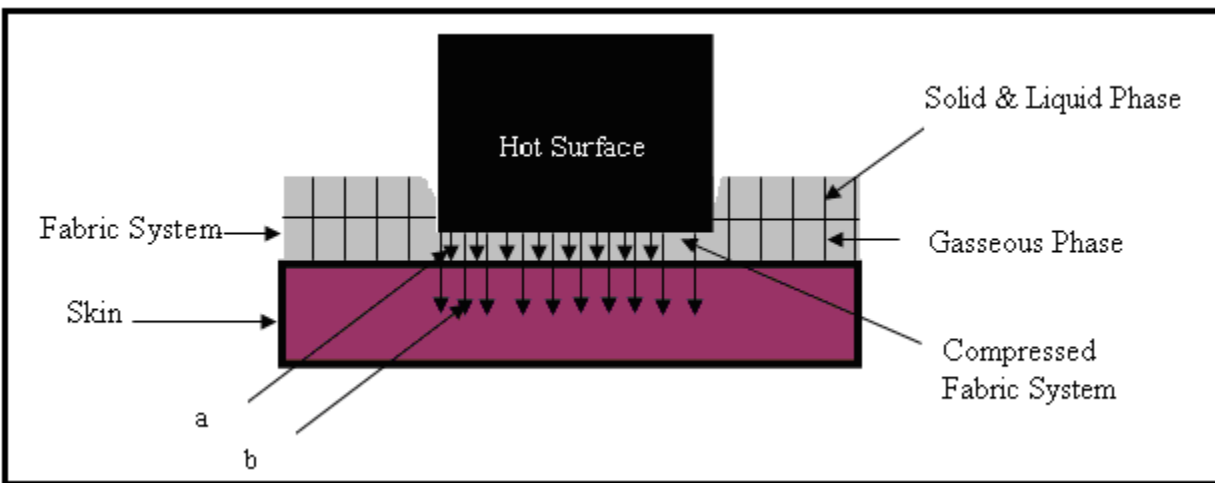


Figure 11. Behavior of thermal energy imposed on a fabric system in a hot surface contact exposure (a = absorbed thermal energy, b = transmitted thermal energy)

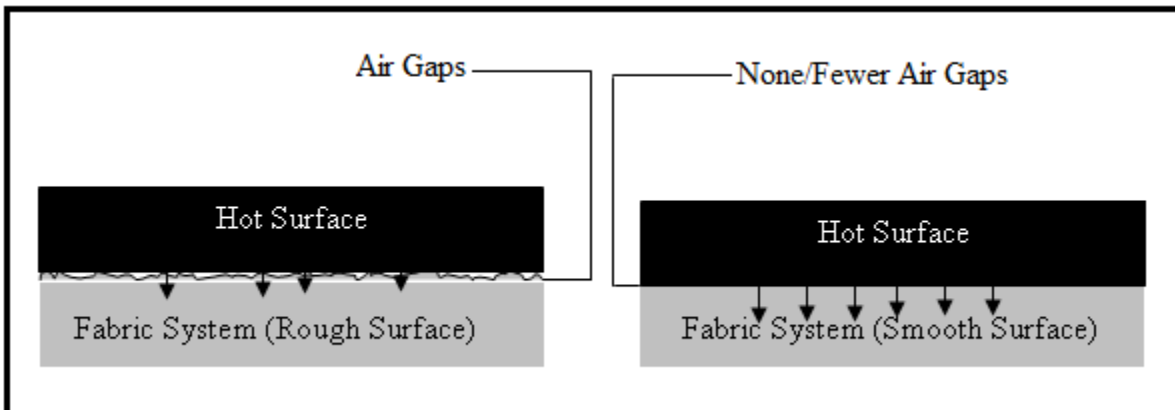


Figure 12. Thermal energy transfer through the interface between hot surface contact and fabric system

Fabric systems AEC and EAC have the same thickness but the thermal protective performance of AEC is almost twice that of EAC in hot surface contact exposure (Table 3). This is because in the EAC fabric system, the moisture barrier is present in the outer layer, whereas, in the AEC fabric system the moisture barrier is present in the inner layer. The moisture barrier in the EAC fabric system was in direct contact with the hot surface. In particular, the polyurethane coated side of the moisture barrier contacted the hot surface and was noted to catch fire and melt easily. This is because the ignition temperature of polyurethane, which is reported to be (~370°C) (Bryner, Madrzykowski, & Grosshandler, n.d.; Klyosov, 2007, p. 480) is lower than the temperature of the hot surface and lower than the ignition temperature of Kevlar[®]/PBI shell fabric (~700°C). Melting or ignition of the moisture barrier does not maintain the integrity of the fabric system, which enhances the transfer of thermal energy toward the skin, reducing the time required to generate a second-degree burn. A molten surface on moisture barrier also reduces the contact resistance between the hot surface and the fabric system; in turn, causing the poor thermal protective performance of the fabric system. These phenomena are less pronounced for the AEC fabric system as the outer layer in this fabric system comprises a Kevlar[®]/PBI fabric that has high ignition temperature (~600°C) and high surface roughness; consequently, the integrity of the fabric system is maintained and it efficiently slows down heat flow toward the skin. The findings for fabric systems AE and EA can be similarly compared; these fabric systems have the same thickness and air permeability but the burn time is higher (i.e., higher protection) for AE than EA (Table 3) due to the position of the moisture barrier which is in the inner layer of AE and in the outer layer of EA (notably, in EA fabric system, the polyurethane coated side of moisture barrier gets exposed to hot surface contact). For flame exposure, the position of the polyurethane coating in the AEC and EAC fabric systems had minimal effect on the thermal

protective performance. In this test, the specimen is engulfing in flame, preventing observations of the fabric surface during the test exposure, but is thought that much of the thermal energy from the flame is diverted away from the fabric surface. The ignitability of the polyurethane coated moisture barrier is insignificant and the integrity of the EAC fabric system is maintained similar to the AEC fabric system. As a consequence, the thermal protective performance of EAC fabric system does not differ significantly from AEC fabric system in the flame exposure.

4.1.2 Thermal protective performance in steam, hot-water splash, and hot-water immersion with compression exposures

The thermal protective performances of the selected fabric systems were measured in terms of second-degree burn time under steam, hot-water splash, and hot-water immersion with compression exposures. These thermal protective performances or second-degree burn times are shown in Table 5.

Table 5. Thermal Protective performance (second-degree burn time in seconds) in steam, hot-water splash, and hot-water immersion with compression exposures

Fabric construction	Fabric systems	Second-degree burn time in seconds						
		Steam	Hot-water splash	Hot-water immersion with compression				
				56 kPa 75°C	56 kPa 85°C	56 kPa 95°C	14 kPa 85°C	28 kPa 85°C
Single-layered	A	0.40	2.70	5.29	3.63	2.05	4.26	4.31
Double-layered	AB	0.60	4.37	6.19	5.82	2.74	6.69	5.92
	AD	0.94	7.28	5.96	6.49	2.78	6.67	6.29
	AE	7.99	60.39	29.99	11.31	9.53	19.72	19.05
	EA	10.38	63.40	32.68	21.57	16.84	23.16	22.96
Triple-layered	AEB	11.51	78.09	57.06	35.12	22.70	40.00	38.10
	AEC	19.31	109.26	48.58	36.25	24.45	36.11	39.52
	AED	21.22	136.07	63.20	42.84	29.84	46.54	44.62
	EAC	25.63	119.57	52.64	40.35	26.04	43.89	42.97

To characterize the textile fabric systems in steam, hot-water splash, and hot-water immersion with compression exposures, their physical properties (thickness, air permeability,

thermal resistance, and evaporative resistance) and second-degree burn times in a particular exposure were normalized following the procedure indicated in section 3.3 titled “Procedure to analyze the experimental results”. After the normalization, t-tests were carried out to analyze the association between fabric system properties and second-degree burn times. Results obtained from the t-tests (T-stat and P-value) are presented in Table 6.

Table 6. Results of t-tests between fabric system properties and second-degree burn times in steam, hot-water splash, and hot-water immersion with compression exposures

Fabric system properties	Second-degree burn time in seconds													
	Steam		Hot-water splash		Hot-water immersion with compression									
					56 kPa 75°C		56 kPa 85°C		56 kPa 95°C		14 kPa 85°C		28 kPa 85°C	
	T-Stat	P-value	T-Stat	P-value	T-Stat	P-value	T-Stat	P-value	T-Stat	P-value	T-Stat	P-value	T-Stat	P-value
Thickness	2.07	0.07	2.05	0.08	1.86	0.09	2.47	0.04	2.11	0.07	2.18	0.07	2.18	0.06
Air permeability	-3.63	0.004	-4.71	0.002	-5.12	0.001	-3.54	0.009	-4.34	0.003	-4.37	0.003	-4.47	0.002
Thermal resistance	1.66	0.14	1.67	0.13	1.44	0.19	1.91	0.10	1.67	0.14	1.69	0.13	1.68	0.14
Evaporative resistance	4.67	0.002	6.74	0.003	8.20	0.0001	5.78	0.0007	6.78	0.0003	7.30	0.0002	7.32	0.0002

According to Table 6, P-values for air permeability and evaporative resistance are less than 0.05; thus, air permeability and evaporative resistance significantly affect fabrics' thermal protective performance in steam, hot-water splash, and hot-water immersion with compression exposures. Although the P-values of thickness (≤ 0.09) are higher than 0.05, thickness is still considered one of the significant properties in steam and hot-water protection (Rossi, et al., 2004). This is because fabric thickness plays an important role in preventing heat transfer through fabric systems. However, thickness may not be so pertinent in steam, hot-water splash, and hot-water immersion with compression exposures since mass transfer occurs through the fabric systems and is the primary cause of skin burn injury. Fabric air permeability and evaporative resistance are more important than thickness when mass transfer (hot-water) results in a skin burn (Keiser, et al., 2010; Keiser, et al., 2008), thus, air permeability and evaporative resistance of the fabric system are expected to be more significant properties in steam, hot-water splash, and hot-water immersion with compression exposures. In Table 6, the T-stat values for thickness and air permeability are positive and negative respectively, indicating that as thickness increases, the time to a second-degree burn also increases, whereas an increase in the air permeability results in a decrease in the time to a second-degree burn. As thick fabric systems provide more thermal insulation than thin fabric systems (Song, et al., 2011a; Song, et al., 2011b), heat transfer is lower and second-degree burn time is higher in thick fabric systems compared to thin fabric systems. However, the presence of air pores in a highly air-permeable fabric system may enhance the transfer of mass and thus reduce the time requirement for a second-degree burn. For example, although the AD fabric system is thicker than the AE fabric system, the second-degree burn time of AD fabric system is less than that of the AE fabric system (Table 5). This difference in second-degree burn times is because the air permeability of

the AD fabric system is higher than the air permeability of the AE fabric system. Furthermore, according to Table 6, P-values of fabric thickness (0.07, 0.08, 0.09, 0.04, 0.07, 0.07, and 0.06) are higher than P-values of fabric air permeability (0.008, 0.002, 0.001, 0.009, 0.003, 0.003, and 0.002), indicating that fabric thickness is a less significant property than fabric air permeability in providing protection against steam and hot-water exposures. These findings can be rationalized by the observation that heat transfer is less expedient than mass transfer in steam, hot-water splash, and hot-water immersion with compression exposures (Keiser, et al., 2010; Keiser, et al., 2008; Keiser & Rossi, 2008). As the P-values of fabric thickness are marginally higher than 0.05 and P-values of fabric air permeability are significantly less than 0.05, it can be inferred that thickness has a minor/marginal impact on thermal protective performance while air permeability has a strong impact on thermal protective performance. The association between air permeability and second-degree burn time under steam, hot-water splash, and hot-water immersion with compression exposures (at a temperature of 75°C and pressure of 56 kPa) are depicted in Figures 13, 14, and 15, respectively. By reflecting on the data in Table 5, it is expected that a similar association could be found under hot-water immersion with compression at other temperatures (85°C and 95°C) and pressures (14 kPa and 28 kPa) as well.

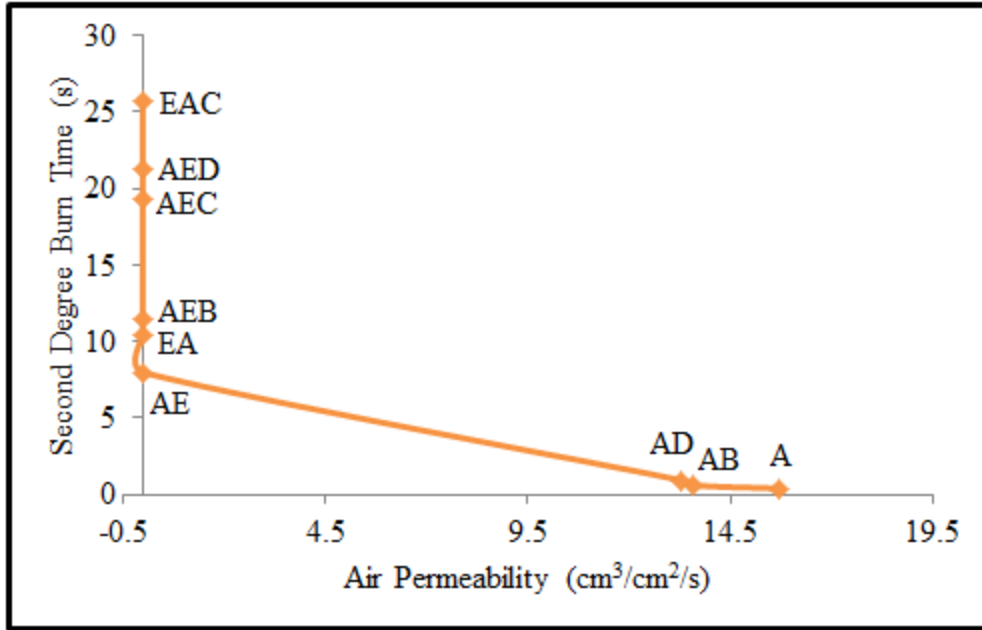


Figure 13. Association between air permeability and second-degree burn time in steam

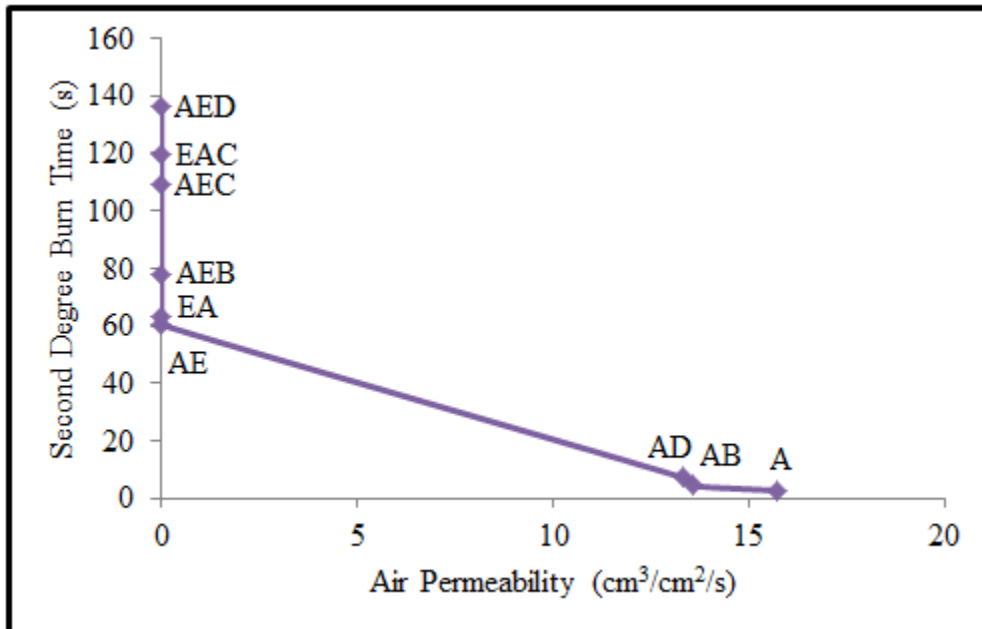


Figure 14. Association between air permeability and second-degree burn time in hot-water splash

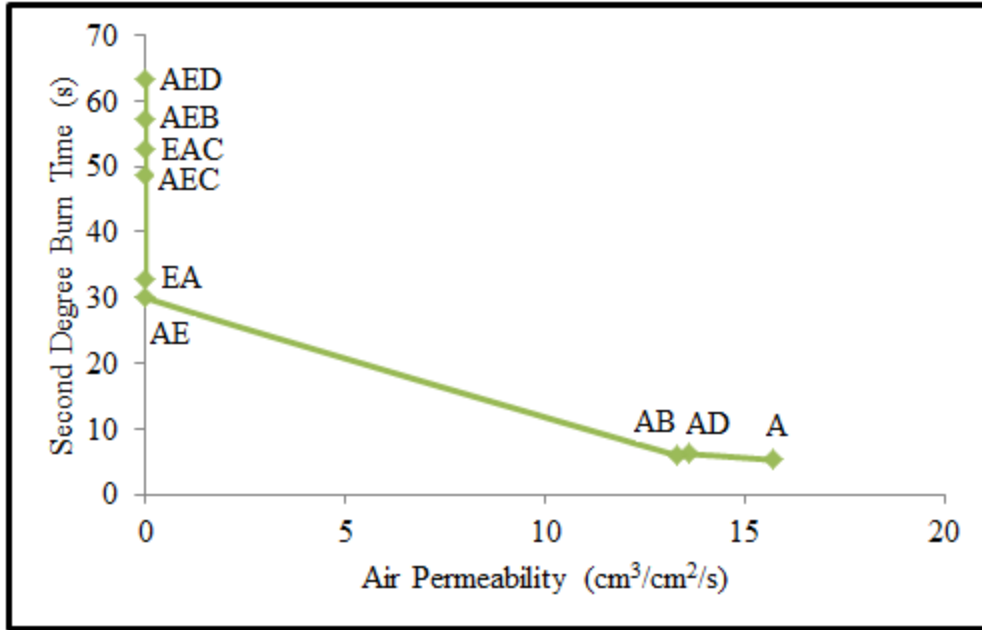


Figure 15. Association between air permeability and second-degree burn time in hot-water immersion with compression at a pressure of 56 kPa and temperature of 75°C

According to Figures 13, 14, and 15, fabric systems with zero air permeability (AE–EAC) show greater second-degree burn times than the fabric systems with higher (> 0) air permeability (A, AB, AD). An inference test confirmed that the second-degree burn time of a fabric system with zero air permeability (an air-impermeable fabric system) is significantly higher than the second-degree burn time of a fabric system with higher air permeability (an air-permeable fabric system). This observation can be explained based on the Darcy’s Law, which associates the mass (steam or water) transfer through a porous medium (fabric system) with other parameters according to the following equation:

$$Q = \frac{-KA(Pb - Pa)}{\mu L} \dots\dots\dots \text{Equation 8}$$

where,

Q = the total discharge of steam or water per unit time (m³/s),

K = fabric permeability (m²),

A = cross sectional area of mass flow (m^2),

P_a = pressure of the steam or hot-water jet (Pa),

P_b = pressure of the steam or hot-water jet after passing through the fabric system (Pa),

μ = viscosity (Pa.s), and

L = fabric thickness (m).

It seems that air-impermeable fabric systems (AE–EAC) do not allow the transfer of steam or water through the fabric systems. As a result, the time requirement for second-degree burn increases and that enhances the thermal protective performance of the air-impermeable fabric systems. From another point of view, as the porosity and tortuosity of an air-impermeable fabric system are very low and high, respectively, the flux or flow of steam or water through the air-impermeable fabric system should also be negligible according to Fick’s law, shown in Equation 9. This low flux or flow of steam or water resulted in comparatively high second-degree burn times in the case of the air-impermeable fabric systems.

$$J = -\frac{D\varepsilon_t\gamma}{\tau} \frac{(C_2 - C_1)}{\delta} \dots\dots\dots \text{Equation 9}$$

where,

J = the flux or flow of mass through the fabric ($mol/m^2.s$),

D = mass diffusion coefficient (m^2/s),

ε_t = porosity of the fabric (dimensionless),

γ = constrictivity of the steam or water (dimensionless),

τ = tortuosity of the fabric (dimensionless),

C_2 = concentration of the steam or water after passing through the fabric (mol/m^3),

C_1 = concentration of the steam or water before passing through the fabric (mol/m^3), and

δ = thickness of the fabric (m) (Cussler, 2009; Kothandaraman, 2006).

Although the AE/EA fabric systems are air-impermeable, their second-degree burn times are significantly lower than the second-degree burn times of the other air-impermeable fabric systems (e.g., AEB, EAC) (Figures 13, 14, and 15). The AE/EA fabric systems are the thinnest of all the air-impermeable fabric systems, and consist of only two layers (Table 2). The triple-layered, thick fabric systems (e.g. AEB, EAC) provide better protection than the double-layered, thin fabric systems (e.g., AE/EA). This is quite reasonable because both hot-water splash and steam apply a certain amount of pressure/load, which ultimately compresses the fabric system, reducing air volumes inside the fabric systems and lowering the thermal insulation afforded by air. Also, fabric systems were tested in compressed condition (on a perforated hot metal surface) in the hot-water immersion and compression exposures, which ultimately lowered the thermal insulation of the fabric systems. In the compressed stage, a triple-layered, thick fabric system contains more air than a double-layered, thin fabric system. As a result, the thermal protective performance of a triple-layered, thick fabric system is better than a double-layered, thin fabric system, especially when heat transfer occurs with steam and hot-water exposures ([Ackerman, et al., 2012](#); [Mandal, et al., 2013a](#); [Song, et al., 2011a](#)). Contact with high pressurized steam, hot-water, and/or perforated hot metal surface might cause thermo-physical properties of the fabric system (e.g., surface tension, thermal conductivity, heat capacity) to change, allowing steam and hot-water to enter the fabric system more easily and thus increasing the chances of scald burns on the wearer. Triple-layered, thick fabric systems can store more hot-water than double-layered, thin fabric systems and would be expected to generate skin burns more slowly. On entering a fabric system, steam may condense into hot-water (Figure 16), and generate scald burns on the wearer ([Keiser, et al., 2008](#); [Shoda, Wang, & Cheng., 1998](#)). In a triple-layered, thick fabric

system, this condensation may occur far away from the skin causing less burn injury than may occur in a double-layered, thin fabric system.

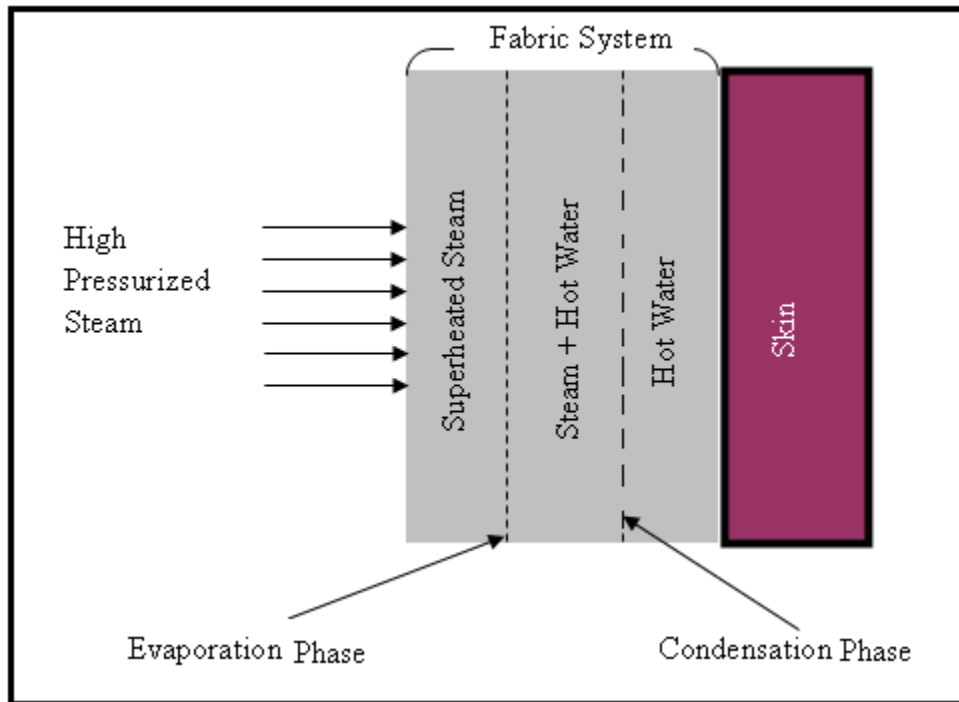


Figure 16. Proposed behavior of high pressurized steam inside a fabric system

The presence of a thermal liner also affects the second-degree burn time or thermal protective performance of multi-layered, thick, impermeable fabric systems. For example, the two outermost layers of the AE (double-layered) and the AEB/AEC/AED (three-layered) fabric systems are the same: shell fabric (A) and moisture barrier (E). However, the AEB/AEC/AED fabric systems comprise an extra layer of thermal liner (B/C/D) in their innermost part (in contact with the wearer's skin). Due to this added thermal liner, the thermal insulation property of the AEB/AEC/AED fabric systems is higher than that of the AE fabric system. Consequently, the AEB/AEC/AED fabric systems can resist heat transfer more effectively than the AE fabric system; that is, the second-degree burn times or thermal protective performances of the AEB/AEC/AED fabric systems are higher than the thermal protective performance of the AE fabric system. The thickness of a thermal liner is also important to thermal protective

performance. For example, there is a gradual increase in the thickness of the thermal liners in AEB, AEC, and AED fabric systems. Thus, the overall thicknesses of AEB, AEC, and AED fabric systems also gradually increase. As expected, thermal protective performance generally increases in the order of AEB, AEC, and AED under all types of thermal exposures. Notably, the thermal protective performance of AEB fabric system is higher than AEC fabric system in a few hot-water immersion and compression exposures, where the water temperature (75°C) or compression pressure (14 kPa) are low. This may be because of the structural difference between the thermal liners B and C. The thermal liner B comprises two thin Nomex[®] oriented webs along with a plain weave Nomex[®] fabric layer, whereas, the thermal liner C comprises one Nomex[®] needle-felted batt along with a plain weave Nomex[®] fabric layer (Table 1).

It has also been found that impermeable fabric systems comprising the same number of layers (double-layered or triple-layered) and thickness show significant differences in second-degree burn time under steam, hot-water splash, and hot-water immersion with compression exposures (P-value < 0.05) (Figures 13, 14, and 15). Although AE and EA fabric systems have the same number of layers and thickness, the thermal protective performance of the EA fabric system is higher than that of the AE fabric system in these exposures (Table 5). Similar observations can be made for AEC and EAC fabric systems where, although the fabric systems are of same thickness, the thermal protective performance of the EAC fabric system is higher than that of the AEC fabric system in these exposures (Table 5). These results can be rationalized by considering the difference in position of the moisture barrier in the protective fabric systems. To understand these results, heat and mass transfer are depicted (Figure 17) through two differently configured impermeable fabric systems comprising the same number of layers and the same thickness: System 1 comprises a moisture barrier in its outermost layer; System 2

comprises a shell fabric in its outermost layer and the moisture barrier in its innermost layer. In Figure 17, Systems 1 and 2 shows that incoming steam or hot-water is deflected from the moisture barrier upon contact. If the moisture barrier is in the outermost layer of the fabric system (System 1), much of the mass hazard is deflected away long before it reaches the wearer's skin. If the moisture barrier is in the innermost layer of the fabric system (System 2), the steam or hot-water is transmitted close to the wearer's skin. Thus, a burn injury is less likely to happen in System 1 that is analogous to fabric systems EA and EAC than in System 2 that is analogous to fabric systems AE and AEC. Contextually, it is interesting that the effects of the moisture barrier position in steam and hot-water exposures are opposite to the hot surface contact exposure. This opposite behaviour is most likely due to the different thermal energy transfer mechanisms in hot surface contact exposure versus steam and hot-water exposures.

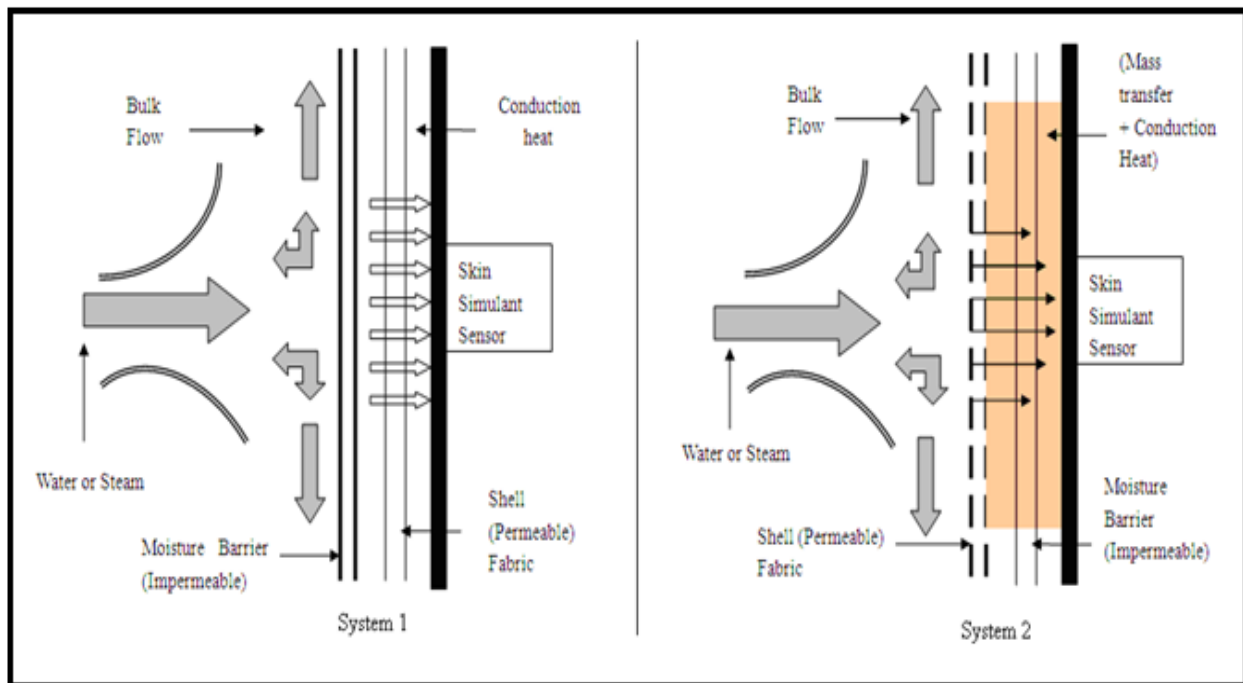


Figure 17. Heat and mass transfer mechanisms through fabric systems in steam and hot-water exposures

Furthermore, in the case of steam and hot-water splash exposures, the P-values of air permeability and evaporative resistance are considerably close (Table 6). Essentially, fabric air

permeability and evaporative resistance have similar effects on second-degree burn time. However, the data in Table 6 demonstrate that P-values of air permeability are much higher than the P-values of evaporative resistance under hot-water immersion with compression exposures (at different temperatures and pressures). This indicates that evaporative resistance is a highly significant property affecting second-degree burn time in hot-water immersion with compression exposures. Relationships between fabric evaporative resistance and second-degree burn time at different temperatures and pressures are shown in Figure 18 to individually explain and compare the exposures in detail.

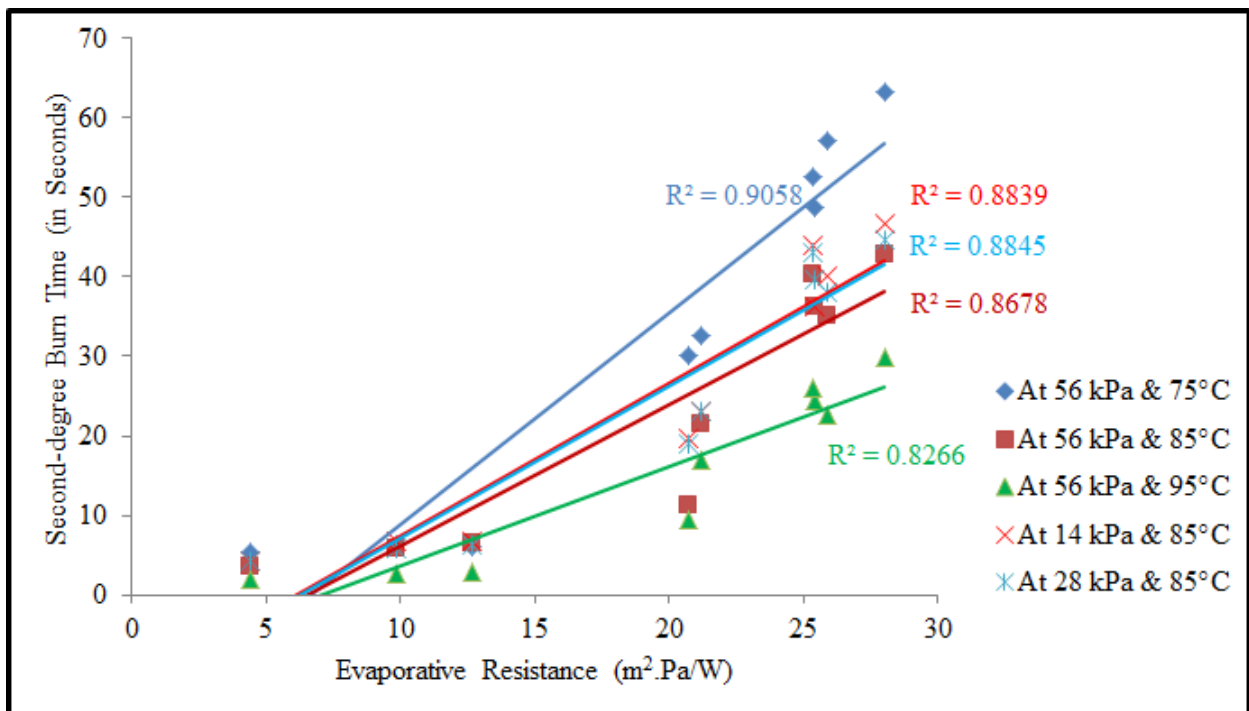


Figure 18. Relationship between fabric evaporative resistance and second-degree burn time in hot-water immersion with compression exposure of different temperatures and pressures

According to Figure 18, it is clear that R^2 values between evaporative resistance and second-degree burn times are different at different temperatures (75°C, 85°C, and 95°C) and constant pressure (56 kPa). From Figure 18, it is also evident that R^2 values are gradually decreasing with increasing temperatures. It means that evaporative resistance has a different

level of impact on second-degree burn time at different temperatures and it has the maximum impact at the lowest temperature (e.g., 75°C) in comparison to the highest temperature (e.g., 95°C). Basically, evaporative resistance controls the amount of mass (hot-water) transfer through a fabric system; hence, it does control the thermal protective performance (second-degree burn time) of the fabric systems. At low temperatures, a fabric system with high evaporative resistance may not allow significant mass transfer through the fabric system and this can increase the second-degree burn times or enhance the thermal protective performance of the fabric system. However, the water molecules (in the hot-water bath) spread slightly further apart from each other and their speed elevates at high temperatures. In this situation, water molecules can easily or forcefully penetrate through the fabric system. Eventually, evaporative resistance has less impact on second-degree burn time or thermal protective performance of the fabric system at high temperatures. Additionally, Figure 18 confirms that the second-degree burn times of the fabric systems are generally lower at the high temperatures in comparison to the low temperatures. This is because of the comparatively easy and quick penetration of water molecules through fabric systems at the high temperatures. Interestingly, it is also evident from Figure 18 that R^2 values between evaporative resistance and second-degree burn time are similar at different pressures (14 kPa and 28 kPa) and at constant temperature (85°C). From this, it can be inferred that the changes of pressure do not affect the amount of water molecules penetration through the fabric systems. As a consequence, evaporative resistance has a similar effect on second-degree burn time at different pressures. In this context, it is notable that the second-degree burn time at 28 kPa is slightly lower than the second-degree burn time at 14 kPa. This is because the fabric systems get highly compressed against the perforated hot metal surface at high pressure (28 kPa) (Figure 8). During the compression, the conductive heat transfer (q)

predominates through the fabric systems based on Equation 10 (Lienhard & Lienhard, 2011; Song, 2009),

$$q = \frac{\Delta_{HF}}{\Delta X_H / (k_H A) + 1 / (h_{HF} A) + \Delta X_F / [(1 - \frac{V_A}{V_F})k_\gamma + \frac{V_A}{V_F} k_\alpha] A} \dots\dots\dots \text{Equation 10}$$

where,

Δ_{HF} = temperature difference between the hot surface and the fabric (K),

ΔX_H = thickness of the hot surface (m),

k_H = thermal conductivity of the hot surface (W/m.K),

A = contact area between the hot surface and the fabric (m^2),

$1/h_{HF}$ = thermal contact resistance between the hot surface and the fabric depending upon their surface roughness ($m^2.K/W$),

ΔX_F = thickness of the fabric (m),

V_A = air volume of the fabric (m^3),

V_F = volume of the fabric (m^3),

k_γ = thermal conductivity of the solid fiber phase of the fabric (W/m.K), and

k_α = thermal conductivity of the gaseous air phase of the fabric (W/m.K).

This conductive heat transfer may cause significant burns on wearers. At high compression, the thickness of the fabric systems and the trapped dead air within the fabric systems tremendously decrease, which ultimately increases the thermal conductivity of the fabric systems. This increase in thermal conductivity causes more heat transfer through the fabric systems and lowers their thermal protective performance. This high compression also lowers the surface roughness of the fabric system resulting in low trapped air layers on the surface. This situation lowers the second-degree burn time or thermal protective performance of the fabric systems. In this context, Mandal, et al. (2015) mention that the conductive heat transfers is more

prominent in the hot-water immersion with compression exposure than the typical hot-water splash exposure. They concluded that the transfer of both mass and conductive heat through fabrics significantly lower the second-degree burn times or thermal protective performance of the fabric systems under hot-water immersion with compression in comparison to the hot-water splash. Contextually, it has also been observed that the differences in second-degree burn times or thermal protective performance under hot-water splash and hot-water immersion with compression (at different temperatures and compression pressures) are not significant for single-layered fabric systems; however, these differences are significant for triple-layered fabric systems. This is likely because changes in the thermo-physical properties (e.g., density, thermal conductivity, volumetric heat capacity) of the triple-layered fabric systems under hot-water splash and hot-water immersion with compression (at different temperatures and compression pressures) are more significant than in the single-layered fabric systems.

4.2 Empirical analysis of thermal protective performance of fabrics under various thermal exposures

Based on the discussion in Section 4.1, it is clear that the thermal protective performance of fabric systems varies under different thermal exposures. This section 4.1 further identifies different significant fabric properties that affect thermal protective performance under these thermal exposures. Thickness and thermal resistance are the significant fabric properties that affect thermal protective performance under flame, radiant heat, and hot surface contact exposures. Fabric thickness, air permeability, and evaporative resistance are the significant properties that affect thermal protective performance under steam, hot-water splash, and hot-water immersion with compression exposures. These significant fabric properties for thermal protective performance under these thermal exposures are summarised in Table 7.

Table 7. Significant fabric properties that affected thermal protective performance under various thermal exposures

Thermal protective performance	Significant fabric properties			
	Thickness	Air permeability	Thermal resistance	Evaporative resistance
Flame	✓		✓	
Radiant heat	✓		✓	
Hot surface contact	✓		✓	
Steam	✓	✓		✓
Hot-water splash	✓	✓		✓
Hot-water immersion with compression	✓	✓		✓

In the following sections, by employing these significant fabric properties (Table 7), thermal protective performance of a fabric system under a specific thermal exposure is predicted using MLR and ANN modelling techniques (sections 4.2.1 and 4.2.2). Subsequently, these MLR and ANN models are compared to identify the best fit models for predicting thermal protective performance (section 4.2.3). The best fit models are further used in the saliency test to identify the relevance or relative importance of each significant property on the thermal protective performance of a fabric system in a particular thermal exposure (section 4.2.4).

4.2.1 MLR models

The MLR models for predicting the thermal protective performance of fabric systems under various thermal exposures [(e.g., flame, radiant heat, hot surface contact, steam, hot-water splash, hot-water immersion with compression at different temperatures (75°C, 85°C, and 95°C) and pressures(14 kPa and 28 kPa)] are presented in Equations 11-20. In these models, the respective fabric properties that significantly affected the thermal protective performance of fabric systems under a particular thermal exposure were employed in StatCrunch™ 5.0 software according to the MLR modelling method described in section 3.3.1.

$$(\text{Performance})_{\text{Flame}} = 0.45 + 4.70 \times \text{Thickness} - 1.61 \times \text{Thermal resistance} \dots\dots\dots \text{Equation 11}$$

$$(\text{Performance})_{\text{Radiantheat}} = -0.46 + 6.64 \times \text{Thickness} - 1.53 \times \text{Thermal resistance} \dots \text{Equation 12}$$

$$(\text{Performance})_{\text{Hot surface}} = 1.02 + 5.61 \times \text{Thickness} - 55.69 \times \text{Thermal resistance} \dots \text{Equation 13}$$

$$(\text{Performance})_{\text{Steam}} = -5.09 + 1.13 \times \text{Thickness} + 0.07 \times \text{Air permeability} + 0.75 \times \text{Evaporative resistance} \dots \text{Equation 14}$$

$$(\text{Performance})_{\text{Hot-water splash}} = -25.47 + 3.57 \times \text{Thickness} + 0.12 \times \text{Air permeability} + 4.59 \times \text{Evaporative resistance} \dots \text{Equation 15}$$

$$(\text{Performance})_{\text{Immersion (75° C)}} = -9.07 - 0.11 \times \text{Thickness} + 0.07 \times \text{Air permeability} + 2.36 \times \text{Evaporative resistance} \dots \text{Equation 16}$$

$$(\text{Performance})_{\text{Immersion (85° C)}} = -6.07 + 3.01 \times \text{Thickness} - 0.07 \times \text{Air permeability} + 1.20 \times \text{Evaporative resistance} \dots \text{Equation 17}$$

$$(\text{Performance})_{\text{Immersion (95° C)}} = -4.65 + 0.92 \times \text{Thickness} + 0.01 \times \text{Air permeability} + 0.98 \times \text{Evaporative resistance} \dots \text{Equation 18}$$

$$(\text{Performance})_{\text{Immersion (14kPa)}} = -6.01 + 1.57 \times \text{Thickness} - 0.02 \times \text{Air permeability} + 1.52 \times \text{Evaporative resistance} \dots \text{Equation 19}$$

$$(\text{Performance})_{\text{Immersion (28kPa)}} = -5.43 + 1.75 \times \text{Thickness} - 0.10 \times \text{Air permeability} + 1.45 \times \text{Evaporative resistance} \dots \text{Equation 20}$$

4.2.2 ANN models

In order to predict the thermal protective performance by ANN models, the ANN modelling method described in section 3.3.2 was followed. Here, the values of significant fabric properties for thermal protective performance under a particular thermal exposure (Table 7) were employed to code the computer programs for ANN models using MATLAB software. The coding of these software programs for ANN models is presented in Appendices 10-19. These coded programs were executed in the MATLAB software for predicting the thermal protective performance under each specified thermal exposure. A generic code for ANN models that can be used to predict thermal protective performance under various thermal exposures is presented below:

```

load dataset.txt;
input=dataset(1:9,1:2); % input data.
target=dataset(1:9,3); % target data.
[inputn,meani,stdi,targetn,meant,stdt] = prestd(input',target');
% preprocessing or normalizing the data with mean at zero and standard deviation 1.
M=[5 1]; %Size of ith layer, for NI layers.
net = newff(minmax(inputn),M,{'tansig','purelin'},'traingdm');
% creating the feedforward backpropagation (gradient descent with momentum) neural network.
% here newff defines feedforward network architecture.
% first argument minmax(inputn) defines range of input and initializes the network parameters.
% second argument defines the structure of the network. There is 1 hidden and 1 output layer.
% 5 is the number of the nodes in the first hidden layer.
% 1 is the number of nodes in the output layer.
% next the activation functions in the layers are defined.
% in the first hidden layer, there are 5 tansig functions.
% in the output layer, there is 1 linear function.
net.trainParam.epochs=3000; % number of epochs/iterations.
net.trainParam.lr=0.3; % learning rate.
net.trainParam.mc=0.6; % momentum.
net=train(net,inputn,targetn);
y=sim(net,inputn);
% to simulate the trained network on the original input data.
output=poststd(y,meant,stdt); % to convert output back to the original scale.
[output target] % predicted data vs actual data.
title('Comparison between actual targets and predictions')
d=[output-target].^2; % to calculate square error between actual and predicted values.
mse=mean(d) % to calculate the mean square error (mse).
rmse=sqrt(mse) % to calculate the root mean square error (rmse).
[m,b,r]=postreg(output',target') % use of regression analysis to judge the network performance.
Rsquare=r.^2 % to calculate the Coefficient of Determination ( $R^2$ ).
save net % to save the trained network 'net'.
load net % to load the trained network 'net'.
newinput = [3.49 0.151];
newinputn = trastd(newinput',meani,stdi);
newoutputn = sim(net,newinputn);
newoutput = poststd(newoutputn',meant,stdt)

```

4.2.3 Comparison between MLR and ANN models

In this section, the MLR and ANN models obtained (in sections 4.2.1 and 4.2.2) for predicting the thermal protective performance under each thermal exposure are statistically compared according to the method described in section 3.3. The predicting performance parameters [R^2 , Root Mean Square Error (RMSE), P-values] of these MLR and ANN models are presented in Table 8.

Table 8. The R^2 , RMSE, and P-values of the MLR and ANN models

Thermal exposure	Model	R^2	RMSE	P-value
Flame	MLR	0.95	1.43	< 0.0001
	ANN	0.97	0.91	
Radiant heat	MLR	0.98	1.16	< 0.0001
	ANN	0.99	0.69	
Hot surface contact	MLR	0.70	2.92	0.005
	ANN	0.82	2.16	
Steam	MLR	0.57	5.95	0.01
	ANN	0.97	1.53	
Hot-water splash	MLR	0.71	6.10	0.002
	ANN	0.98	2.41	
Hot-water immersion with compression (at 56 kPa and 75°C)	MLR	0.80	9.64	0.0002
	ANN	0.98	1.19	
Hot-water immersion with compression (at 56 kPa and 85°C)	MLR	0.76	7.35	0.0006
	ANN	0.97	2.01	
Hot-water immersion with compression (at 56 kPa and 95°C)	MLR	0.75	5.14	0.0006
	ANN	0.98	1.43	
Hot-water immersion with compression (at 14 kPa and 85°C)	MLR	0.80	6.97	0.0002
	ANN	0.98	1.87	
Hot-water immersion with compression (at 28 kPa and 85°C)	MLR	0.82	6.64	0.0001
	ANN	0.99	1.22	

Table 8 presents that the prediction models are valid as all of the P-values are less than 0.05. In a comparison between the MLR and ANN models under all thermal exposures [(i.e., flame, radiant heat, hot surface contact, steam, hot-water splash, hot-water immersion with compression at different temperatures (75°C, 85°C, and 95°C) and pressures (14 kPa and 28 kPa)], it can be identified that the R^2 values of MLR models are lower than the ANN models;

hence, the predictability of the ANN models works better than the MLR models. Moreover, the prediction errors (RMSE) by the ANN models are much lower than the MLR models. In summary, the ANN models perform better than the MLR models for thermal protective performance prediction in terms of the precision and accuracy. Thus, it is worthwhile to use the ANN models for predicting the thermal protective performance of the fabric systems under all types of thermal exposures.

4.2.4 Relative importance of each significant fabric property on thermal protective performance

Based on the previous section, it is clear that ANN models can effectively predict the thermal protective performance of fabric systems under various thermal exposures – flame, radiant heat, hot surface contact, steam, hot-water splash, and hot-water immersion with compression. In this section, these ANN models are used to analyze the relative importance of significant properties on thermal protective performance of fabric systems under all of these thermal exposures. For this, a saliency test is conducted by eliminating only one designated significant property from an ANN model at a time. In this test, the increase in RMSE value in the saliency test compared to the original model is considered as the indicator of importance of the eliminated significant property; the eliminated property that generates the highest RMSE is inferred as the prime significant property for thermal protective performance. The results of the saliency tests for all the ANN models are shown in Table 9.

Table 9. The results of saliency tests

Thermal protective performance	Excluded significant property	RMSE	% increase in RMSE	Rank
Flame	Thickness	0.95	4.40	1
	Thermal resistance	0.92	1.10	2
Radiant heat	Thickness	0.69	0.00	2
	Thermal resistance	0.77	11.59	1
Hot surface contact	Thickness	2.18	0.92	2
	Thermal resistance	2.56	18.52	1
Steam	Thickness	3.42	123.53	1
	Air permeability	1.60	4.58	2
	Evaporative resistance	1.59	3.92	3
Hot-water splash	Thickness	11.49	376.76	1
	Air permeability	2.60	7.88	2
	Evaporative resistance	2.54	5.39	3
Hot-water immersion with compression (at 56 kPa and 75°C)	Thickness	1.46	22.69	3
	Air permeability	1.79	50.42	2
	Evaporative resistance	2.47	107.56	1
Hot-water immersion with compression (at 56 kPa and 85°C)	Thickness	2.18	8.46	3
	Air permeability	2.42	20.40	2
	Evaporative resistance	2.65	31.84	1
Hot-water immersion with compression (at 56 kPa and 95°C)	Thickness	1.80	25.87	1
	Air permeability	1.61	12.59	2
	Evaporative resistance	1.80	25.87	1
Hot-water immersion with compression (at 14 kPa and 85°C)	Thickness	1.99	6.42	2
	Air permeability	1.96	4.81	3
	Evaporative resistance	2.37	26.74	1
Hot-water immersion with compression (at 28 kPa and 85°C)	Thickness	1.47	20.49	1
	Air permeability	1.23	0.82	3
	Evaporative resistance	1.29	5.74	2

Based on Table 9, it is notable that the thickness of fabric systems dominates over the thermal resistance for predicting thermal protective performance under flame exposure; whereas, thermal resistance of fabric systems dominates over the thickness for predicting thermal protective performance under radiant heat and hot surface contact exposures. Thus, thickness is the most important property for predicting thermal protective performance under flame exposure, and thermal resistance primarily affects the prediction of thermal protective performance under radiant heat and hot surface contact exposures. As the modes of heat transfer in these exposures

are different, it is expected that different properties could predominantly contribute in predicting thermal protective performance under these exposures. Furthermore, thickness and air permeability of fabric systems dominates over evaporative resistance during the prediction of thermal protective performance under steam and hot-water splash exposures. In the exposures of hot-water immersion with compression at 75°C and 85°C, evaporative resistance and air permeability of fabric systems predominate over thickness for predicting thermal protective performance; however, thickness and evaporative resistance primarily affect the prediction of thermal protective performance under the exposures of hot-water immersion with compression at 95°C, 14 kPa, and 28 kPa. Here, thickness and evaporative resistance have the same contribution in predicting thermal protective performance at 95°C. Also, the predominance of thickness and evaporative resistance are completely reversed in the exposures of hot-water immersion with compression at 14 kPa and 28 kPa. It is also notable from Table 9 that the percentage (%) increase in RMSE is generally high in the case of steam, hot-water splash, and hot-water immersion with compression exposures in comparison to the flame, radiant heat, and hot surface contact exposures. This difference is because mass transfer primarily occurs in the case of steam, hot-water splash, and hot-water immersion with compression exposures; whereas, heat transfer predominates in the case of flame, radiant heat, and hot surface contact exposures.

Chapter 5

Summary and Conclusion

In this PhD study, the thermal protective performance of textile fabrics used in firefighters' clothing was investigated under various laboratory-simulated thermal exposures – flames, radiant heat, hot surface contact, steam, hot-water splash, and hot-water immersion with compression. For this, the thermal protective performance of the fabrics with different physical properties was evaluated in terms of time required to generate a second-degree burn on a wearer's skin. Subsequently, various fabric properties affecting the performance were statistically identified and the reasons for the importance of these fabric properties were explained according to theories of heat and mass transfer through fabrics. By employing the significant fabric properties, MLR and ANN models were used to predict and explain the thermal protective performances of the fabrics under the thermal exposures.

The findings from this study demonstrate that thermal protective performance of fabric systems varies according to the characteristics of the fabric systems and the type of thermal exposures. The thickness of a fabric system primarily controls its thermal protective performance in flame and radiant heat exposures. Insulation from flame and radiant heat exposures is found to be provided by air volumes inside the fabric system that prohibited thermal energy transfer to the sensor (i.e., human skin). In other exposures (i.e., hot surface contact, high pressurized steam, hot-water splash, and hot-water immersion with compression), a certain amount of pressure is imposed on the fabric system. This pressure caused fabric compression which reduced both the contact resistance between the fabric system and the sensor (human skin) and the air volume insulation provided by fabric system, enhancing heat transfer toward the sensor and reducing the protective performance of the fabric system. Thermo-physical properties (e.g., thermal

conductivity, heat capacity) of the fabric systems did change in various thermal exposures. Hence, fabric systems may char or pyrolyze, reducing their thermal protective performance. In addition to the heat delivered in steam and hot-water (splash, and immersion with compression) exposures, mass transfer through the fabric system may present another primary concern. The study suggests that impermeable fabric systems can reduce mass transfer and enhance thermal protective performance. Better protection is obtained by stopping or minimizing the mass transfer at the initial contact point in steam and hot-water exposures. Otherwise, a significant amount of condensed steam and hot-water may be stored inside the fabric system and might be instantaneously delivered to the human skin. This delivery of condensed steam and/or hot-water transmits the thermal energy to the human skin and that causes significant skin burns. Also, depending upon the hot-water temperature and compression pressure, a different amount of heat and/or mass (hot-water) might be stored inside or transmitted through the fabric system in hot-water immersion with compression exposure; this situation may influence the thermal protective performance of fabric systems under hot-water immersion with compression exposures. From this study, it can be concluded that an air-impermeable fabric can be efficiently used to produce thermal protective clothing. However, this air-impermeable clothing may cause heat stress or discomfort for firefighters through ineffective dissipation of their sweat-vapor ([Rossi, 2003](#); [Song, et al., 2011a](#)). Notably, the air-impermeable moisture barrier should be vapor-permeable to dissipate the metabolic-heat and sweat-vapor generated from firefighters' bodies in order to prevent heat strain ([Moein & Torvi, 2011](#); [Song, et al., 2011a](#)). It can also be concluded that thickness and thermal resistance are the significant fabric properties that affect thermal protective performance of fabric systems under flame, radiant heat, and hot surface contact exposures; and thickness, air permeability, and evaporative resistance are the significant fabric properties for

thermal protective performance of fabric systems under steam, hot-water splash, and hot-water immersion with compression exposures.

By employing the above mentioned significant fabric properties in the MLR and ANN models, thermal protective performance of fabric systems are predicted under various thermal exposures. The results indicate that the ANN models outperformed the MLR models in predicting thermal protective performance; here, the three-layered feed-forward back propagation ANN models with five neurons in the hidden layer are found as the best fit models to effectively predict thermal protective performance. By using the ANN models in saliency testing, it can be concluded that the different fabric properties primarily affect the prediction of thermal protective performance under various thermal exposures. In summary, thickness is the key fabric property to predict thermal protective performance in flame exposures; thermal resistance is the key fabric property to predict thermal protective performance in radiant heat and hot surface contact exposures; thickness and air permeability are the key fabric properties for predicting thermal protective performance under steam and hot-water splash exposures; air permeability and evaporative resistance are the key in predicting thermal protective performance under hot-water immersion with compression exposure at low temperatures (75°C and 85°C); and thickness and evaporative resistance are the key for predicting thermal protective performance under hot-water immersion with compression at high temperature (95°C) and different pressures (14 kPa and 28 kPa). Here, it can be concluded that the mode of heat and/or mass transfer is different under various thermal exposures; as a result, different key fabric properties influence the prediction of thermal protective performance under various thermal exposures.

Overall, this PhD study acknowledges the thermal protective performance of fabrics used

in the firefighters' clothing under various thermal exposures that are faced by firefighters. Interestingly, this study demonstrates a new finding on the thermal protective performance of fabrics under the significant and unexplored area of thermal exposure to hot-water immersion with compression. This study also holistically characterizes the fabric properties that affect the thermal protective performance, and empirically analyzes the thermal protective performance under the thermal exposures. This study further advances the field of textile/materials science through better understanding of heat and mass transfer in fabrics. This understanding is useful to develop an integrated knowledge on fabric properties, heat and mass transfer through fabrics under various thermal exposures, and thermal protective performance of fabrics. Eventually, this PhD study would help to build an improved understanding of the materials used in the firefighters' clothing. Based on this PhD research findings, a number of peer-reviewed papers are published and presented in the international journals and conferences ([Mandal, et al., 2013a](#); [Mandal, et al., 2014](#); [Mandal, et al., 2015](#); [Mandal & Song, 2011](#); [Mandal, Lu, & Song, 2013b](#); [Mandal & Song, 2012a](#); [Mandal & Song, 2012b](#); [Mandal & Song, 2014a](#); [Mandal & Song, 2014b](#); [Mandal & Song, 2014c](#); [Mandal & Song, 2014d](#); [Mandal & Song, 2015](#); [Mandal & Song, 2016](#)). Notably, the performance prediction accuracy of the MLR models of this study may be affected by the input variables of some mutually dependent significant fabric properties (e.g., thickness and thermal resistance). In future, these MLR models can be further improved by considering only the mutually independent variables. Also, this research is limited to the characterization and prediction of thermal protective performance of fabrics for firefighters' clothing. In future, this study could be extended to the development or engineering of new fabric testing standards and materials for thermal protective clothing. Such clothing will provide optimal occupational safety and health for on-duty firefighters in Canada and worldwide.

References

- Abbott, N. J., & Schulman, S. (1976). Protection from fire: nonflammable fabrics and coatings. *Journal of Coated Fabrics*, 6(1), 48-64.
- Abdel-Rehim, Z. S., Saad, M. M., Ei-Shakankery, M., & Hanafy, I. (2006). Textile fabrics as thermal insulator, *Autex Research Journal*, 6(3), 148-161.
- Ackerman, M. Y., Crown, E. M., Dale, J. D., Murtaza, G., Batcheller, J., & Gonzalez, J. A. (2012). Development of a test apparatus/method and material specifications for protection from steam under pressure. *Performance of Protective Clothing and Equipment: Emerging Issues and Technologies, 9th Vol., STP1544*, 308-328.
- Agresti, A., & Franklin, C. (2009). *Statistics- the art and science of learning from data*. USA: Prentice Hall.
- Andersson, C. J. (1999). Relationship between physical textile properties and human comfort during wear trials of chemical biological protective garment systems. MSc Thesis, University of Alberta, Edmonton, Canada.
- Arpaci, V. S. (1966). *Conduction Heat Transfer*. USA: Addison-Wesley Publication Company.
- Arpaci, V. S. & Larsen, P. S. (1984). *Convection Heat Transfer*. USA: Prentice Hall.
- Arupjoyti, S., & Iragavarapu, S. (1998). New electrotopological descriptor for prediction of boiling points of alkanes and aliphatic alcohols through artificial neural network and multiple linear regression analysis. *Computers and Chemistry*, 22(6), 512-522.
- ASTM International. (1987). ASTM D 4108: Standard test method for thermal protective performance of materials for clothing by open-flame method. Annual Book of ASTM Standards (Vol. 7.01, 9 pp.). West Conshohocken, PA, USA.

ASTM International. (1996). ASTM D 1777: Standard test method for thickness of textile material. Annual Book of ASTM Standards (Vol. 7.01, 5 pp.). West Conshohocken, PA, USA.

ASTM International. (2004). ASTM D 737: Standard test method for air permeability of textile fabrics. Annual Book of ASTM Standards (Vol. 7.01, 5 pp.). West Conshohocken, PA, USA.

ASTM International. (2008a). ASTM F 1939: Standard test method for radiant heat resistance of flame resistant clothing materials with continuous heating. Annual Book of ASTM Standards (Vol. 11.03, 12 pp.). West Conshohocken, PA, USA.

ASTM International. (2008b). ASTM F 2702: Standard test method for radiant heat performance of flame resistant clothing materials with burn injury prediction. Annual Book of ASTM Standards (Vol. 11.03, 17 pp.). West Conshohocken, PA, USA.

ASTM International. (2008c). ASTM F 2701: Standard test method for evaluating heat transfer through materials for protective clothing upon contact with a hot liquid splash. Annual Book of ASTM Standards (Vol. 11.03, 8 pp.). West Conshohocken, PA, USA.

ASTM International. (2008d). ASTM F 1060: Standard test method for thermal protective performance of materials for protective clothing for hot surface contact. Annual Book of ASTM Standards (Vol. 11.03, 7 pp.). West Conshohocken, PA, USA.

ASTM International. (2009). ASTM D 3776: Standard test method for mass per unit area (weight) of fabric. Annual Book of ASTM Standards (Vol. 7.01, 5 pp.). West Conshohocken, PA, USA.

ASTM International. (2013a). ASTM D 4850: Standard terminology relating to fabrics and fabric test methods. Annual Book of ASTM Standards (Vol. 7.02, 11 pp.). West Conshohocken, PA, USA.

- ASTM International. (2013b). ASTM F 2703: Standard test method for unsteady-state heat transfer evaluation of flame resistant materials for clothing with burn injury prediction. Annual Book of ASTM Standards (Vol. 11.03, 12 pp.). West Conshohocken, PA, USA.
- ASTM International. (2013c). ASTM F 1930: standard test method for evaluation of flame resistant clothing for protection against flash fire simulations using an instrumented manikin. Annual Book of ASTM Standards (Vol. 11.03, 12 pp.). West Conshohocken, PA, USA.
- ASTM International. (2014a). ASTM D 1518: Standard test method for thermal resistance of batting systems using a hot plate. Annual Book of ASTM Standards (Vol. 7.01, 6 pp.). West Conshohocken, PA, USA.
- ASTM International. (2014b). ASTM E 1354: Standard test method for heat and visible smoke release rates for materials and products using an oxygen consumption calorimeter. Annual Book of ASTM Standards (Vol. 4.07, 20 pp.). West Conshohocken, PA, USA.
- ASTM International. (2015). ASTM D 1776: Standard practice for conditioning and testing textiles. Annual Book of ASTM Standards (Vol. 7.01, 4 pp.). West Conshohocken, PA, USA.
- Barker, R. L. (2005, January). A review of gaps and limitations in test methods for first responder protective clothing and equipment. USA: National Personal Protection Technology Laboratory, 1-98.
- Barker, R. L., Guerth-Schacher, C., Grimes, R. V., & Hamouda, H. (2006). Effects of moisture on the thermal protective performance of firefighter protective clothing in low-level radiant heat exposures. *Textile Research Journal*, 76(1), 27-31.
- Barker, R. L., Hamouda, H., Shaley, I., & Johnson, J. (1999). Review and evaluation of thermal sensors for use in testing firefighters protective clothing. USA: National Institute of Standards and Technology, 1-49.

- Barker, R. L., & Lee, Y. M. (1987). Analyzing the transient thermophysical properties of heat-resistant fabrics in TPP exposures. *Textile Research Journal*, 57(6), 331-338.
- Batra, S. K., & Pourdeyhimi, B. (2012). *Introduction to Nonwoven Technology*, USA: DEStech Publications.
- Bear, J. (1972). *Dynamics of Fluids in Porous Media*, USA: Dover Publications.
- Benisek, L., & Phillips, W. A. (1979). Evaluation of flame retardant clothing assemblies for protection against convective heat flames. *Clothing and Textile Research Journal*, 7(9), 2-20.
- Benisek, L., & Phillips, W. A. (1981). Protective clothing fabrics: part II. against convective heat (open-flame) hazards . *Textile Research Journal*, 51(3), 191-196.
- Bergman, T. L., Lavine, A. S., Incropera, F. P., & Dewitt, D. P. (2011). *Fundamentals of Heat and Mass Transfer*. USA: John Wiley & Sons Incorporation.
- Bryner, N., Madrzykowski, D., & Grosshandler, W. (n.d.). Reconstructing the station nightclub fire- materials testing and small scale experiments. Retrieved from <http://fire.nist.gov/bfrlpubs/fire07/PDF/f07062.pdf>
- Burnmeister, L. C. (1993). *Convective Heat Transfer*, USA: Wiley Publications.
- CGSB (2001). CGSB 78.1: Thermal protective performance of materials for clothing. CGSB (11 pp.), Ottawa, Canada.
- Chitrphiromsri, P., & Kuznetsov, A. V. (2005). Modeling heat and moisture transport in firefighter protective clothing during flash fire exposure. *Heat and Mass Transfer*, 41(3), 206-215.
- Cussler, E. L. (2009). *Diffusion Mass Transfer in Fluid Systems*. UK: Cambridge University Press.

- Dale, J. D., Crown, E. M., Ackerman, M. Y., Leung, E., & Rigakis, K. B. (1992). Instrumented manikin evaluation of thermal protective clothing. In J. P. McBriarty & N. W. Henry (Eds.), *Performance of Protective Clothing, ASTM STP 1133* (pp. 717-733). USA: American Society for Testing and Materials.
- Eni, E. U. (2005). Developing test procedures for measuring stored thermal energy in firefighter protective clothing. MSc Thesis. North Carolina State University, Raleigh, USA.
- Fahy, R. F., LeBlanc, P. R., & Molis, J. L. (2014, June). Firefighter fatalities in the United States- 2012. USA: National Fire Protection Association, 1-30.
- Foster, J. A., & Roberts, G. V. (1995). Measurements of the firefighters environments- summary report. *Fire Engineers Journal*, 55(178), 30-34.
- Gholamreza F., & Song, G. (2013). Laboratory evaluation of thermal protective clothing performance upon hot liquid splash. *The Annals of Occupational Hygiene*, 57(6), 805-822.
- Haghi, A. K. (2011). *Heat & Mass Transfer in Textiles*. Canada: World Scientific and Engineering Academy and Society.
- Hassoun, M. H. (1995). *Fundamentals of Artificial Neural Networks*. USA: The MIT Press.
- Heath, D. W. (2000). A liquid cooled heat flux transducer for use in evaluating the thermal protective performance of firefighters' clothing. MSc Thesis. North Carolina State University, Raleigh, USA.
- Henriques, F. C. (1947). Studies of thermal injury; the predictability and the significance of thermally induced rate processes leading to irreversible epidermal injury. *Archives of Pathology*, 43(5) 489-502.

- Henriques, F. C., & Moritz, A. R. (1947). Studies of thermal injury I. The conduction of heat to and through skin and the temperatures attained therein: a theoretical and an experimental investigation. *The American Journal of Pathology*, 23(4), 530-549.
- Hsu, S. T. (1963). *Engineering Heat Transfer*. USA: Van Nostrand Company.
- Hui, C. L., & Ng, S. F. (2009). Predicting seam performance of commercial woven fabrics using multiple logarithm regression and artificial neural networks. *Textile Research Journal*, 79(18), 1649-1657.
- ISO. (1995). ISO 9151: Protective clothing against heat and flame – determination of heat transmission on exposure to flame. ISO (14 pp.). Geneva, Switzerland.
- ISO. (2014). ISO 11092: Textiles – physiological effects – measurement of thermal and water-vapor resistance under steady-state conditions (sweating guarded-hotplate test). ISO (15pp.). Geneva, Switzerland.
- Jalbani, S. H., Ackerman, M. Y., Crown, E. M., Keulen, M., & Song, G. (2012). Apparatus for use in evaluating protection from low pressure hot water jets. *Performance of Protective Clothing and Equipment: Emerging Issues and Technologies, 9th Vol., STP1544*, 329-339.
- Kahn, S. A., Patel, J. H., Lentz, C. W., & Bell, D. E. (2012). Firefighter burn injuries: predictable patterns influenced by turnout gear. *Journal of Burn Care & Research*, 33(1), 152-156.
- Karter, M. J. (2013a, September). Fire loss in the United States during 2012. USA: National Fire Protection Association, 1-42.
- Karter, M. J. (2013b, December). Patterns of firefighter fireground injuries. USA: National Fire Protection Association, 1-27.
- Karter, M. J., & Molis, J. L. (2013, October). U.S. firefighter injuries- 2012. USA: National Fire Protection Association, 1-28.

- Keiser, C., Becker, C., & Rossi, R. M. (2008). Moisture transport and absorption in multilayer protective clothing fabrics. *Textile Research Journal*, 78(7), 604-613.
- Keiser, C., & Rossi, R. M. (2008). Temperature analysis for the prediction of steam formation and transfer in multilayer thermal protective clothing at low level thermal radiation. *Textile Research Journal*, 78(11), 1025-1035.
- Keiser, C., Wyss, P., & Rossi, R. M. (2010). Analysis of steam formation and migration in firefighters' protective clothing using X-ray radiography. *International Journal of Occupational Safety and Ergonomics*, 16(2), 217-229.
- Klyosov, A. A. (2007). *Wood-Plastic Composites*. New Jersey: John Wiley & Sons Inc.
- Kothandaraman, C. P. (2006). *Fundamentals of Heat and Mass Transfer*. New Delhi: New Age International Publishers.
- Lawson, J. R. (1996, August). Fire fighter's protective clothing and thermal environments of structural fire fighting. USA: National Institute of Standards and Technology, 1-22.
- Lawson, J. R. (1997, August). *Thermal environments of structural firefighting and thermal tests for firefighters' protective clothing*. Second International Conference on Fire Research and Engineering, Maryland, USA.
- Lawson, J. R., Twilley, W. H., & Malley, K. S. (2000, April). Development of a dynamic compression test apparatus for measuring thermal performance of fire fighters' protective clothing. USA: National Institute of Standards and Technology, 1-24.
- Lee, Y. M., & Barker, R. L. (1986). Effect of moisture on the thermal protective performance of heat-resistant fabrics. *Journal of Fire Sciences*, 4(5), 315-330.
- Lienhard, J. H., & Lienhard, J. H. (2011). *A Heat Transfer Textbook*. USA: Phlogiston Press.

- Lu, Y., Li, J., Li, X., & Song, G. (2013a). The effect of air gaps in moist protective clothing on protection from heat and flame, *Journal of Fire Sciences*, 31(2), 99-111.
- Lu, Y., Song, G., Ackerman, M. Y., Paskaluk, S. A., & Li, J. (2013b). A new protocol to characterize thermal protective performance of fabrics against hot liquid splash. *Experimental Thermal and Fluid Science*, 46, 37-45.
- Lu, Y., Song, G., Li, J., & Paskaluk, S. (2013c). Effect of an air gap on the heat transfer of protective materials upon hot liquid splashes. *Textile Research Journal*, 83(11), 1156-1169.
- Lu, Y., Song, G., Zeng, H., Zhang, L., & Li, J. (2014). Characterizing factors affecting the hot liquid penetration performance of fabrics for protective clothing. *Textile Research Journal*, 84(2), 174-186.
- Majumdar, P. K., & Majumdar, A. (2004). Predicting the breaking elongation of ring spun cotton yarns using mathematical, statistical and artificial neural networks models. *Textile Research Journal*, 74(7), 652-655.
- Makinen, H. (2008). Firefighters protective clothing. In R. A. Scott (Ed.), *Textiles for Protection* (pp. 622-647). England: Woodhead Publishing.
- Mandal, S., Lu, Y., & Song, G. (2013b, April). *Characterization of thermal protective clothing under hot-water and pressurized steam exposure*. The 2013 Herman and Myrtle Goldstein Student Paper Competition organized by AATCC, South Carolina, USA.
- Mandal, S., Lu, Y., Wang, F., & Song, G. (2014). Characterization of thermal protective clothing under hot water and pressurized steam exposure. *AATCC Journal of Research*, 1(5), 7-16.
- Mandal, S., & Song, G. (2011, May). *Characterization of protective textile materials for various thermal hazards*. Fiber Society Spring Conference, Kowloon, Hong Kong.

- Mandal, S., & Song, G. (2012a, August). *Modeling of thermal protective performance of commercial woven fabric using artificial neural network*. 9th International Meeting for Manikins and Modeling, Tokyo, Japan.
- Mandal, S., & Song, G. (2012b, May) *Modeling for predicting the performances of thermal protective clothing*. 5th European Conference on Protective Clothing and NOKOBETEF 10, Valencia, Spain.
- Mandal, S., & Song, G. (2014a). An empirical analysis of thermal protective performance of fabrics used in protective clothing. *The Annals of Occupational Hygiene*, 58(8), 1065-1077.
- Mandal, S., & Song, G. (2014b). Characterizing fabric materials of firefighters' protective clothing in hot-water immersion and compression. Proceedings of 2014 AATCC International Conference. p. 77-86. Asheville, North Carolina: AATCC.
- Mandal, S., & Song, G. (2014c, April). *Characterizing fabric materials of firefighters' protective clothing in hot-water immersion and compression*. The 2014 Herman and Myrtle Goldstein Student Paper Competition organized by AATCC, North Carolina, USA.
- Mandal, S., & Song, G. (2014d, May). *Analyzing the parameters of thermal protective fabrics under hot-water immersion and compression*. Fiber Society Spring Conference, Liberec, Czech Republic. (Poster)
- Mandal, S., & Song, G. (2015). Thermal sensors for performance evaluation of protective clothing against heat and fire: a review. *Textile Research Journal*, 85(1), 101-112.
- Mandal, S., & Song, G. (2016). Characterizing fabrics in firefighters' protective clothing: hot-water immersion and compression. *AATCC Journal of Research*, 3(2), 8-15.

- Mandal, S., Song, G., & Gholamreza, F. (2015). A novel protocol to characterize the thermal protective performance of fabrics in hot-water exposures. *Journal of Industrial Textiles*. doi 10.1177/1528083715580522
- Mandal, S., Song, G., Ackerman, M., Paskaluk, S., & Gholamreza, F. (2013a). Characterization of textile fabrics under various thermal exposures. *Textile Research Journal*, 83(10), 1005-1019.
- Massenaux, G. (2003). Introduction to nonwovens. In W. Albrecht, H. Fuchs, & W. Kittelmann (Eds.), *Nonwoven Fabrics: Raw Materials, Manufacture, Applications, Characteristics, Testing Processes*. Germany: Wiley-VCH.
- MATLAB*. (n.d.). Retrieved from <http://www.mathworks.com/products/matlab/>
- Moein, R., & Torvi, D. A. (2011). Assessment of factors affecting the continuing performance of firefighters protective clothing. *Fire Technology*, 47, 565-599.
- Morris, G. J. (1953). Thermal properties of textile materials. *Journal of the Textile Institute Transactions*, 44(10), T449-T476.
- Murrells, C. M., Tao, X. M., Xu, B. G., & Cheng, K. P. S. (2009). An artificial neural network model for the prediction of spirality of fully relaxed single jersey fabrics. *Textile Research Journal*, 79(3), 227-234.
- Murtaza, G. (2012). Development of fabrics for steam and hot water protection. MSc Thesis. University of Alberta, Edmonton, Canada
- NFPA. (2013). NFPA 1971: Standard on protective ensembles for structural fire fighting and proximity fire fighting. 2013 NFPA 1971 Handbook (145 pp.). Quincy, MA, USA.
- Orme, J. G., & Orme, T. C. (2009). *Multiple Regression with Discrete Dependent Variables*. United Kingdom: Oxford University Press.

- Perkins, R. M. (1979). Insulative values of single-layer fabrics for thermal protective clothing. *Textile Research Journal*, 49(4), 202-205.
- Pynckels, F., Kiekens, P., Sette, S., Van-Langenhove, L., & Impe, K. (1995). Use of neural nets for determining the spinnability of fibres. *Journal of Textile Institute*, 86(3), 425-437.
- Rossi, R. (2003). Firefighting and its influence on the body. *Ergonomics*, 46(10), 1017-1033.
- Rossi, R., Indelicato, E., & Bolli, W. (2004). Hot steam transfer through heat protective clothing layers. *International Journal of Occupational Safety and Ergonomics*, 10(3), 239-245.
- Rossi, R., & Zimmerli, T. (1994, January). *Influence of humidity on the radiant, convective and contact heat transmission through protective clothing materials*. Fifth International Symposium on Performance of Protective Clothing: Improvement through Innovation, San Francisco, USA.
- Sati, R., Crown, E., Ackerman, M., Gonzalez, J., & Dale, J. D. (2008). Protection from steam at high pressure: development of a test device and protocol. *International Journal of Occupational Safety and Ergonomics*, 14(1), 29-41.
- Shalev, I., & Barker, R. L. (1983). Analysis of heat transfer characteristics of fabrics in an open flame exposure. *Textile Research Journal*, 53(8), 475-482.
- Shalev, I., & Barker, R. L. (1984). Protective fabrics: a comparison of laboratory methods for evaluating thermal protective performance in convective/radiant exposures. *Textile Research Journal*, 54(10), 648-654.
- Shoda, A., Wang, C. Y., & Cheng, P. (1998). Simulation of constant pressure steam injection in a porous medium. *International Communication on Heat Mass Transfer*, 25(6), 753 – 762.
- Siegel, R., & Howell, J. (2002). *Thermal Radiation Heat Transfer*. London: Taylor & Francis.

- Song G. (2004). Modeling thermal protection outfit for fire exposures. PhD Thesis. North Carolina State University, Raleigh, USA.
- Song, G. (2009). Thermal insulation properties of textiles and clothing. In J. T. Williams (Ed.), *Textiles for Cold Weather Apparel* (pp. 19-32). England: Woodhead Publishing.
- Song, G., Cao, W., & Gholamreza, F. (2011b). Analyzing thermal stored energy and effect on protective performance. *Textile Research Journal*, 81(11), 120-135.
- Song, G., Chitraphiromsri, P., & Ding, D. (2008). Numerical simulations of heat and moisture transport in thermal protective clothing under flash fire conditions. *International Journal of Occupational Safety and Ergonomics*, 14(1), 89-106.
- Song, G., Paskaluk, S., Sati, R., Crown, E. M., Dale, J. D., & Ackerman, M. (2011a). Thermal protective performance of protective clothing used for low radiant heat protection. *Textile Research Journal*, 81(3), 311-323.
- StatCrunch*. (n.d.). Retrieved from <http://www.statcrunch.com/learn-about/what-is.html>
- Stull, J. O. (1997). Comparison of conductive heat resistance and radiant heat resistance with thermal protective performance of fire fighter protective clothing. In O. S. Jeffrey & D. S. Arthur (Eds.), *Performance of Protective Clothing, ASTM STP 1273* (pp. 248-269). USA: American Society for Testing and Materials.
- Sun, G., Yoo, H. S., Zhang, X. S., & Pan, N. (2000). Radiant protective and transport properties of fabrics used by wildland firefighters. *Textile Research Journal*, 70(7), 567-573.
- The Fallen*. (n.d.). Retrieved from <http://www.cfff.ca/EN/fallen.html>
- Torvi, D. A. (1997). Heat transfer in thin fibrous materials under high heat flux conditions. PhD Thesis. University of Alberta, Edmonton, Canada.

- Torvi, D. A., & Dale, J. D. (1998). Effect of variation in thermal properties on the performance of flame resistant fabrics for flash fires. *Textile Research Journal*, 68(11), 787-796.
- Torvi, D. A., & Dale, J. D. (1999). Heat transfer in thin fibrous materials under high heat flux. *Fire Technology*, 35(3), 210-231.
- Torvi, D. A., Dale, J. D., & Faulkner, B. (1999). Influence of air gaps on bench-top test results of flame resistant fabrics. *Journal of Fire Protection Engineering*, 10(1), 1-12.
- Torvi, D. A., & Threlfall, T. G. (2006). Heat transfer model of flame resistant fabrics during cooling after exposure to fire. *Fire Technology*, 42(1), 27- 48.
- Wen, S. (2014). Physiological strain and physical burden in chemical protective coveralls. PhD Thesis, University of Alberta, Edmonton, Canada.
- Yan, X., & Su, X. G. (2009). *Linear Regression Analysis – Theory and Computing*. Singapore: World Scientific.
- Yegnanarayana, B. (2006). *Artificial Neural Networks*. New Delhi: Prentice-Hall of India Private Limited.
- Zaefizadeh, M., Khayatnezhad, M., & Gholamin, R. (2011). Comparison of multiple linear regression (MLR) and artificial neural networks (ANN) in predicting the yield using its components in hullless barley. *Journal of Agricultural and Environmental Science*, 10(1), 60-64.
- Zhu, F., Zhang, W., & Chen, M. (2007). Investigation of material combinations for fire-fighter's protective clothing on radiant protective and heat-moisture transfer performance. *Fibres and Textiles in Eastern Europe*, 15(1), 72-75.

Appendices

Appendix 1. Mass and thickness of fabrics used in this work

Fabric types	Specimens	Total weight (g/196.35cm ²)	Mass ^a (g/m ²)	Thickness ^b (mm)			Air permeability ^c (cm ³ /cm ² /s)		
				IS ^d	M ^e	CV%	IS	M	CV%
A	1	4.87	248	0.69	0.69	2.45	15.75	15.71	2.40
	2			0.69			15.67		
	3			0.71			16.10		
	4			0.69			15.93		
	5			0.66			16.25		
	6			0.71			15.63		
	7			0.69			16.06		
	8			0.69			15.35		
	9			0.66			15.15		
	10			0.69			15.25		
B	1	4.10	209	1.63	1.63	1.40	43.74	43.19	2.50
	2			1.60			43.52		
	3			1.60			44.27		
	4			1.63			43.33		
	5			1.63			43.52		
	6			1.68			42.95		
	7			1.63			44.64		
	8			1.65			42.76		
	9			1.63			42.39		
	10			1.63			40.79		
C	1	5.68	289	2.17	2.13	2.48	41.81	40.62	2.31
	2			2.15			41.61		
	3			2.11			41.20		
	4			2.01			40.59		
	5			2.16			38.83		
	6			2.06			39.56		
	7			2.15			40.39		
	8			2.17			40.18		
	9			2.14			41.40		
	10			2.15			40.59		
D	1	6.89	351	3.18	3.18	2.29	38.15	38.43	2.50
	2			3.34			39.01		
	3			3.15			37.95		
	4			3.12			36.83		
	5			3.18			38.96		
	6			3.05			37.95		
	7			3.20			37.28		
	8			3.18			39.98		

	9			3.18			39.17		
	10			3.20			39.00		
E	1	4.15	211	0.87	0.85	2.28	0.00	0	NA
	2			0.85			0.00		
	3			0.89			0.00		
	4			0.84			0.00		
	5			0.82			0.00		
	6			0.84			0.00		
	7			0.86			0.00		
	8			0.84			0.00		
	9			0.86			0.00		
	10			0.86			0.00		

^aMeasured according to ASTM D 3776 (ASTM International, 2009).

^bMeasured according to ASTM D 1777 under 1kPa pressure (ASTM International, 1996).

^cMeasured according to ASTM D 737 under air pressure differential 125Pa (ASTM International, 2004).

^dIS = Individual Specimens; ^eM = Mean

Appendix 2. Thickness and air permeability of fabrics systems

Fabric systems	Specimens	Thickness ^a (mm)			Air permeability ^b (cm ³ /cm ² /s)		
		Individual specimen	Mean	CV%	Individual specimen	Mean	CV%
A	1	0.69	0.69	2.45	15.75	15.71	2.40
	2	0.69			15.67		
	3	0.71			16.10		
	4	0.69			15.93		
	5	0.66			16.25		
	6	0.71			15.63		
	7	0.69			16.06		
	8	0.69			15.35		
	9	0.66			15.15		
	10	0.69			15.25		
AB	1	2.11	2.18	2.26	13.01	13.59	2.48
	2	2.11			13.82		
	3	2.21			13.55		
	4	2.18			13.47		
	5	2.16			13.36		
	6	2.18			13.81		
	7	2.18			13.13		
	8	2.26			13.81		
	9	2.24			13.97		
	10	2.21			13.92		
AD	1	3.59	3.53	2.09	13.22	13.30	2.21
	2	3.53			13.19		
	3	3.58			13.24		
	4	3.53			12.77		
	5	3.57			13.47		
	6	3.66			13.70		
	7	3.41			13.81		
	8	3.53			13.20		
	9	3.43			13.19		
	10	3.51			13.22		
AE	1	1.42	1.42	0.60	0.00	0	NA
	2	1.42			0.00		
	3	1.42			0.00		
	4	1.42			0.00		
	5	1.40			0.00		
	6	1.40			0.00		
	7	1.42			0.00		
	8	1.42			0.00		
	9	1.42			0.00		
	10	1.42			0.00		

EA	1	1.42	1.42	0.96	0.00	0	NA
	2	1.42			0.00		
	3	1.43			0.00		
	4	1.42			0.00		
	5	1.39			0.00		
	6	1.39			0.00		
	7	1.42			0.00		
	8	1.42			0.00		
	9	1.42			0.00		
	10	1.42			0.00		
AEB	1	2.82	2.88	2.25	0.00	0	NA
	2	2.87			0.00		
	3	2.95			0.00		
	4	2.90			0.00		
	5	2.92			0.00		
	6	2.95			0.00		
	7	2.90			0.00		
	8	2.92			0.00		
	9	2.79			0.00		
	10	2.77			0.00		
AEC	1	3.61	3.49	2.48	0.00	0	NA
	2	3.35			0.00		
	3	3.51			0.00		
	4	3.53			0.00		
	5	3.35			0.00		
	6	3.43			0.00		
	7	3.53			0.00		
	8	3.53			0.00		
	9	3.56			0.00		
	10	3.51			0.00		
AED	1	4.29	4.23	2.04	0.00	0	NA
	2	4.31			0.00		
	3	4.24			0.00		
	4	4.29			0.00		
	5	4.01			0.00		
	6	4.27			0.00		
	7	4.19			0.00		
	8	4.22			0.00		
	9	4.24			0.00		
	10	4.27			0.00		
EAC	1	3.61	3.49	2.50	0.00	0	NA
	2	3.35			0.00		
	3	3.51			0.00		
	4	3.53			0.00		
	5	3.35			0.00		

	6	3.42			0.00		
	7	3.53			0.00		
	8	3.53			0.00		
	9	3.56			0.00		
	10	3.48			0.00		

^aMeasured according to ASTM D 1777 under 1kPa pressure ([ASTM International, 1996](#)).

^bMeasured according to ASTM D 737 under air pressure differential 125Pa ([ASTM International, 2004](#)).

Appendix 3. Thermal and evaporative resistances of fabrics systems

Fabric systems	Specimens	Thermal resistance ^a (K·m ² /W)			Evaporative resistance ^b (m ² ·Pa/W)		
		Individual specimen	Mean	CV%	Individual specimen	Mean	CV%
A	1	0.0732	0.073	1.28	4.3	4.40	2.27
	2	0.073			4.5		
	3	0.0715			4.4		
AB	1	0.119	0.117	1.30	10.0	9.87	1.17
	2	0.117			9.8		
	3	0.116			9.8		
AD	1	0.168	0.169	1.36	12.8	12.70	0.79
	2	0.168			12.7		
	3	0.172			12.6		
AE	1	0.094	0.095	1.22	20.6	20.70	0.84
	2	0.094			20.6		
	3	0.096			20.9		
EA	1	0.094	0.095	1.05	21.1	21.17	0.27
	2	0.095			21.2		
	3	0.096			21.2		
AEB	1	0.128	0.129	1.18	26.0	25.90	0.39
	2	0.131			25.9		
	3	0.129			25.8		
AEC	1	0.149	0.151	1.15	24.9	25.40	1.97
	2	0.152			25.9		
	3	0.152			25.4		
AED	1	0.181	0.184	1.44	27.4	28.03	2.15
	2	0.186			28.6		
	3	0.185			28.1		
EAC	1	0.150	0.151	1.38	25.4	25.37	0.60
	2	0.153			25.5		
	3	0.149			25.2		

^aMeasured according to ASTM D 1518 (ASTM International, 2014a).

^bMeasured according to ISO 11092 (ISO, 2014).

Appendix 4. Thermal protective performance of fabric systems under flame exposure

Fabric Systems	Specimens	Thermal Protective Performance ^a (Second-degree Burn Time in Seconds)		
		Values	Mean	CV (%)
A	1	2.68	2.75	2.22
	2	2.80		
	3	2.76		
AB	1	12.86	12.81	1.76
	2	13.00		
	3	12.56		
AD	1	16.27	16.59	1.68
	2	16.70		
	3	16.79		
AE	1	9.40	9.58	2.41
	2	9.50		
	3	9.84		
EA	1	5.86	5.72	2.21
	2	5.62		
	3	5.67		
AEB	1	12.01	11.79	2.22
	2	11.86		
	3	11.50		
AEC	1	15.91	15.74	2.48
	2	16.01		
	3	15.29		
AED	1	20.93	20.84	1.07
	2	21.01		
	3	20.59		
EAC	1	15.80	15.47	2.47
	2	15.05		
	3	15.55		

^aMeasured according to modified ISO 9151 (ISO, 1995).

Appendix 5. Thermal protective performance of fabric systems under radiant heat exposure

Fabric Systems	Specimens	Thermal Protective Performance ^a (Second-degree Burn Time in Seconds)		
		Values	Mean	CV (%)
A	1	4.65	4.64	2.39
	2	4.74		
	3	4.52		
AB	1	11.58	11.90	2.50
	2	11.94		
	3	12.17		
AD	1	23.63	24.18	2.20
	2	24.69		
	3	24.22		
AE	1	9.48	9.22	2.49
	2	9.06		
	3	9.11		
EA	1	7.99	7.91	2.02
	2	7.73		
	3	8.02		
AEB	1	17.30	17.60	2.29
	2	17.45		
	3	18.06		
AEC	1	22.69	23.19	1.87
	2	23.39		
	3	23.48		
AED	1	27.16	27.93	2.43
	2	28.17		
	3	28.45		
EAC	1	21.09	20.59	2.11
	2	20.29		
	3	20.40		

^aMeasured according to modified ASTM E 1354 (ASTM International, 2014b).

Appendix 6: Thermal protective performance of fabric systems under hot surface contact exposure

Fabric Systems	Specimens	Thermal Protective Performance ^a (Second-degree Burn Time in Seconds)		
		Values	Mean	CV (%)
A	1	1.48	1.51	2.02
	2	1.54		
	3	1.52		
AB	1	4.83	4.77	2.43
	2	4.85		
	3	4.64		
AD	1	6.71	6.87	2.48
	2	7.05		
	3	6.86		
AE	1	5.20	5.16	1.14
	2	5.18		
	3	5.09		
EA	1	3.45	3.54	2.43
	2	3.62		
	3	3.56		
AEB	1	9.47	9.45	2.29
	2	9.65		
	3	9.22		
AEC	1	16.42	16.27	2.12
	2	15.88		
	3	16.52		
AED	1	17.46	17.30	2.36
	2	17.61		
	3	16.84		
EAC	1	7.19	7.22	2.38
	2	7.06		
	3	7.40		

^aMeasured according to modified ASTM F 1060 ([ASTM International, 2008d](#)).

Appendix 7: Thermal protective performance of fabric systems under steam exposure

Fabric Systems	Specimens	Thermal Protective Performance (Second-degree Burn Time in Seconds)		
		Values	Mean	CV (%)
A	1	0.40	0.40	2.50
	2	0.41		
	3	0.39		
AB	1	0.59	0.60	1.91
	2	0.61		
	3	0.61		
AD	1	0.95	0.94	2.21
	2	0.96		
	3	0.92		
AE	1	7.86	7.99	2.11
	2	7.93		
	3	8.18		
EA	1	10.42	10.38	2.01
	2	10.56		
	3	10.15		
AEB	1	11.34	11.51	1.99
	2	11.42		
	3	11.77		
AEC	1	18.90	19.31	2.05
	2	19.69		
	3	19.34		
AED	1	20.85	21.22	2.26
	2	21.76		
	3	21.04		
EAC	1	26.28	25.63	2.20
	2	25.26		
	3	25.35		

Appendix 8: Thermal protective performance of fabric systems under hot-water splash exposure

Fabric Systems	Specimens	Thermal Protective Performance ^a (Second-degree Burn Time in Seconds)		
		Values	Mean	CV (%)
A	1	2.69	2.70	2.26
	2	2.65		
	3	2.77		
AB	1	4.34	4.37	1.73
	2	4.46		
	3	4.32		
AD	1	7.30	7.28	2.35
	2	7.10		
	3	7.44		
AE	1	60.28	60.39	1.58
	2	59.49		
	3	61.39		
EA	1	62.98	63.40	0.88
	2	63.18		
	3	64.03		
AEB	1	76.07	78.09	2.40
	2	8.43		
	3	79.78		
AEC	1	108.10	109.26	1.09
	2	110.47		
	3	109.20		
AED	1	138.48	136.07	1.97
	2	133.19		
	3	136.53		
EAC	1	118.15	119.57	2.28
	2	117.85		
	3	122.71		

^aMeasured according to modified ASTM F 2701 (ASTM International, 2008c).

Appendix 9: Thermal protective performance of fabric systems under hot-water immersion with compression exposure

Fabric Systems	Specimens	Thermal Protective Performance (Second-degree Burn Time in Seconds)														
		At 56 kPa and 75°C			At 56 kPa and 85°C			At 56 kPa and 95°C			At 14 kPa and 85°C			At 28 kPa and 85°C		
		Value	Mean	CV (%)	Value	Mean	CV (%)	Value	Mean	CV (%)	Value	Mean	CV (%)	Value	Mean	CV (%)
A	1	5.24	5.29	2.50	3.60	3.63	2.45	2.01	2.05	2.31	4.35	4.26	1.96	4.26	4.31	0.97
	2	5.19			3.56			2.03			4.19			4.34		
	3	5.44			3.73			2.10			4.23			4.32		
AB	1	6.21	6.19	1.39	5.94	5.82	2.38	2.70	2.74	2.14	6.54	6.69	2.17	5.84	5.92	1.13
	2	6.27			5.67			2.72			6.69			5.96		
	3	6.10			5.86			2.81			6.83			5.95		
AD	1	5.87	5.96	2.38	6.61	6.49	2.42	2.76	2.78	2.25	6.55	6.67	2.50	6.26	6.29	1.06
	2	5.88			6.54			2.73			6.86			6.37		
	3	6.12			6.31			2.85			6.60			6.25		
AE	1	29.84	29.99	0.50	11.03	11.31	2.43	9.63	9.53	1.70	19.88	19.72	1.14	18.81	19.05	1.44
	2	29.98			11.58			9.61			19.81			18.99		
	3	30.14			11.32			9.34			19.46			19.35		
EA	1	32.76	32.68	0.32	22.03	21.57	2.13	17.25	16.84	2.17	23.08	23.16	0.81	22.73	22.96	0.91
	2	32.56			21.58			16.74			23.02			23.13		
	3	32.71			21.11			16.54			23.37			23.03		
AEB	1	56.47	57.06	1.47	34.73	35.12	1.22	22.68	22.70	1.26	40.29	40.00	1.34	38.00	38.10	0.40
	2	56.69			35.04			22.99			39.38			38.03		
	3	58.02			35.58			22.42			40.32			38.28		
AEC	1	48.25	48.58	1.50	35.73	36.25	1.25	24.05	24.45	1.43	36.14	36.11	0.54	39.04	39.52	1.07
	2	48.08			36.57			24.60			36.29			39.68		
	3	49.42			36.45			24.70			35.90			39.84		
AED	1	64.95	63.20	2.41	43.04	42.84	0.54	29.67	29.84	0.53	45.95	46.54	1.10	44.24	44.62	0.79
	2	62.15			42.59			29.88			46.78			44.93		
	3	62.50			42.90			29.98			46.88			44.70		
EAC	1	53.58	52.64	2.45	39.69	40.35	1.67	25.53	26.04	1.69	43.62	43.89	1.10	41.97	42.97	2.04
	2	53.18			40.31			26.30			43.61			43.33		
	3	51.17			41.04			26.28			44.45			43.61		

Appendix 10: ANN coding for predicting thermal protective performance under flame exposure

```

input=[0.69 0.073;2.18 0.117;3.53 0.169;1.42 0.095;1.42 0.095;2.88 0.129;3.49 0.151;4.23
0.184;3.49 0.151]; % input data.
target=[2.75;12.81;16.59;9.58;5.72;11.79;15.74;20.84;15.47]; % target data.
[inputn,meani,stdi,targetn,meant,stdt] = prestd(input',target');
% preprocessing or normalizing the data with mean at zero and standard deviation 1
M=[5 1]; % size of ith layer, for NI layers.
netflame = newff(minmax(inputn),M,{'tansig','purelin'},'traingdm');
% creating the feedforward backpropagation (gradient descent with momentum) neural network.
% here newff defines feedforward network architecture.
% first argument minmax(inputn) defines range of input and initializes the network parameters.
% second argument defines the structure of the network. There is 1 hidden and 1 output layer.
% 5 is the number of the nodes in the first hidden layer.
% 1 is the number of nodes in the output layer.
% next, the activation functions in the layers are defined.
% in the first hidden layer, there are 5 tansig functions.
% in the output layer, there is 1 linear function.
netflame.trainParam.epochs=3000; % number of epochs/iterations.
netflame.trainParam.lr=0.3; % learning rate.
netflame.trainParam.mc=0.6; % momentum.
netflame=train(netflame,inputn,targetn);
y=sim(netflame,inputn);
% to simulate the trained network on the original input data.
output=poststd(y',meant,stdt); % to convert y back to the original scale.
[output target] % predicted data vs actual data
title('Comparison between actual targets and predictions')
d=[output-target].^2; % to calculate square error between actual and predicted values.
mse=mean(d) % to calculate the mean square error (mse).
rmse=sqrt(mse) % to calculate the root mean square error (rmse).
[m,b,r]=postreg(output',target') % use of regression analysis to judge the network performance.
Rsquare=r.^2 % to calculate the Coefficient of Determination (R2).
save netflame % to save the trained network 'netflame'.
load netflame % to load the trained network 'netflame'.
% newinput = [3.49 0.151];
% newinputn = trstd(newinput',meani,stdi);
% newoutputn = sim(netflame,newinputn);
% newoutput = poststd(newoutputn',meant,stdt)

```

Appendix 11: ANN coding for predicting thermal protective performance under radiant heat exposure

```

input=[0.69 0.073;2.18 0.117;3.53 0.169;1.42 0.095;1.42 0.095;2.88 0.129;3.49 0.151;4.23
0.184;3.49 0.151]; % input data.
target=[4.64;11.9;24.18;9.22;7.91;17.6;23.19;27.93;20.59]; % target data.
[inputn,meani,stdi,targetn,meant,stdt] = prestd(input',target');
% preprocessing or normalizing the data with mean at zero and standard deviation 1.
M=[5 1]; % size of ith layer, for NI layers.
netrh = newff(minmax(inputn),M,{'tansig','purelin'},'traingdm');
% creating the feedforward backpropagation (gradient descent with momentum) neural network.
% here newff defines feedforward network architecture.
% first argument minmax(inputn) defines range of input and initializes the network parameters.
% second argument defines structure of the network. There is 1 hidden and 1 output layer.
% 5 is the number of the nodes in the first hidden layer.
% 1 is the number of nodes in the output layer.
% next, the activation functions in the layers are defined.
% in the first hidden layer, there are 5 tansig functions.
% in the output layer, there is 1 linear function.
netrh.trainParam.epochs=3000; % number of epochs/iterations.
netrh.trainParam.lr=0.3; % learning rate.
netrh.trainParam.mc=0.6; % momentum.
netrh=train(netrh,inputn,targetn);
y=sim(netrh,inputn);
% to simulate the trained network on the original input data.
output=poststd(y',meant,stdt); % to convert y back to the original scale.
[output target] % predicted data vs actual data.
title('Comparison between actual targets and predictions')
d=[output-target].^2; % to calculate square error between actual and predicted values.
mse=mean(d) % to calculate the mean square error (mse).
rmse=sqrt(mse) % to calculate the root mean square error (rmse).
[m,b,r]=postreg(output',target') % use of regression analysis to judge the network performance.
Rsquare=r.^2 % to calculate the Coefficient of Determination (R2).
save netrh % to save the trained network 'netrh'.
load netrh % to load the trained network 'netrh'.
% newinput = [3.49 0.151];
% newinputn = trastd(newinput',meani,stdi);
% newoutputn = sim(netrh,newinputn);
% newoutput = poststd(newoutputn',meant,stdt)

```

Appendix 12: ANN coding for predicting thermal protective performance under hot surface contact exposure

```
input=[0.69 0.073;2.18 0.117;3.53 0.169;1.42 0.095;1.42 0.095;2.88 0.129;3.49 0.151;4.23
0.184;3.49 0.151]; % input data.
target=[1.51;4.77;6.87;5.16;3.54;9.45;16.27;17.3;7.22]; % target data.
[inputn,meani,stdi,targetn,meant,stdt] = prestd(input',target');
% preprocessing or normalizing the data with mean at zero and standard deviation 1.
M=[5 1]; % size of ith layer, for NI layers.
neths = newff(minmax(inputn),M,{'tansig','purelin'},'traingdm');
% creating the feedforward backpropagation (gradient descent with momentum) neural network.
% here newff defines feedforward network architecture.
% first argument minmax(inputn) defines range of input and initializes the network parameters.
% second argument defines the structure of the network. There is 1 hidden and 1 output layer.
% 5 is the number of the nodes in the first hidden layer.
% 1 is the number of nodes in the output layer.
% next, the activation functions in the layers are defined.
% in the first hidden layer, there are 5 tansig functions.
% in the output layer, there is 1 linear function.
neths.trainParam.epochs=3000; % number of epochs/iterations.
neths.trainParam.lr=0.3; % learning rate.
neths.trainParam.mc=0.6; % momentum.
neths=train(neths,inputn,targetn);
y=sim(neths,inputn);
% to simulate the trained network on the original input data.
output=poststd(y',meant,stdt); % to convert y back to the original scale.
[output target] % predicted data vs actual data.
title('Comparison between actual targets and predictions')
d=[output-target].^2; % to calculate square error between actual and predicted values.
mse=mean(d) % to calculate the mean square error (mse).
rmse=sqrt(mse) % to calculate the root mean square error (rmse).
[m,b,r]=postreg(output',target') % use of regression analysis to judge the network performance.
Rsquare=r.^2 % to calculate the Coefficient of Determination (R2).
save neths % to save the trained network 'neths'.
load neths % to load the trained network 'neths'.
% newinput = [3.49 0.151];
% newinputn = trastd(newinput',meani,stdi);
% newoutputn = sim(neths,newinputn);
% newoutput = poststd(newoutputn',meant,stdt)
```

Appendix 13: ANN coding for predicting thermal protective performance under steam exposure

```

input=[0.69 15.71 4.4;2.18 13.59 9.87;3.53 13.3 12.7;1.42 0 20.7;1.42 0 21.17;2.88 0 25.9;3.49 0
25.4;4.23 0 28.03;3.49 0 25.37]; % input data.
target=[0.4;0.6;0.94;7.99;10.38;11.51;19.31;21.22;25.63]; % target data.
[inputn,meani,stdi,targetn,meant,stdt] = prestd(input',target');
% preprocessing or normalizing the data with mean at zero and standard deviation 1.
M=[5 1]; % size of ith layer, for NI layers.
netsteam = newff(minmax(inputn),M, {'tansig','purelin'},'traingdm');
% creating the feedforward backpropagation (gradient descent with momentum) neural network.
% here newff defines feedforward network architecture.
% first argument minmax(inputn) defines range of input and initializes the network parameters.
% second argument defines the structure of the network. There is 1 hidden and 1 output layer.
% 5 is the number of the nodes in the first hidden layer.
% 1 is the number of nodes in the output layer.
% next, the activation functions in the layers are defined.
% in the first hidden layer, there are 5 tansig functions.
% in the output layer, there is 1 linear function.
netsteam.trainParam.epochs=3000; % number of epochs/iterations.
netsteam.trainParam.lr=0.3; % learning rate.
netsteam.trainParam.mc=0.6; % momentum.
netsteam=train(netsteam,inputn,targetn);
y=sim(netsteam,inputn);
% to simulate the trained network on the original input data.
output=poststd(y',meant,stdt); % to convert y back to the original scale.
[output target] % predicted data vs actual data.
title('Comparison between actual targets and predictions')
d=[output-target].^2; % to calculate square error between actual and predicted values.
mse=mean(d) % to calculate the mean square error (mse).
rmse=sqrt(mse) % to calculate the root mean square error (rmse).
[m,b,r]=postreg(output',target') % use of regression analysis to judge the network performance.
Rsquare=r.^2 % to calculate the Coefficient of Determination (R2).
save netsteam % to save the trained network 'netsteam'.
load netsteam % to load the trained network 'netsteam'.
% newinput = [3.49 0 25.4];
% newinputn = trstd(newinput',meani,stdi);
% newoutputn = sim(netsteam,newinputn);
% newoutput = poststd(newoutputn',meant,stdt)

```

Appendix 14: ANN coding for predicting thermal protective performance under hot-water splash exposure

```
input=[0.69 15.71 4.4;2.18 13.59 9.87;3.53 13.3 12.7;1.42 0 20.7;1.42 0 21.17;2.88 0 25.9;3.49 0
25.4;4.23 0 28.03;3.49 0 25.37]; % input data.
target=[2.7;4.37;7.28;60.39;63.4;78.09;109.26;136.07;119.57]; % target data.
[inputn,meani,stdi,targetn,meant,stdt] = prestd(input',target');
% preprocessing or normalizing the data with mean at zero and standard deviation 1.
M=[5 1]; % size of ith layer, for NI layers.
netsplash1 = newff(minmax(inputn),M,{'tansig','purelin'},'traingdm');
% creating the feedforward backpropagation (gradient descent with momentum) neural network.
% here newff defines feedforward network architecture.
% first argument minmax(inputn) defines range of input and initializes the network parameters.
% second argument defines the structure of the network. There is 1 hidden and 1 output layer.
% 5 is the number of the nodes in the first hidden layer.
% 1 is the number of nodes in the output layer.
% next, the activation functions in the layers are defined.
% in the first hidden layer, there are 5 tansig functions.
% in the output layer, there is 1 linear function.
netsplash1.trainParam.epochs=3000; % number of epochs/iterations.
netsplash1.trainParam.lr=0.3; % learning rate.
netsplash1.trainParam.mc=0.6; % momentum.
netsplash1=train(netsplash1,inputn,targetn);
y=sim(netsplash1,inputn);
% to simulate the trained network on the original input data.
output=poststd(y',meant,stdt); % to convert y back to the original scale.
[output target] % predicted data vs actual data
title('Comparison between actual targets and predictions')
d=[output-target].^2; % to calculate square error between actual and predicted values.
mse=mean(d) % to calculate the mean square error (mse).
rmse=sqrt(mse) % to calculate the root mean square error (rmse).
[m,b,r]=postreg(output',target') % use of regression analysis to judge the network performance.
Rsquare=r.^2 % to calculate the Coefficient of Determination (R2).
save netsplash1 % to save the trained network 'netsplash1'.
load netsplash1 % to load the trained network 'netsplash1'.
% newinput = [3.49 0 25.4];
% newinputn = trstd(newinput',meani,stdi);
% newoutputn = sim(netsplash1,newinputn);
% newoutput = poststd(newoutputn',meant,stdt)
```

Appendix 15: ANN coding for predicting thermal protective performance under hot-water immersion and compression exposure at 56 kPa and 75°C

```

input=[0.69 15.71 4.4;2.18 13.59 9.87;3.53 13.3 12.7;1.42 0 20.7;1.42 0 21.17;2.88 0 25.9;3.49 0
25.4;4.23 0 28.03;3.49 0 25.37]; % input data.
target=[5.29;6.19;5.96;29.99;32.68;57.06;48.58;63.2;52.64]; % target data.
[inputn,meani,stdi,targetn,meant,stdt] = prestd(input',target');
%preprocessing or normalizing the data with mean at zero and standard deviation 1.
M=[5 1]; % size of ith layer, for NI layers.
netimmersion75 = newff(minmax(inputn),M,{'tansig','purelin'},'traingdm');
% creating the feedforward backpropagation (gradient descent with momentum) neural network.
% here newff defines feedforward network architecture.
% first argument minmax(inputn) defines range of input and initializes the network parameters.
% second argument defines the structure of the network. There is 1 hidden and 1 output layer.
% 5 is the number of the nodes in the first hidden layer.
% 1 is the number of nodes in the output layer.
% next, the activation functions in the layers are defined.
% in the first hidden layer, there are 5 tansig functions.
% in the output layer, there is 1 linear function.
netimmersion75.trainParam.epochs=3000; % number of epochs/iterations.
netimmersion75.trainParam.lr=0.3; % learning rate.
netimmersion75.trainParam.mc=0.6; % momentum.
netimmersion75=train(netimmersion75,inputn,targetn);
y=sim(netimmersion75,inputn);
% to simulate the trained network on the original input data.
output=poststd(y',meant,stdt); % to convert y back to the original scale.
[output target] % predicted data vs actual data.
title('Comparison between actual targets and predictions')
d=[output-target].^2; % to calculate square error between actual and predicted values.
mse=mean(d) % to calculate the mean square error (mse).
rmse=sqrt(mse) % to calculate the root mean square error (rmse).
[m,b,r]=postreg(output',target') % to judge the network performance, use of regression analysis
Rsquare=r.^2 % to calculate the Coefficient of Determination (R2).
save netimmersion75 % to save the trained network 'netimmersion75'.
load netimmersion75 % to load the trained network 'netimmersion75'.
% newinput = [3.49 0 25.4];
% newinputn = trastd(newinput',meani,stdi);
% newoutputn = sim(netimmersion75,newinputn);
% newoutput = poststd(newoutputn',meant,stdt)

```

Appendix 16: ANN coding for predicting thermal protective performance under hot-water immersion and compression exposure at 56 kPa and 85°C

```

input=[0.69 15.71 4.4;2.18 13.59 9.87;3.53 13.3 12.7;1.42 0 20.7;1.42 0 21.17;2.88 0 25.9;3.49 0
25.4;4.23 0 28.03;3.49 0 25.37]; % input data.
target=[3.63;5.82;6.49;11.31;21.57;35.12;36.25;42.84;40.35]; % target data.
[inputn,meani,stdi,targetn,meant,stdt] = prestd(input',target');
% preprocessing or normalizing the data with mean at zero and standard deviation 1.
M=[5 1]; % size of ith layer, for NI layers.
netimmersion85 = newff(minmax(inputn),M,{'tansig','purelin'},'traingdm');
% creating the feedforward backpropagation (gradient descent with momentum) neural network.
% here newff defines feedforward network architecture.
% first argument minmax(inputn) defines range of input and initializes the network parameters.
% second argument defines the structure of the network. There is 1 hidden and 1 output layer.
% 5 is the number of the nodes in the first hidden layer.
% 1 is the number of nodes in the output layer.
% next, the activation functions in the layers are defined.
% in the first hidden layer, there are 5 tansig functions.
% in the output layer, there is 1 linear function.
netimmersion85.trainParam.epochs=3000; % number of epochs/iterations.
netimmersion85.trainParam.lr=0.3; % learning rate.
netimmersion85.trainParam.mc=0.6; % momentum.
netimmersion85=train(netimmersion85,inputn,targetn);
y=sim(netimmersion85,inputn);
% to simulate the trained network on the original input data.
output=poststd(y',meant,stdt); % to convert y back to the original scale.
[output target] % predicted data vs actual data.
title('Comparison between actual targets and predictions')
d=[output-target].^2; % to calculate square error between actual and predicted values.
mse=mean(d) % to calculate the mean square error (mse).
rmse=sqrt(mse) % to calculate the root mean square error (rmse).
[m,b,r]=postreg(output',target') % use of regression analysis to judge the network performance.
Rsquare=r.^2 % to calculate the Coefficient of Determination (R2).
save netimmersion85 % to save the trained network 'netimmersion85'.
load netimmersion85 % to load the trained network 'netimmersion85'.
% newinput = [3.49 0 25.4];
% newinputn = trstd(newinput',meani,stdi);
% newoutputn = sim(netimmersion85,newinputn);
% newoutput = poststd(newoutputn',meant,stdt)

```

Appendix 17: ANN coding for predicting thermal protective performance under hot-water immersion and compression exposure at 56 kPa and 95°C

```

input=[0.69 15.71 4.4;2.18 13.59 9.87;3.53 13.3 12.7;1.42 0 20.7;1.42 0 21.17;2.88 0 25.9;3.49 0
25.4;4.23 0 28.03;3.49 0 25.37]; % input data.
target=[2.05;2.74;2.78;9.53;16.84;22.7;24.45;29.84;26.04]; % target data.
[inputn,meani,stdi,targetn,meant,stdt] = prestd(input',target');
% preprocessing or normalizing the data with mean at zero and standard deviation 1.
M=[5 1]; % size of ith layer, for NI layers.
netimmersion95 = newff(minmax(inputn),M,{'tansig','purelin'},'traingdm');
% creating the feedforward backpropagation (gradient descent with momentum) neural network.
% here newff defines feedforward network architecture.
% first argument minmax(inputn) defines range of input and initializes the network parameters.
% second argument defines the structure of the network. There is 1 hidden and 1 output layer.
% 5 is the number of the nodes in the first hidden layer.
% 1 is the number of nodes in the output layer.
% next, the activation functions in the layers are defined.
% in the first hidden layer, there are 5 tansig functions.
% in the output layer, there is 1 linear function.
netimmersion95.trainParam.epochs=3000; % number of epochs/iterations.
netimmersion95.trainParam.lr=0.3; % learning rate.
netimmersion95.trainParam.mc=0.6; % momentum.
netimmersion95=train(netimmersion95,inputn,targetn);
y=sim(netimmersion95,inputn);
% to simulate the trained network on the original input data.
output=poststd(y',meant,stdt); % to convert y back to the original scale.
[output target] % predicted data vs actual data.
title('Comparison between actual targets and predictions')
d=[output-target].^2; % to calculate square error between actual and predicted values.
mse=mean(d) % to calculate the mean square error (mse).
rmse=sqrt(mse) % to calculate the root mean square error (rmse).
[m,b,r]=postreg(output',target') % use of regression analysis to judge the network performance.
Rsquare=r.^2 % to calculate the Coefficient of Determination (R2).
save netimmersion95 % to save the trained network 'netimmersion95'.
load netimmersion95 % to load the trained network 'netimmersion95'.
% newinput = [3.49 0 25.4];
% newinputn = trastd(newinput',meani,stdi);
% newoutputn = sim(netimmersion95,newinputn);
% newoutput = poststd(newoutputn',meant,stdt)

```

Appendix 18: ANN coding for predicting thermal protective performance under hot-water immersion and compression exposure at 14 kPa and 85°C

```

input=[0.69 15.71 4.4;2.18 13.59 9.87;3.53 13.3 12.7;1.42 0 20.7;1.42 0 21.17;2.88 0 25.9;3.49 0
25.4;4.23 0 28.03;3.49 0 25.37]; % input data.
target=[4.26;6.69;6.67;19.72;23.16;40;36.11;46.54;43.89]; % target data.
[inputn,meani,stdi,targetn,meant,stdt] = prestd(input',target');
% preprocessing or normalizing the data with mean at zero and standard deviation 1.
M=[5 1]; % size of ith layer, for NI layers.
netimmersion2p = newff(minmax(inputn),M,{'tansig','purelin'},'traingdm');
% creating the feedforward backpropagation (gradient descent with momentum) neural network.
% here newff defines feedforward network architecture.
% first argument minmax(inputn) defines range of input and initializes the network parameters.
% second argument defines the structure of the network. There is 1 hidden and 1 output layer.
% 5 is the number of the nodes in the first hidden layer.
% 1 is the number of nodes in the output layer.
% next, the activation functions in the layers are defined.
% in the first hidden layer, there are 5 tansig functions.
% in the output layer, there is 1 linear function.
netimmersion2p.trainParam.epochs=3000; % number of epochs/iterations.
netimmersion2p.trainParam.lr=0.3; % learning rate.
netimmersion2p.trainParam.mc=0.6; % momentum.
netimmersion2p=train(netimmersion2p,inputn,targetn);
y=sim(netimmersion2p,inputn);
% to simulate the trained network on the original input data.
output=poststd(y',meant,stdt); % to convert y back to the original scale.
[output target] % predicted data vs actual data.
title('Comparison between actual targets and predictions')
d=[output-target].^2; % to calculate square error between actual and predicted values.
mse=mean(d) % to calculate the mean square error (mse).
rmse=sqrt(mse) % to calculate the root mean square error (rmse).
[m,b,r]=postreg(output',target') % use of regression analysis to judge the network performance.
Rsquare=r.^2 % to calculate the Coefficient of Determination (R2).
save netimmersion2p % to save the trained network 'netimmersion2p'.
load netimmersion2p % to load the trained network 'netimmersion2p'.
% newinput = [3.49 0 25.4];
% newinputn = trstd(newinput',meani,stdi);
% newoutputn = sim(netimmersion2p,newinputn);
% newoutput = poststd(newoutputn',meant,stdt)

```

Appendix 19: ANN coding for predicting thermal protective performance under hot-water immersion and compression exposure at 28 kPa and 85°C

```

input=[0.69 15.71 4.4;2.18 13.59 9.87;3.53 13.3 12.7;1.42 0 20.7;1.42 0 21.17;2.88 0 25.9;3.49 0
25.4;4.23 0 28.03;3.49 0 25.37]; % input data.
target=[4.31;5.92;6.29;19.05;22.96;38.1;39.52;44.62;42.97]; % target data.
[inputn,meani,stdi,targetn,meant,stdt] = prestd(input',target');
% preprocessing or normalizing the data with mean at zero and standard deviation 1.
M=[5 1]; % size of ith layer, for NI layers.
netimmersion4 = newff(minmax(inputn),M,{'tansig','purelin'},'traingdm');
% creating the feedforward backpropagation (gradient descent with momentum) neural network.
% here newff defines feedforward network architecture.
% first argument minmax(inputn) defines range of input and initializes the network parameters.
% second argument defines the structure of the network. There is 1 hidden and 1 output layer.
% 5 is the number of the nodes in the first hidden layer.
% 1 is the number of nodes in the output layer.
% next, the activation functions in the layers are defined.
% in the first hidden layer, there are 5 tansig functions.
% in the output layer, there is 1 linear function.
netimmersion4.trainParam.epochs=3000; % number of epochs/iterations.
netimmersion4.trainParam.lr=0.3; % learning rate.
netimmersion4.trainParam.mc=0.6; % momentum.
netimmersion4=train(netimmersion4,inputn,targetn);
y=sim(netimmersion4,inputn);
% to simulate the trained network on the original input data.
output=poststd(y',meant,stdt); % to convert y back to the original scale.
[output target] % predicted data vs actual data.
title('Comparison between actual targets and predictions')
d=[output-target].^2; % to calculate square error between actual and predicted values.
mse=mean(d) % to calculate the mean square error (mse).
rmse=sqrt(mse) % to calculate the root mean square error (rmse).
[m,b,r]=postreg(output',target') % use of regression analysis to judge the network performance.
Rsquare=r.^2 % to calculate the Coefficient of Determination (R2).
save netimmersion4 % to save the trained network 'netimmersion4'.
load netimmersion4 % to load the trained network 'netimmersion4'.
% newinput = [3.49 0 25.4];
% newinputn = trastd(newinput',meani,stdi);
% newoutputn = sim(netimmersion4,newinputn);
% newoutput = poststd(newoutputn',meant,stdt)

```